c.1

PARTICLE VIBRATION at the BOUNDARY in TURBULENT SHEAR FLOW

by

DAVID PETER JONES

B. Sc., The University of British Columbia, 1976

A THESIS SUBMITTED IN PARTIAL FULFILMENT OF

THE REQUIREMENTS FOR THE DEGREE OF

MASTER OF SCIENCE

in

THE FACULTY OF GRADUATE STUDIES

(Department of Geography)

We accept this thesis as conforming

to the required standard

THE UNIVERSITY OF BRITISH COLUMBIA

April 1981

In presenting this thesis in partial fulfilment of the requirements for an advanced degree at the University of British Columbia, I agree that the Library shall make it freely available for reference and study. I further agree that permission for extensive copying of this thesis for scholarly purposes may be granted by the Head of my Department or by his representatives. It is understood that copying or publication of this thesis for financial gain shall not be allowed without my written permission.

Department of Geography

The University of British Columbia
2075 Wesbrook Place
Vancouver, Canada
V6T 1W5

Date March 10 1981

ABSTRACT

Observations were made of the vibratory motion of individual gravel particles near the threshold of motion in a flume. Since it is not known what flow-boundary parameters modify the pressure and velocity fluctuations, a phenomenological approach was used.

The study focuses on the processes and conditions that result in vibration and on the factors that modify the vibration frequency. Four hypotheses that may provide an explanation for the vibration were investigated:

a) mechanical instability of the particles;

b) self excitation arising from wake shedding;

c) wake interaction or vorticity amplification leading to vibration;

d) excitation arising from turbulent bursting.

Individual particles were observed to exhibit irregular vibratory motion. Measurements of the vibration period of gravel in water were found to conform to the scaling relationship proposed by Rao, Narasimha and Badri Narayanan (1971) for the period of turbulent bursts in air and water. Measurements taken by Vanoni (1964) and Sutherland (1967) for the motion of sand in water and by Lyles (1970) for sand in air are shown also to conform to this scaling relationship. As flow parameters approach the threshold condition for a particle, the non-dimensional vibration period consistently decreases towards a value of approximately five. This possibly may provide an objective criterion to determine the threshold of motion.

On this criterion, there appears to be no basis for differentiating entrainment mechanisms for coarse sand and gravel - at least for normally loose boundaries. The present work supports the modification of Sutherland's entrainment mechanism by Sumer and Oğuz (1978): Rather than a transverse vortex whose lower most portion rotates in the same direction as the mean flow, they propose that the vortex rotates counter to the mean flow. This would be consistent with observations obtained in flow visualization studies (Offen and Kline, 1975) and the correspondence found between particle vibration frequency and the burst periodicity found in this work.

Particle vibration and entrainment are considered to result from local, temporarily adverse pressure gradients imposed on the wall by high speed fluid sweeps that form transverse vortices as part of the turbulent burst sequence.

TABLE OF CONTENTS

Page

LIST OF TABLES

LIST OF FIGURES

LIST OF SYMBOLS

a	Principal axis length
b	Intermediate axis length
c	Minor axis length
D	Diameter of equivalent sphere
d	Flow depth
F_D	Drag force
F_f	Frictional force
F_g	Gravitational force
F_L	Lift force
F_n	Contact and restraining force
Fr	Froude number
F_v	Viscous force
g	Gravitational constant
k	Roughness density
p	Pressure
p'	RMS pressure fluctuation
Re	Reynolds number
Re	Momentum-thickness Reynolds number
Re_*	Particle Reynolds number
S	Slope
Sp	Maximum projection sphericity
Tm	Period measured by hot wire anemometer
Tv	Period measured by visual observations
T^*	Non-dimensional period

T_p^* Non-dimensional period for particles

U_∞ Free stream velocity

u Instantaneous longitudinal velocity

u' RMS horizontal velocity fluctuation

U* Shear velocity

v Instantaneous vertical velocity

v' RMS vertical velocity fluctuation

α Angle of inclination from horizontal

δ Boundary layer thickness taken as flow depth

δ^* Displacement thickness

θ Momentum thickness

a Orientation of principal axis

λ_e Downstream spacing of roughness element

ν Kinematic viscosity

ρ_s Sediment density

ρ_f Fluid density

σ Variance

τ Shear stress

$1/\psi_c$ Entrainment function

ACKNOWLEDGEMENTS

I would like to thank my supervisor, Dr. Michael Church, for his assistance and advice throughout all aspects of this study. In particular I am grateful for his unflagging patience and encouragement.

I am also indebted to members of my committee, particularly Dr. O. Slaymaker who read an early version of the manuscript and provided helpful suggestions. I also wish to thank Dr. T. Hickin who kindly provided access to the flume installation in the Department of Geography, Simon Fraser University.

The author is grateful to Mr. R. Leslie for technical assistance, Miss J. Haggerstone for assistance with the drafting and Miss S. Rear for typing two copies of the manuscript.

Financial support for this project was received by the author through a National Science and Engineering Research Council Scholarship and grants from the National Research Council to Dr. M. Church.

I would also like to thank Miss B. Martin for her encouragement without which this manuscript might never have been completed.

CHAPTER 1

1.1 INTRODUCTION

1.1.1 The research problem

In studies of the threshold conditions required for the entrainment of non-cohesive particles, several investigators have reported the occurrence of vibratory motion of particles prior to translation. No satisfactory explanation for the existence of this motion has been offered. The present investigation examines the oscillatory motion of coarse sands and gravels that occurs prior to entrainment. This is achieved by conducting experiments to examine four alternative hypotheses for the mechanism that produces particle vibration, and their consequences. The hypotheses are that vibration is induced primarily by:

1) mechanical instability of the particle in the flow;
2) oscillatory forces arising due to vortex shedding from a particle;
3) advected eddies interacting with particles downstream;
4) response of particles to turbulent bursting in the vicinity.

1.1.2 Rationale and basis

As early as 1936, Shields, in his classic experiments on the threshold of motion, noted the occurrence of particle vibration prior to entrainment. Subsequent investigators have also observed the phenomenon but, aside from Lyles (1970), no consideration appears to have been given to either the importance of, or processes that result in particle vibration. Phenomena such as particle vibration may provide a means of obtaining some insight

into sediment entrainment.

In the present study, attention is restricted to depth limited flows where turbulence arises when fluid is sheared by gravitational forces. In such flows, the production of turbulent energy is concentrated in the region immediately adjacent to the wall (Kim et. al., 1971). Recent flow visualization and velocity correlation measurements have disclosed a deterministic sequence of complex fluid motions that occurs randomly in time and space (reviewed in Offen and Kline; 1975). The energy concentration associated with the deterministic sequence of fluid motions is expected to have important implications for the response and subsequent behavior of a compliant boundary of non-cohesive particles. The detailed mechanics of sediment entrainment must depend on the characteristics of the turbulent structure as well as specific bed configurations.

For turbulent flows over a boundary of non-cohesive particles typical of depth limited alluvial streams, fluid forces of sufficient magnitude may occur that individual particles are entrained. In order to estimate bed stability, scour potential or sediment transport in alluvial channels, it is necessary to be able to determine the threshold conditions below which no particle movement occurs. The standard approach to determine the threshold condition is to use the mean properties of the turbulent flow, such as shear stress or velocity (Shields, 1936; Gessler, 1971). Since the individual particles respond to the instantaneous fluctuating forces impinging on the bed, considerable uncertainty may arise in the determination of the threshold condition by the standard approach. At the threshold of motion the mean overturning moment and mean forces can be computed, at least for uniform elements, if the distributions

of mean fluid pressure and velocity are known. In order to estimate the fluctuating forces it is necessary to know the spectrum of the fluctuating pressure at the wall, the space-time correlation of the pressure fluctuations on the particle surface, the space-time correlation of the wall fluctuating pressure and the three components of the fluctuating velocity in the vicinity of the particle, as well as a possible particle admittance frequency.

The incident turbulent flow is the prime cause of wall pressure fluctuations that are modified by wake eddies shed from upstream roughness elements, eddies shed from the object itself, flow separation and re-attachment to the particle surface, and the oscillatory motion and mechanical instability of the particle. In order to make further progress in our understanding of the threshold condition and the processes sustaining particle motion, it is useful to ascertain which of the preceding mechanisms provide dominant contributions to the fluctuating forces. If no one mechanism is dominant it would be useful to ascertain the relative importance of each mechanism.

The analytic intractability of the turbulent flow problem has resulted in an emphasis on experimental investigations. These studies have in turn been frustrated by the inherent complexity of three-dimensional turbulent flows which makes it difficult to interpret either qualitative or quantitative measurements. Rather than making extensive temporal recordings of the pressure and velocity fluctuations that could be related to initial particle motion, it was considered more fruitful to make inferences from simple observations.

Reports in the literature and new observations of vibratory motion of gravel prior to entrainment suggested that an investigation of this phenomenon

might provide some insight into factors that determine the threshold of motion. Conditions influencing the vibratory frequency, as well as the range of sizes exhibiting motion, might suggest different entrainment mechanisms for different sized materials. Furthermore, systematic observations of a consistent pattern of behavior of particles as threshold is approached may provide further insight.

The purpose of the present qualitative observations is to examine such factors as mechanical stability, a deterministic condition; a stochastic process such as particle interaction via wake shedding; or random flow conditions that may modify the critical threshold condition defined on the basis of mean flow parameters. Such information will provide some means of discriminating between different processes that affect the entrainment mechanism. Qualitative observations of these phenomena however will be suggestive rather than conclusive support for any proposed hypothesis.

Ultimately an increased understanding of the conditions that control sediment entrainment will help in the development of more physically sound sediment transport formulations (eg. particle step length in Einstein's bed load function) or new conditions governing particle behavior may be developed. An improved understanding of the mechanics of entrainment could provide more accurate estimates of flow parameters controlling threshold and live bed conditions and hence the range of applicability of sediment transport formulae.

The present study focusses on the processes and conditions that result in vibration prior to entrainment and the factors that modify the vibration frequency.

1.2 TURBULENT BOUNDARY LAYERS

1.2.1 Boundary layer flows

Free surface, depth limited flows are a sub-group of boundary layer flows that may be either laminar or turbulent. Boundary layer flows are those in which the character of the wall and the distance from that surface determine characteristics such as velocity and shear stress distribution. Boundary layers are delimited by a 'thickness' where the velocity reaches 99% of the free stream velocity (Massey, 1975). The presence of a free surface results in a problem of definition of the thickness of the boundary layer and the free stream velocity.

Laminar boundary layer flows, where the fluid behavior is marked by the absence of lateral diffusion and dominance of viscous effects, are the exception rather than the rule in geophysical flows. Virtually all boundary layer flows of geophysical interest are turbulent. Bradshaw (1971) gives the most concise definition of turbulence:

> Turbulence is a three dimensional time-dependent motion in which vortex stretching causes velocity fluctuations to spread to all wavelengths between a minimum determined by viscous forces and a maximum determined by the boundary conditions of the flow. It is the usual state of flow at high Reynolds numbers (p. 17).

A complete list and discussion of the characteristics of turbulence may be found in Tennekes and Lumley (1972) or Reynolds (1974). Further attention and discussion will be restricted to those characteristics that directly affect the present study.

Turbulence may be generated either by frictional forces created by flow over and around fixed walls or by the flow of layers of fluid with different velocities past one another. Differences in the nature of the generated turbulence make it useful to distinguish between these two types. The former case, where a gradient in the mean velocity away from the wall occurs, exhibits anisotropic turbulence. This may be designated as shear-flow or wall turbulence (Hinze, 1975) to differentiate it from free turbulence that may be more nearly isotropic. Open channel flows typically have large velocity gradients, particularly near the basal boundary, and are highly anisotropic.

Highly sheared or turbulent fluid flow over either a smooth or rough wall results in a region where the wall characteristics condition the flow. This boundary layer may be composed of three major, intergrading zones of flow (Middleton and Southard, 1978).

The zone immediately adjacent to the wall, where the velocity tends towards zero, is dominated by viscosity and is called the viscous sublayer. For hydrodynamically rough surfaces where the height of the roughness elements is greater than the thickness of the viscous sublayer, turbulent fluctuations may disrupt this layer sufficiently that it becomes indistinguishable from the next zone.

Immediately above the viscous sublayer is the turbulence generation or wake layer where the production of turbulent kinetic energy is concentrated. Energy is abstracted from the highly sheared mean flow to produce turbulent eddies that carry momentum both outward to the free surface and inward toward

the wall. For sufficiently rough boundaries, this zone extends right to the wall. The scaling parameters for this region are the shear velocity U_* and the roughness size D.

Above the turbulence generating zone is an outer region where the larger scales of turbulence are more efficient at transporting momentum. This results in a decrease in the shear and reduced velocity gradients. For relative roughness $d/D \gg 3$, the outer region occupies most of the flow depth from the free surface to fairly near the wall. Scaling parameters are the mean velocity U or free stream velocity U_∞ , and the flow depth d.

In depth limited flows, the development of the boundary layer is constrained by the presence of a free surface. Aside from effects of surface waves, the presence of a free surface redistributes the turbulent energy from the vertical component to the horizontal down-stream and cross-stream velocity components via the pressure-velocity correlation. Except for the pioneering work of Kennedy (1969), the role of the free surface has hardly been investigated and is assumed to have negligible affects on the flow-boundary interaction except where the relative depth is less than three.

1.2.2 Mean properties of the flow

The time dependent nature of turbulence means that it may be viewed as a stochastic process. Classical work assumed that the process was Gaussian, empirical support being provided by early experimental studies investigating the distribution of the velocity fluctuations. Increasing evidence suggests that the process is non-Gaussian (Nordin et. al, 1972; Nowell, 1978).

However, no critical assessment has been made of Einstein and El Samni's (1949) conclusion that the pressure fluctuations are normally distributed. If the distributions of either the velocity or pressure fluctuations are non-Gaussian, the role of exceptionally large or small events (fluctuations) will become important. In this report, it will be demonstrated that quasi-periodic turbulent fluctuations play a significant role in the response of non-cohesive bed materials and particle motion.

The definition of turbulence given by Bradshaw (1971) implicitly recognizes that turbulence may be characterized by one or more length and time scales. Length scales have an upper bound constrained by the dimensions of the flow field and a lower bound where molecular diffusion occurs. The mean flow is independent of viscous forces and the integral or macroscale of motion, L, responsible for extracting energy from the mean flow, normally scales with distance from the boundary (Tennekes and Lumley, 1972). Micro-scales, where viscosity first becomes significant, may also be defined.

Analogous scales can be obtained for the temporal characteristics of the turbulence. The integral time scale T_E is a ratio of the distance from the boundary and the appropriate velocity. The integral time scale may be an important measure of the duration of the fluctuating forces present within the turbulent flow (Jackson, 1976).

Along with appropriate spatial and temporal scales of motion, turbulent flows may be characterized by measures of the turbulence intensity. This number is defined as the ratio of the root mean square of the velocity fluctu-

ations to the mean velocity. For hydrodynamically smooth boundaries, turbulence intensities will be only a few percent while a strongly sheared flow over a rough boundary will have turbulence intensities in excess of 20% close to the bed. As the boundary roughness increases, Grass (1971) found that the longitudinal intensity decreased while the vertical intensity increased.

1.2.3 Flow interaction with a rough boundary

Any body placed in a fluid flow is an obstruction that will interact with the fluid to create a forward three-dimensional turbulent boundary layer. The flow approaching the upstream face of a bluff body continuously decelerates because the face acts as a stagnation plate. The decelerating fluid will tend to accumulate in front of the bluff body, becoming very unstable and creating high levels of turbulence intensity. Immediately upstream of the stagnation zone, a bound standing vortex occurs with a strongly diverging flow around the side of the body.

The strongly divergent flow stretches the vortex filaments leading to vorticity amplification (Sadeh and Cermak, 1972). The increased turbulence intensity arising from the vorticity amplification occurs at selected lengths larger than the 'neutral scale", resulting in the concentration of energy at lower frequencies. The neutral scale is determined by the hydraulic diameter of the body and the free stream velocity (Sadeh and Cermak, 1972). Below the neutral scale, energy is dissipated by viscous forces more rapidly than it is amplified. For an array of bluff bodies it might be expected that the turbulent energy is concentrated at specific low frequencies that dominate the flow. This would then be expected to create a significant frequency or length scale

in the flow-boundary interaction.

On the basis of the response of a boundary layer, Morris (1955) differentiated three different types of flow-boundary interactions: isolated roughness, wake interaction and skimming, that resulted from the spacing of the roughness elements and their interaction with the flow. Skimming flow occurs for densely packed roughness elements. Flow obstruction and mutual protection in the vicinity of the bed results in the flow being displaced to the top of the roughness elements. Nowell (1978) found that skimming flow occurred when the roughness concentration, defined as the ratio of the plan area of the roughness elements to the total surrounding area, exceeded 1/12. Isolated block roughness occurs when roughness elements act as individual wake shedding blocks with no wake interaction. Wake development and dissipation occur completely before the next block is encountered.

Intermediate between skimming and isolated flow is wake interaction flow where wakes from the roughness elements interact to increase significantly the flow resistance (Nowell, 1978; Nowell and Church, 1979). This occurs for intermediate roughness densities between about 1/16 and 1/48.

Associated with the turbulence intensity are the Reynolds stresses, the major effect of momentum transfer, that are a function of the velocity fluctuations. For a constant Reynolds number, Grass (1971) found that placing 2 mm sand and 9 mm pebbles on an initially smooth boundary increased the effective shear stress by approximately 40 and 90 per cent respectively. Brown and Thomas (1977) showed that the wall shear stress in a boundary layer

over a smooth surface can be divided into a slowly varying component and a high frequency, large amplitude component corresponding to large and small scale motions. From their work, it appears that there is a specific phase in the low frequency wall fluctuations at which the high frequency component will occur. The wavelength of the low frequency component associated with the large scale turbulence is of the order of 2δ long at the wall.

1.3 BOUNDARY CONDITIONS

1.3.1 Nature of a compliant boundary

In alluvial open channel flows, the bed is composed of individual non-cohesive particles of varying sizes and shapes. These bed materials may interact with the flow, which in turn will modify the distribution and morphology of the bed materials. While the concentration of effective roughness elements will have a profound effect upon the boundary layer flow, modification of the wall morphology by the fluid force may also be a significant factor in changing the flow characteristics. To date, studies of the turbulent structure in a fluid have predominantly been confined to conditions where either smooth or rough boundaries are rigid. Even when coarse sand or gravel have been used for the roughness elements, the boundary is frequently rigid since the particles have been glued or otherwise fixed to the bed (Thompson, 1963; Grass, 1971; Francis, 1973; Fenton and Abbot, 1977). While specification of the roughness density may be adequate to characterize a rigid boundary, bed configurations that occur on a deformable boundary suggest that further differentiations would be useful. While distinct bedforms such as ripples and dunes occurring in fine materials are important,

attention in the present discussion will be restricted primarily to coarse materials, $d > 2$ mm, exhibiting no bedforms.

1.3.2 Bed texture and structure

The geometry of the bed roughness elements may be considered passive for the purpose of differentiating flow characteristics. This, however, does not take adequate account of the morphology and response of a deformable boundary. Rather than differentiating the roughness spacing, the bed may be defined as packed when adjacent particles are touching or restraining each other; crowded when there are many particles in the neighbourhood, but they are not generally restraining each other; sparse when there are few particles in the neighbourhood and coherent wakes are maintained so that wake interaction may occur; or isolated where particles are sufficiently removed from each other that wake shedding does not dominate the flow structure. Neighbourhood might be defined as the largest area possible whose morphology can be modified without initiating a change in the mean flow characteristics. Assuming relatively uniform particle size, both packed and crowded bed conditions will exhibit skimming flow.

The packing arrangement of a compliant boundary composed of non-cohesive particles may also be described as normal, overloose and underloose or imbricated (Church and Gilbert, 1975; see Figure 1). The packing arrangement may severely restrict the ability of the bed to respond to processes occurring within the turbulent flow. A normal boundary is one in which individual particles are loosely and randomly arranged with neither a dispersed nor imbricated packing. An overloose boundary exists when the particles are found

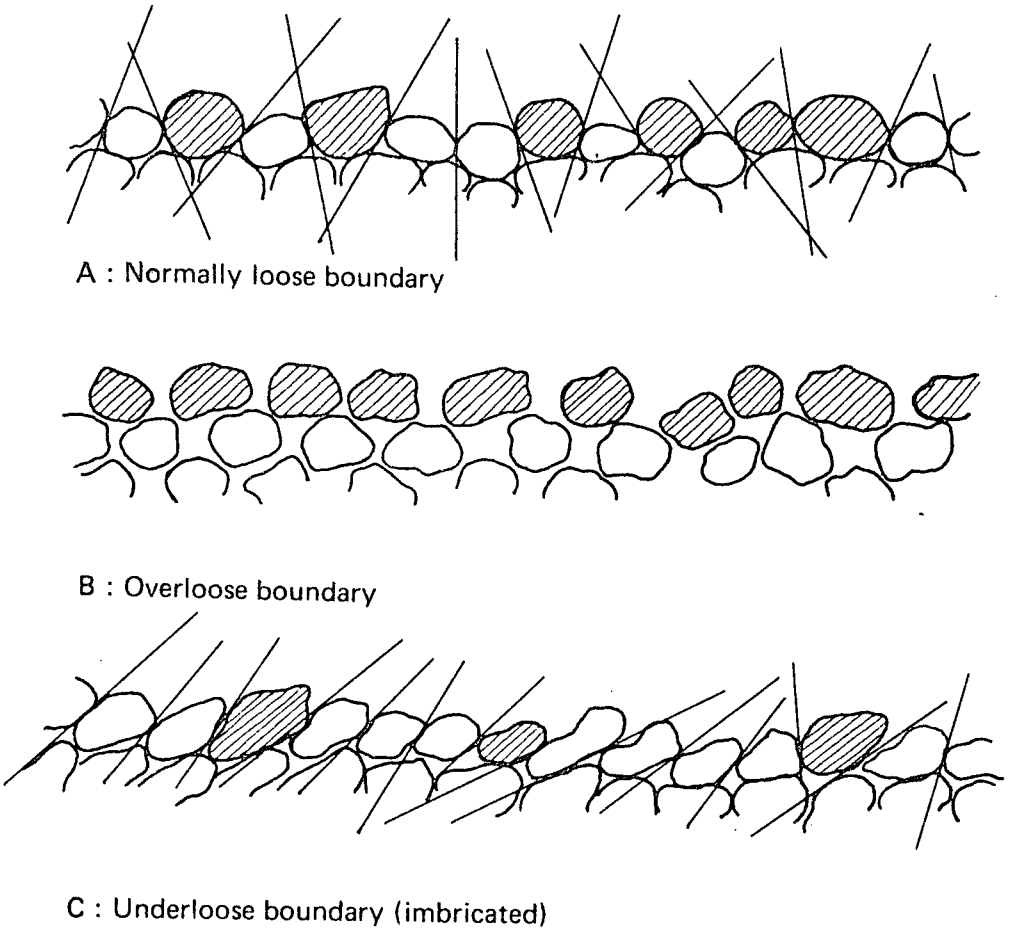

Fig. 1. Boundary packing arrangements (After Church and Gilbert, 1975). The tangential lines in A and C indicate the direction of the frictional forces F_f that constrain the possible motion of individual clasts.

in a dilated state with an "open" packing arrangement. In contrast, an underloose or imbricated state refers to the interlocking or close packing of particles. This last configuration is common in gravel and cobble bed rivers.

The existence of varying particle size distributions and support arrangements will modify some packing configurations. Restricting attention to coarse material, the simplest and most unnatural case is a single layer of gravel on a rigid boundary. The distribution of the gravel may range from isolate to crowded. By placing gravel on a rigid boundary, the effects of local bed configuration, particle support and relative protrusion can be reduced or eliminated.

A more realistic configuration is that of isolate gravel on a sand bed. Some of the characteristics of this bed condition have been investigated (Leopold, Emmett and Myrick, 1966; Koster, 1974) but little work has been done in relating the response of the bed materials to the processes occurring in the flow.

Lastly, the most natural configuration is a mixture of sand and gravel. In this case, the presence of sand between the coarse material is expected to promote stability and modify the response of bed materials to impinging turbulent fluctuations.

In this thesis, emphasis will be placed on the processes occurring within the turbulent flow that affect the response of a compliant boundary. Investigations were conducted with gravel, ranging from isolate to crowded

packing on a rigid boundary and with graded mixtures of gravel with varying quantities of interstitial sand.

1.4 ANTECEDENTS TO THIS WORK

1.4.1 Introduction

An extensive literature exists that deals with the transport of solid particles in a moving fluid. Francis (1973) asserted that this literature could be divided into three categories. First he identified that body of work which dealt with the total solids flow and the characteristics of the fluid i.e. bulk sediment transport. A second category included studies of the formation and effects of bed forms. Francis discriminated a third group whose aim is to determine the threshold of motion.

For conditions near the threshold of motion, the response of individual particles will depend not only on the types of forces experienced by the particle, but also on the nature of the turbulence structure and the energy mechanisms. While simple static analyses of the forces are useful, they do not provide any insight into the processes initiating the forces. Observations of particle vibration prior to entrainment may provide an alternate estimate of the pressure and velocity fluctuations impinging on the particle, yielding insights into the processes initiating the particle forces.

1.4.2 Turbulence structure

In depth-limited boundary layers, three regions may be discriminated based upon the distribution of the mean and fluctuating properties of the

flow (Middleton and Southard, 1978; Nowell and Church, 1979). For $y/d > 0.35$, encompassing most of the outer region, the turbulence intensity steadily decreases toward the surface. For relative depths $y/d < 0.2$, the turbulence characteristics are very dependent upon the roughness density. For low roughness densities, wake interactions are small and the fluctuating properties of the turbulence increase all the way to the wall, In the region $0.2 < y/d < 0.35$, the turbulence properties are nearly constant for a sufficiently dense roughness. Nowell and Church (1979) found that the development of a wake layer, where wakes shed from upstream roughness elements interact to determine flow properties of the region, was particularly evident for intermediate roughness densities (1/16 - 1/22). For high roughness concentrations, the flow shifted its origin to the top of the roughness elements. The development of a wake layer resulting from wake interaction may be particularly effective in modifying a boundary of non-cohesive particles but this has not been investigated to date.

White (1940) was the first to recognize the importance of fluctuating velocities resulting from the turbulent flow in modifying the entrainment of individual particles. Sutherland (1967), however, appears to have been the first investigator who made explicit observations of turbulence near the wall in order to explain the mechanism of particle entrainment. Sutherland noted the tendency for grains (0.564 mm diameter) on the bed to move in a series of short, intermittent bursts. Dye injections, in conjunction with motion photography, showed a correlation between grain motion and large disturbances of dye in the viscous sublayer, suggesting that the dye ejections resulted from the intrusion of turbulent eddies into the sublayer. From these observations he hypothesized that particle entrainment and lift-up was due to

an incoming eddy rotating so that its lower most portion is in the direction of the mean flow.

Flow visualization techniques, in conjunction with hot film anemometry, have subsequently disclosed a complex, quasi-ordered flow structure consisting of a deterministic sequence of fluid motions. Despite difficulties imposed by sampling limitations and the inability to make unique inferences of eddy structure based on velocity-correlation measurements, organized fluid motions termed 'bursts' and 'sweeps' have been identified. A considerable degree of structural organization within the flow is required before individual patterns can be perceived. Such organization appears to be present, at least over smooth boundaries, while the recognition of spatial patterns over rough surfaces becomes increasingly difficult.

While the presence of an organized structure in the boundary layer is now generally recognized, a variety of conceptual models that attempt to explain the quasi-deterministic sequence of events called a 'burst' have been presented (Kline et. al., 1967; Corino and Brodkey, 1969; Kim et. al., 1971; Offen and Kline, 1974, 1975; Brown and Thomas, 1977; Praturi and Brodkey, 1978). The different nomenclature used by these investigators, alternate Eulerian and Lagrangrian frames of reference and the different perspectives derived from either visualization techniques or velocity correlation measurements create some difficulty in obtaining a consistent picture. With few exceptions, observations have been made over smooth rigid boundaries. To date, possible relations between the turbulent structure and the response of a deformable boundary of cohesionless material remain neglected.

In the case of a turbulent boundary layer over a smooth, rigid surface the models agree on the existence of two distinct zones: a wall region and an outer region (Nychas, Hershey and Brodkey, 1973; Offen and Kline, 1975). Although there are some differences in the precise division between these two zones, the wall region incorporates the viscous sublayer and turbulence generation zone of Middleton and Southard (1978).

The wall region or inner zone is distinguished by a viscous sublayer displaying spanwise alternations of high and low speed streaks of fluid that experience episodic disruption by transverse vortices, causing the subsequent lift-up of the low speed streaks. The essential characteristics of this zone such as the spanwise spacing of the streaks are scaled by inner variables, shear velocity U_* and kinematic viscosity ν.

The thickness of the viscous sublayer scales with the roughness element size D, U_*, and ν. When the non-dimensional thickness $D^+ = DU_*/\nu$ exceeds about 70 (Yalin, 1977), the roughness elements completely disrupt the viscous sublayer and it ceases to exist as a reasonably behaved region. Grass (1971) found that the roughness elements in such a flow disrupt the inner layer sufficiently that no organized pattern of sublayer streaks could be distinguished.

The transverse vortex that appears responsible for the lift-up of the slow speed streaks over the smooth boundary arises when a high speed fluid element (a 'sweep' in the nomenclature of Offen and Kline, 1974,1975) is directed towards the wall. This fluid rapidly advances over the lower velocity fluid in the inner region giving rise to a transverse vortex at the

front between the high and low speed fluid. The transverse vortex adjacent to the wall impresses a temporary adverse pressure gradient, leading to the lift up and ejection of the low momentum fluid. At increasing distance from the wall, this low momentum fluid oscillates rapidly and breaks up into a chaotic motion termed a 'burst'. Individual burst-sweep events occur randomly in time and space but their sequence, referred to as a burst cycle, appears to be deterministic. At present there is insufficient information to decide on the beginning of the sequence although Praturi and Brodkey (1978) suggest that accelerated fluid moving towards the wall from the outer region precedes and probably initiates a burst.

Hydrogen bubble visualization techniques provide simultaneous longitudinal and vertical velocity profiles so that some measure of the interaction between the inner and outer regions can be obtained. Linked pairs of conditionally averaged velocity profiles show that the minimum local longitudinal velocities are directly correlated with peaked regions of positive vertical velocities. This corresponds to observations of the ejection of low momentum fluid from the wall region ($u' < 0$, $v' > 0$)(Grass, 1971). These results are in accord with continuity requirements. Similarly, maximum local longitudinal velocities are found to correlate with peaked regions of negative vertical velocities ($u' > 0$, $v' < 0$). Both the fluid ejections and inrush or sweep phases result in a very high positive Reynolds stress at the boundary and form an important part of the general momentum transfer mechanism.

Grass (1971) found that independent of the roughness concentration, negative vertical velocities associated with inrush phases of a turbulent

burst exhibit strong positive correlation over a significant proportion of the flow depth. On this basis he suggested that the interaction between the inner and outer regions of flow are affected by the overall flow boundary conditions influencing the outer regions rather than the wall parameters. This implies that turbulent bursting and hence particle vibration should be independent of the roughness concentration of the wall. The recent work of Brown and Thomas (1977) has provided additional evidence to suggest that the large scale structures of the outer region give rise to a characteristic response in the region near the wall. This response is observed as a high frequency, large amplitude wall shear fluctuation which is thought to be directly connected with the bursting phenomenon.

The turbulent structure of the outer region is dominated by the bursting process which Rao, Narasimha and Badri Narayanan (1971) found to be scaled by outer variables, free stream velocity U_∞ and the boundary layer depth δ, independent of the wall structure. The non-dimensional period of the large organized structures, found by Brown and Thomas (1977) to be inclined at an angle of about 18°, is $T^+ = TU_\infty / \delta \approx 5$.

The models of the turbulent flow structure proposed by either Offen and Kline (1975) or Pratura and Brodkey (1978) are based primarily on flow visualization over smooth boundaries. At present there is an extreme paucity of data regarding the applicability of these models to hydrodynamically rough and/or deformable boundaries. Grass (1971), in a unique study, compared the effects of various surface roughnesses on the turbulent flow over hydraulically smooth, transitional and rough boundary conditions. These surface roughness

conditions were varnished marine plywood, 2 mm Leighton Buzzard sand and 9 mm rounded pebbles.

Using the hydrogen bubble technique, Grass found that the magnitude of the velocity fluctuations was between two and three times the local mean velocity for all three surfaces. On the basis of conditional sampling, he concluded that the general fluid ejection process is a common feature of the flow structure irrespective of boundary roughness.

The major difference in the flow structure over the hydrodynamically rough surface is the absence of well organized spanwise alternating high and low speed streaks that are present over smooth surfaces. This may be attributed in part to the absence of a viscous sublayer although Grass, noting the extremely violent ejections of fluid from between the interstices of the roughness elements, suggested that different modes of instability might occur for different roughness conditions.

1.4.3 Initiation of motion

Fluid flowing over a surface of non-cohesive material exerts a shear stress or force on each individual particle. In the absence of a horizontal slope, the forces acting on a single cohesionless grain are of two opposing types: those forces such as gravity which keep the grain in place, and forces such as lift or drag acting to change the position of the particle. A threshold or incipient condition (of motion) occurs when the balance of mobilizing and restraining forces is reached, then surpassed. For the condition wherein the mobilizing forces exceed the restraining forces, the

combined mobilizing forces may be referred to as critical or threshold forces.

The forces acting on an individual particle are summarized in Figure 2. The gravity force F_g acting through the center of mass is the grain volume times the submerged specific weight $g(\rho s - \rho f)$, where ρs, ρf are the particle and fluid densities respectively. If the effective diameter of an equivalent sphere is D, the total volume is $\pi D^3/6$ so that the total gravity force is:

$$F_g = \frac{\pi}{6} D^3 g \ (\rho_s - \rho_f)$$

The effective gravitational component that resists motion will be $F_g \sin\alpha$, where α is the angle that the direction of easiest motion makes with the horizontal (Figure 2).

Many investigators (Shields, 1936; White, 1940; Bagnold, 1941; Chepil, 1959) have suggested that the angle α can be closely approximated by the mass angle of repose. The term mass angle of repose refers to the angle at which loose material will stand when piled and averages about 33° for well rounded sand, increasing for larger material. Miller and Byrne (1966), in a series of experiments, determined that the angle α for individual grains on a fixed bed of similar grains was much larger, being in the range of 45 - 70 degrees. For grains smaller than the average size in the fixed bed, the angle is larger while for those grains that are larger than the average bed size, the angle is reduced. This is a consequence of sheltering and the effectiveness of imbrication which only works between grains of more or less similar size. The lower values for grains larger than the bed average

A

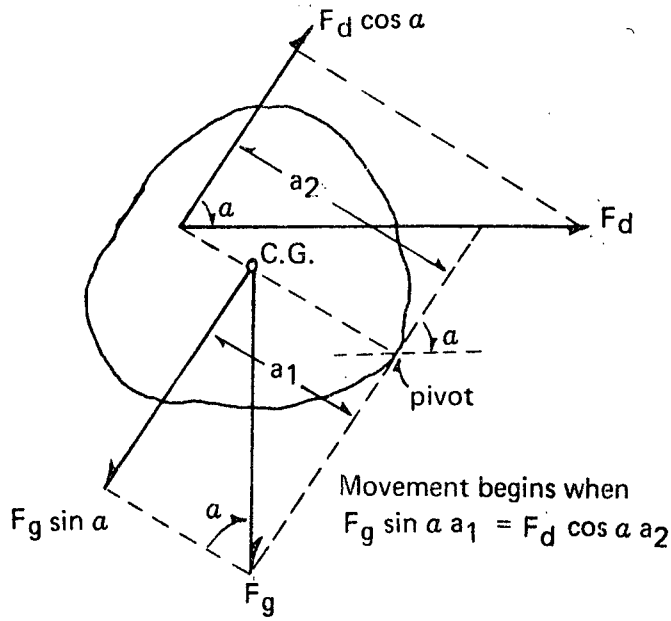

B

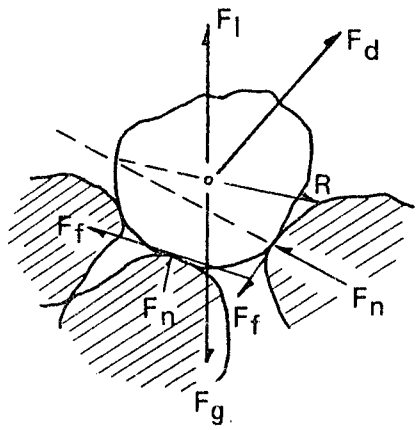

Fig. 2. A) Analysis of moments acting on a grain at the beginning of motion (After Middleton and Southard, 1978).

B) Forces acting on a grain resting on a bed of similar grains.

suggest that other things being equal, the larger than average grains may be easier to move (Miller and Byrne, 1966) depending on whether lift or drag is the predominant force initiating motion. Little difference for the angle of repose was found between the immersed and dry cases when the grains are non-spherical and with a significant angularity.

Supporting and frictional forces, F_n, F_f depend upon the orientation of the supporting grains as well as the shape of the grains under consideration. In effect, these forces are determined by different bed conditions, loose, normal or imbricated packing. The usual practice in the analysis of incipient motion is to consider a statistical average representing typical conditions so that the supporting force F_n and frictional force F_f become proportional to the gravity force F_g and hence do not have to be considered separately (Gessler, 1971).

The fluid forces of lift and drag add vectorially to produce a resultant force that acts in a downstream direction (Figure 2). For fully turbulent flow over hydrodynamically rough boundaries the viscous forces F_v become negligible and are usually neglected. The resultant force may either lift the grain over the surrounding particles or rotate the grain about a pivot. In the case where motion is about a pivot, the balance is between the fluid forces acting upward in the direction of easiest movement and the gravitational component acting downward in the opposite direction. The gravitational component acts through the particle's center of gravity while the fluid forces may act at some distance above the center of gravity. Therefore, in order to determine the condition for the threshold of motion, moments (a force times

the vertical distance from the pivot) rather than forces should be used (Middleton and Southard, 1978). Incorporation of the moments introduces grain shape as an important additional parameter. Grains of the same size or weight may have widely varying ratios of the moment arms for the fluid and gravity forces. These ratios will most likely vary from one group of particles to another and have a corresponding effect in modifying the critical threshold criterion.

If the threshold of motion of individual particles is examined, atypical behavior may be expected as a result of unusual grain configurations that deviate from a statistical average. This suggests that in interpreting behavior of specific particles, it is important to determine whether the behavior is atypical and whether it has any statistical significance.

The direction of easiest movement is highly variable from grain to grain depending upon particle geometry, local packing and the degree of exposure of the particle to the flow. Various combinations are summarized in Figure 3. Only the direction of the gravity force is well defined. The restraining forces are primarily affected by the arrangements of the adjacent particles while the mobilizing fluid forces are affected by the slope and exposure of the particle. The direction and magnitude of the fluid forces arising from the effects of viscosity, lift and drag are extremely variable both spatially and temporally. Even for a uniform, steady flow, fluctuations in the magnitude of lift and drag forces occur because of velocity and pressure fluctuations.

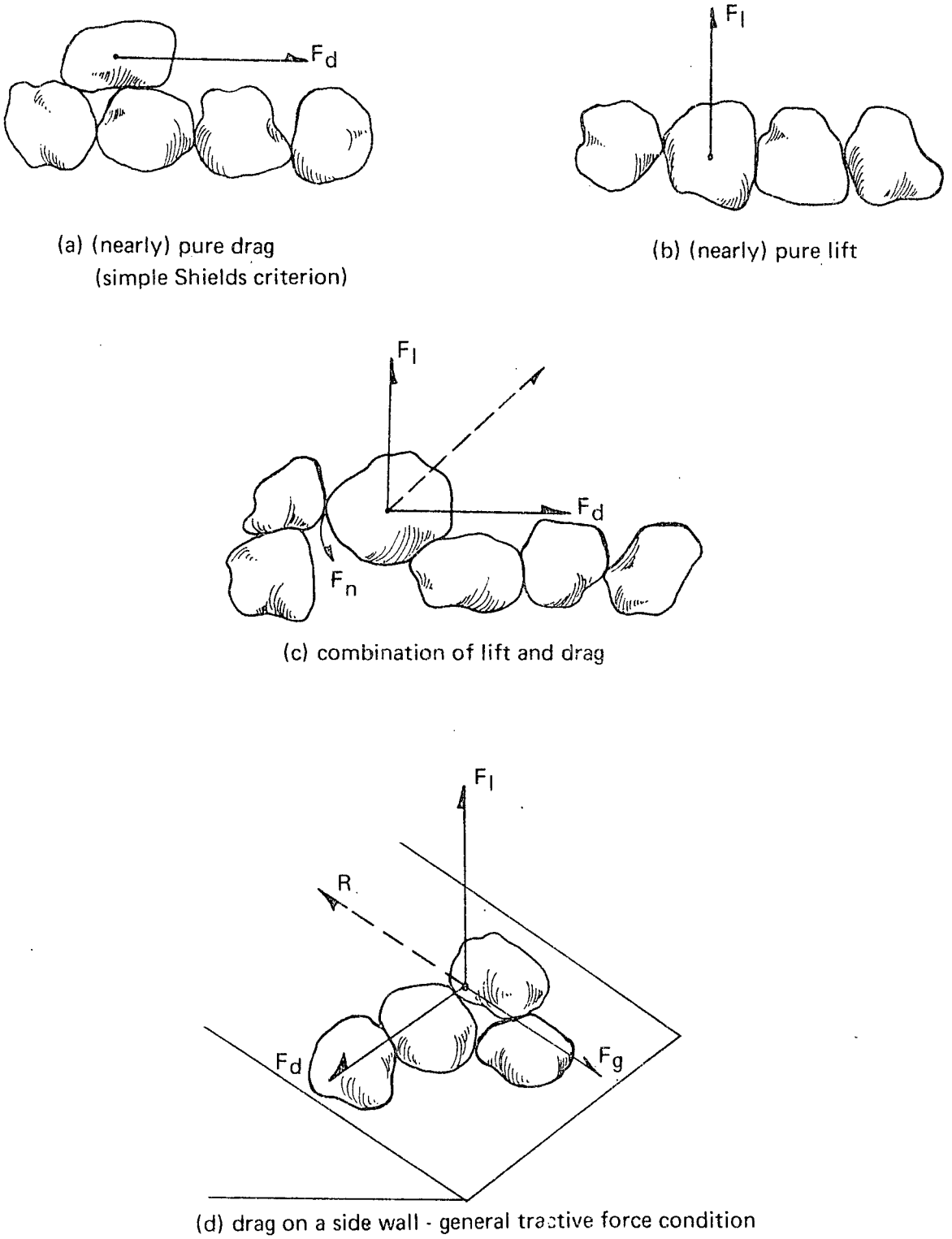

(a) (nearly) pure drag
(simple Shields criterion)

(b) (nearly) pure lift

(c) combination of lift and drag

(d) drag on a side wall - general tractive force condition

Fig. 3. Variation of net forces on a particle depending on local bed configuration and slope.

Due to the large number of grains with irregular shape and packing that are present on a typical boundary, it is not possible to determine individual values for the threshold of motion. By utilizing mean values and dimensional arguments, Shields (1936) combined the parameters of interest into a non-dimensional form now known as the Shields relation. These parameters are the density of the sediment ρ_s, grain diameter D, fluid density ρ_f, kinematic viscosity of the fluid ν, shear stress τ and the acceleration of gravity g. The parameters may be combined to give the dimensionless relationship:

$$\frac{1}{\psi} = \frac{\tau}{(\rho_s - \rho_f)gD} = \frac{\rho u_*^2}{(\rho_s - \rho_f)gD} = f\left(\frac{U_* D}{\nu}\right)$$

where U_* is the shear velocity and the dimensionless group U_*D/ν is known as the particle Reynolds number Re_*. For the threshold condition of sediment motion, the non-dimensional stress function is denoted by $1/\psi_c$ and is called the Shields criterion.

For large values of Re^*, the particles disrupt the viscous sublayer and the entrainment function assumes a constant value. This is to be expected, since in the absence of a viscous sublayer, viscosity exerts a negligible effect and the entrainment function becomes independent of Re_*. The entrainment function $1/\psi_c$ has a minimum value around 0.3 for a particle Reynolds number of about 10. (Yalin and Karahan, 1979). Around this minimum value, the grain size will approximate the depth of the viscous sublayer. As the particle Reynolds number decreases, grains are completely enveloped within the viscous sublayer and the entrainment function converges to values obtained for entrainment in a laminar flow (Yalin and Karahan, 1979).

Thus grains within a restricted size range (0.2 - 1 mm) where the particle Reynolds number conforms approximately to the minimum in the Shields function will be subjected to both a viscous drag and surface drag arising from wake shedding. In the domain where these forces may not be exclusive of each other, the additive effect may result in a minimum critical shear stress for entrainment. The minimum may also be due in part to the packing arrangements, since for fine material, co-planar packing becomes increasingly difficult and relative protrusion will be important (Fenton and Abbott, 1977).

The Shields relation is the usual criterion for the initiation of motion of particles but a number of assumptions limit its effective application. This function assumes a steady, uniform flow over a flat bed of particles that are of uniform size and shape. In particular, the difficulty posed by poorly sorted sediment becomes apparent in alluvial gravel streams that exhibit bed armoring. The beginning of particle movement however is a stochastic phenomenon that depends not only on the average fluid motions but also on the size of the turbulent deviations from the average (Yalin, 1977). Observations of flows over beds of non-cohesive sediment show that when the sediment motion begins it is unsteady and that it occurs intermittently in changing isolated patches. When the mean velocity and shear stress are increased, the frequency of movement and its intensity are seen to increase.

The random and sporadic movement of particles near the threshold suggests that the forces acting to move particles fluctuate just as velocities in turbulent flows fluctuate. These fluctuating forces, impinging on a mechanically unstable particle, may lead to the phenomenon of particle vibration.

Both the spatial and temporal characteristics of the fluctuating forces may be systematically modified by bed geometry. Wake shedding or vorticity amplification of flow around 'dominant' particles (White, 1940) may preferentially concentrate energy at specific frequencies. Isolated roughness, wake interaction and skimming flow, resulting from flow-boundary interaction, may alter the fluctuating forces on a particle sufficiently that vibratory motion occurs.

Fluctuating forces that contribute to the unsteady and intermittent particle motion may arise from two other mechanisms. Self excitation by alternate shedding of vortices from individual particles may create oscillatory forces of sufficient magnitude to initiate vibratory motion. Lastly, coherent turbulent structures within the flow may be the source of fluctuating forces of sufficient magnitude to initiate particle motion.

1.4.4 Evidence for particle vibration

The initial motion of non-cohesive materials in a fully developed turbulent flow has been noted by a number of observers, but few investigators have attempted to describe precisely the characteristic motions. Gilbert (1914), in his classic experimental studies, was perhaps the first to observe and record incipient particle motion. Descriptions of particle motion were concerned primarily with saltation although the occurrence of particle vibration was mentioned briefly. Particle vibration was observed by Shields (1936), but he made no further reference to direction of movement, frequency or magnitude.

In a study on the saltation of sand, Danel, Durand and Condolios (1953) drew attention to the characteristic trembling and quivering of particles on the bed of a live channel. Sundborg (1956) also made reference to sand particles trembling prior to entrainment while vibration of pebbles up to 20 mm in length was reported by Johansson (1963).

Bisal and Nielsen (1962) investigated incipient motion of soil grains under the influence of pressure gradients in a wind tunnel. In their study, a shallow pan containing a mixture of eroding (0.1 to 0.5 mm) and non-eroding particles (> 0.5 mm) was placed on the viewing stage of a binocular microscope and subjected to a stream of air. Wind velocities were measured with pitot tubes. As the air velocity was increased above about 5.4 ms^{-1}, particles began to vibrate. If the velocity was increased to 6 ms^{-1}, vibrating grains were seen to leave the surface instantaneously as if ejected, with few instances of particles first rolling along the surface. Bisal and Nielsen, concluding that the majority of eroding particles vibrated with increasing intensity as wind speed increased, attributed the motion to impulse forces caused by pressure fluctuations. The mode of vibration is not explicitly stated but appears to be in a horizontal plane (see their Figure 2).

To date there have been few investigations on the pressure fluctuations experienced by non-cohesive particles in water. Einstein and El Samni (1949) measured the instantaneous pressure at the top and bottom of fixed hemispheres but were unable to measure the fluctuations in the pressure difference. Although a considerable literature exists on the role of pressure fluctuations experienced by buildings and other structures in air, only recent technological

advances have allowed the measurement of instantaneous pressure fluctuations over a surface (Surry and Stathopoulos, 1978). Furthermore, caution must be exercised in making any comparison between the role of pressure fluctuations on fixed elastic structures and non-cohesive particles that are free to move.

Urbonas (1968), investigating pressure fluctuations on a particle located in a stilling basin, observed that particles on the bottom of a scour hole were in constant motion, continuously bouncing and moving back and forth on the bottom. In several instances, smaller particles remained at the upstream portion of the test hole, moving slightly back and forth but not downstream, while at other times, an apparently stable rock was observed to 'pop up' into the flow to be moved downstream. The frequency of the oscillating particles may have been quasi-periodic but the observations do not permit quantification of the phenomenon.

Based upon the observations of Bisal and Nielsen (1962), Lyles (1970) hypothesized that particle vibration was a response to fluctuating pressures and velocities caused by turbulent eddies in the flow. He suggested that the particle oscillation frequency would be related to the spectral band containing the maximum turbulent energy. Lyles, however, made no conjectures about either the mechanism producing periodic turbulent eddies or the possible role of a particle admittance frequency.

In the experiments of Lyles (1970; Lyles and Woodruff, 1971), particles placed on the floor of a wind tunnel were observed with a 12 power telescope and recorded by motion photography. The wind tunnel produced nearly uniform

flows with a slightly favorable pressure gradient (0.00029 inch of water per foot). He observed that as the mean speed approached the threshold value, some particles began to vibrate or rock back and forth. Vibrations were seldom steady; after flurries of 3 - 5 vibrations, the particles ceased vibrating momentarily before oscillating again. The average vibration frequency was determined by counting 25 vibrations observed through the telescope which, for 0.59 - 0.84 mm grains, was determined to be 1.8 ± 0.3 Hz. If the wind speed was increased considerably above the threshold, particles moved so rapidly that vibrations could not be observed. Since the oscillatory motion is very irregular and intermittent, averaging over 25 vibrations will tend to underestimate the true vibration frequency when the particles are in motion.

Using a hot wire anemometer, Lyles (1970) measured the fluctuating velocities and obtained a frequency spectrum for the longitudinal component whose peak was found to be 2.3 ± 0.7 Hz. He attributed the difference in the two frequencies to be due to the large differences in the mass density of the erodible particles and fluid rather than to a bias introduced by intermittent particle vibration.

While the particle vibration frequency is very close to the spectral peak of the turbulent kinetic energy, this correspondence does not demonstrate a causal relationship. Questions regarding the origin of the energy at a specific frequency, the energy transfer mechanism to the particle and the role of a particle admittance function need to be addressed.

Particle vibrations similar to that recorded by previous observers were

noted by Nowell (1975) in water using a narrowly graded gravel with a mean size of 30 mm, uniformly packed on the bed of a flume. The intermittent nature of particle vibration was noted. As flow velocities were increased, the number of vibrating particles increased but the frequency of vibration did not appear to alter. Further increases in flow velocity caused vibrating particles to become unstable and to be moved downstream.

Clearly the phenomenon of particle vibration in a moving fluid is real, but it remains uncertain whether vibration is due to a mechanical instability or is related to some periodic component in the turbulent flow. Both the origin of the periodic component and the energy transfer mechanism need investigation in order to determine the importance of vibration in the entrainment process.

1.5 RESEARCH HYPOTHESES

Vibratory motion of individual particles appears to be a precursor to entrainment. Static analysis of the threshold of motion provides neither an adequate description of particle behavior when subjected to random fluctuating forces nor any insight into the fluid processes that excite the particle motion. Heretofore, little attention appears to have been given to flow or bed conditions, other than packing arrangements, that may control or modify the response of individual particles to fluctuating forces.

There are several possible mechanisms whose efficacy to produce vibratory motion may be considered within hypotheses for research. These mechanisms

are mechanical instability of the particle; self-excitation arising from wakes shed from the particle; flow interaction with upstream particles through advected eddies and vorticity amplification; or random excitation by turbulent bursts. The possibility of pressure fluctuations being transmitted through the porous bed was considered unlikely and therefore not pursued further.

Rather than attempt to measure fluctuating pressure and velocity components over the surface of a particle which is itself moving, it was decided to take a more indirect approach. Since it is not known what flow-boundary parameters modify the pressure and velocity fluctuations, a phenomenologic approach was adopted where particle vibration frequencies were measured. It was hoped that this would provide sufficient insight into the flow-boundary interaction that critical experiments or hypotheses could be proposed.

Some limitations in the experimental conditions were accepted because of the primary reliance on visual observations. Use of the vibration frequency is limited by the ability to perceive motion. In some instances the amplitude of the motion was very small and difficult to count while under other conditions large amplitude motion was rather violent and easily defined. Although sophisticated methods such as strain gauges or fine suspension wires would be able to resolve the higher frequencies or lower amplitudes, the present limitations were accepted to avoid restraining or interfering with the particle motion.

1.5.1 Mechanical instability of a particle

For any regular oscillatory motion to occur, a particle must be either conditionally stable or unstable. A stable particle will exhibit no motion unless the fluid forces are sufficient to cause physical translation. Thus the relevant question is what conditions or mechanisms control the vibration frequency? For vibration to occur a mechanical instability may be a necessary but not sufficient condition.

The simplest hypothesis is that particle vibration reflects a mechanical instability driven by random fluctuations in the velocity field. The turbulent flow exhibits a range of length scales with widely varying energy densities so that the particle would respond to the length scale corresponding to the particle admittance frequency. Therefore one would not expect any specific flow structure to be associated with the motion and different particles might exhibit widely varying vibration frequencies.

The concept of an admittance frequency arises in studies of the responses of aero-elastic structures such as buildings subjected to fluctuating force fields. The mechanical admittance is the transfer function between an excitation frequency and the response. Aero-elastic structures will have a peaked admittance function (Figure 4a) corresponding to the natural resonant frequency of the structure (Davenport, 1964). The analogous transfer function for a non-elastic particle is not known and may be either a flat response (Figure 4b) or sharply peaked (Figure 4c).

In the present context it is useful to differentiate between two

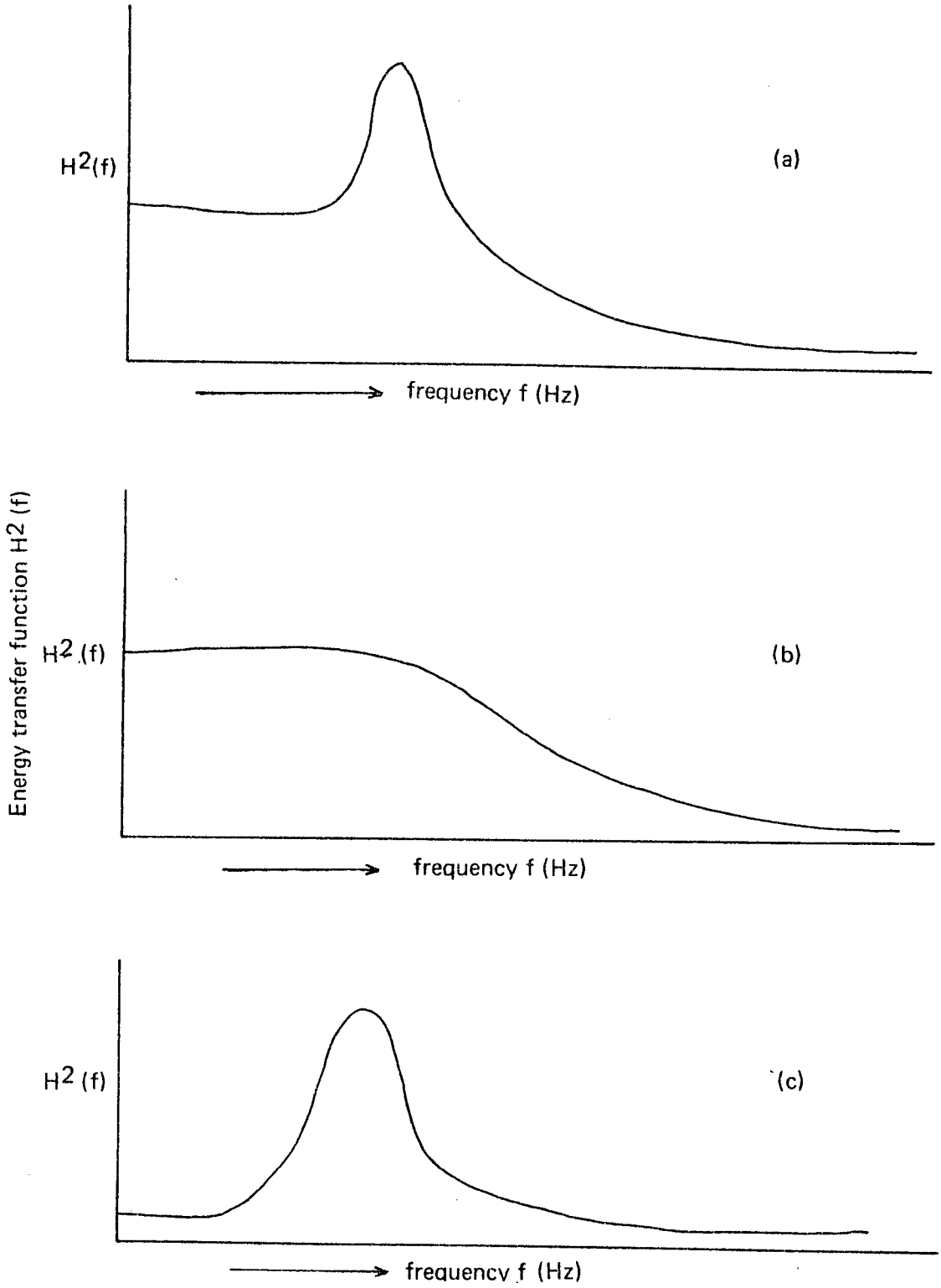

Fig. 4. Schematic diagrams of hypothetical particle admittance functions.

possible transfer functions: a broad, flat response or a transfer function with a preferential frequency response. In the former case, the vibration frequency is apt to be relatively constant for particles of differing sizes and shapes. The particle frequency should correspond to the peak in the turbulent energy spectrum. This peak is not particularly sensitive to flow depth at low Froude numbers (Nowell, 1975), so that the vibration frequency would be expected to remain relatively constant for different flow depths, some variation being expected for different bed roughness conditions.

If the energy transfer is dominated by a narrow frequency band, the particle frequency response would be essentially constant irrespective of the velocity or Froude number but varying in amplitude. Furthermore it is likely that the transfer function would be dependent on particle size and shape so that various particle sizes would exhibit quite different frequencies. The size of the particle will restrict the response to a range of flow perturbations for which $v/f \sim O(D)$.

Irrespective of the response in either case at low frequencies, the response will fall sharply for increasing frequencies since particle inertia will restrict the frequency response. Furthermore, at higher frequencies the energy density will be inadequate to initiate motion.

It is possible, however, that a transfer function is not important in controlling the mode or frequency of vibration. One possibility is that particle vibration is a response to an aerodynamic instability. In effect the particle may be able to 'fly' in the mean flow but once perturbed, the change

of attitude may destroy the lift so it subsides and then is able to take off again. Such a phenomenon would be restricted to particles of favorable shape and attitude.

A second possibility is that of a particle which is 'loosely constrained' by adjacent particles. In response to a fluid force, the particle moves and immediately collides with a nearby particle. A reduction in the fluid force would allow the particle to return toward its original position. Such behavior would not be statistically stable over an ensemble of particles.

Therefore observations that will lend support to the hypothesis of mechanical instability or its variants include the following:

a) Particle vibration should occur irrespective of the boundary configuration and presence of neighbouring particles.

b) If a particle has a flat admittance function the particle vibration frequency should correspond rather closely to the peak in the turbulent energy spectrum and not be particularly sensitive to changes in velocity and flow depth.

c) For particles whose size spans almost two orders of magnitude a similar range in particle vibration period may be expected for constant flow conditions.

d) If aerodynamic instability is an important factor, a specific shape or Zingg class may show preferential vibration.

e) Depending upon the relevance of the particle admittance function, particles responding to random turbulent fluctuations might show a considerable range in particle vibration frequencies.

1.5.2 Vibration due to self-excitation

A bluff body placed in a turbulent flow produces flow separation and the formation of shear layers in the wake downstream of the body. Downstream of the separation point, a growing vortex will be fed by the circulation from the shear layer until the vortex is sufficiently strong to draw fluid from the other shear layer across the wake. The vortex ceases to grow upon interaction with fluid of a different vorticity and the vortex is shed from the body (Gerrard, 1966). The alternate shedding of the vortices may create oscillatory forces of sufficient magnitude to initiate vibration of conditionally stable and unstable particles.

For bluff bodies, the separation point will remain essentially fixed for various Reynolds numbers. If the formation region controlled by the effective hydraulic diameter of the body is reduced, the shear layers are brought closer together, facilitating their interaction and resulting in a decrease of the shedding period (Gerrard, 1966). With increasing turbulence intensity, the shear layer will become more diffuse. With diffused shear layers, a longer time will be required for sufficient vorticity to be drawn across the wake to initiate the vortex shedding. Thus the shedding frequency should decrease (increased period) with increasing turbulence intensities.

For two dimensional bodies whose effective hydraulic diameter is very much less than the length (i.e. a long wire or cylinder), vortices are shed with a regular period (Massey, 1975). Very little work appears to have been conducted on the vortex shedding characteristics of three-dimensional bluff bodies. Random fluctuations arising from the turbulence and 'end' effects

associated with the three dimensional bluff body contribute to a more irregular vortex shedding frequency compared with that of a two dimensional body (Massey, 1975).

Therefore, if vortex shedding is the operative process creating oscillatory forces on the particle, observations that will lend support for to this hypothesis are:

a) Since the oscillatory forces causing vibration would arise from vortex shedding, vibration would be expected to occur on either smooth or rough boundaries irrespective of the presence of other bluff bodies.

b) For increasing particle size with constant flow conditions mean vibration period should increase.

c) For sufficiently small particles that subsist within the viscous sublayer, vortex shedding does not occur so these particles should exhibit no vibratory motion.

d) For large particles, a maximum size should exist above which vibration does not occur. At this scale the fluctuating forces associated with the vortex shedding are not large enough to initiate motion.

e) With increasing turbulent intensity, the vibration period might be expected to increase for a specified particle.

f) For constant flow velocities, the vortex shedding frequency should be independent of flow depth.

1.5.3 Wake interaction and vorticity amplification

The work of Leopold, Emmett and Myrick (1966), Helley (1969) and Nowell (1975) strongly suggested that particle interaction, either by wake

shedding or vortex amplification is a significant factor that may contribute to particle vibration.

Particle vibration may be a response to periodic fluctuations in the velocity-pressure field that arise due to the shedding of wakes by upstream roughness elements. For regular roughness arrays of uniform size, coherent wake shedding and interaction could result in energy being concentrated in a narrow frequency band. The length scale associated with this frequency would be expected to be smaller than the dimension of the roughness elements. For particles much larger than the length scale associated with the concentrated energy, the fluctuating forces would not be sufficiently coherent over the particle to initiate motion. For particles smaller than the appropriate length scale, the vibration frequency might be relatively constant with increasing amplitude as particle size decreases.

Downstream of the roughness elements, significant amounts of the turbulent kinetic energy are transferred to smaller scales of motion within one rotational period or turnover period (Tennekes and Lumley, 1972). This would result in a rapid decrease in the period affecting successively smaller particles at increasing distances from the roughness elements upstream.

Closely associated with the phenomenon of wake shedding is vorticity amplification. Particle vibration may be initiated in response to frequencies that are preferentially amplified by vortex stretching that occurs in the strongly diverging flow about a bluff body. The diverging flow stretches the vortices, resulting in an increase of the rotation velocity and turbulence

intensity (Sadeh and Cermak, 1972).

If either wake shedding or vorticity amplification is important in initiating vibratory motion, support will be provided by the following observations:

a) No motion should occur on either a hydrodynamically smooth or rough boundary in the absence of neighbouring upstream particles.

b) Small material (like coarse sands) is not expected to show evidence of vibration since amplified frequencies or wake interaction affects will rapidly be dominated by viscous effects.

c) There does not appear to be any reason a priori to expect a relationship between flow depth and vibration.

d) The vibration period would be expected to be a function of particle size and flow velocity.

1.5.4 Turbulent bursting

A fourth hypothesis proposes that particle vibration occurs in response to the passage of coherent turbulent structures over the non-cohesive bed material. Either the adverse pressure gradient associated with the high speed sweeps or the high-frequency, large amplitude fluctuations of the wall shear stress may be the primary mechanism initiating vibration.

On the basis of the behavior and characteristics of the turbulent structure (Section 1.4.2), the observations that would support this hypothesis are:

a) Since fluid ejection and sweeps associated with the turbulent bursts occur over both smooth and rough boundaries, particle vibration should be

present in both conditions.

b) The vibration period will be independent of boundary roughness, scaling with outer flow variables of depth and free stream velocity. Varying the flow depth or velocity will affect the vibration period.

c) For constant flow conditions all sizes of material should exhibit the same frequency of vibration. Particle size will, however, be important insofar as it affects the discrimination of burst amplitude and hence the frequency response.

d) Since the period is imposed by conditions in the outer flow, the vibration period should be independent of the position downstream of a roughness element.

CHAPTER 2 EXPERIMENTAL AND OBSERVATIONAL PROCEDURES

2.1 ASSUMPTIONS OF THIS RESEARCH

Turbulent flows may be described formally by the Navier-Stokes equations of motion (Hinze, 1975). In their most general form these equations have defied an explicit solution. In the course of the present study where a recirculating flume was used to model some of the processes that are thought to occur in natural river channels, a number of simplifications and assumptions are made about the equations of motion and general conditions. It is important to recognize these qualifications which may limit the generality of the results.

1. The flow is assumed to be two-dimensional and homogeneous in the horizontal plane. This condition may be approached by a suitable choice of width-depth ratio that will minimize side wall or bank affects. The present work, following Nowell (1975), assumes that a lower limit for the width depth ratio is approximately 6.

Recent work by Knight and MacDonald (1979) indicates that the width depth ratio necessary to ensure two dimensional flow is a function of the relative roughness. Conditions within 95% of a true two dimensional flow were found by Knight and MacDonald to occur at a width-depth ratio of ten for a high bed roughness. For comparable conditions over a smooth boundary the width depth ratio would increase to 180.

For comparative purposes, the width depth ratio was maintained near that of Nowell (1975) rather than increasing the ratio to ensure a more completely two dimensional flow. The extent of the departure from two dimensional flow was minimized by making all observations near the flume center line.

2. If the flow is strictly two dimensional, no local convergence or divergence should occur in the horizontal plane, which implies no secondary circulation. Knight and MacDonald (1979), investigating sidewall correction procedures for flow resistance in flumes, found that momentum transfer occurs across the channel implying that secondary circulation does occur. The importance of this effect is not known.

3. Flume studies of flow over distributed roughness elements provide an adequate representation of turbulent flow conditions that occur in a natural river. Nowell (1975) measured turbulence spectra in the flume and found them comparable to spectral estimates obtained from velocity profiles in the Cheekye river, a small cobble-gravel stream.

4. Gravity is the only body force affecting the motion of gravel particles.

5. The flow is assumed to be stationary, being steady and uniform along the channel. Nowell (1975), using the same flume, conducted an intensive investigation and found no detectable spatial variation in the flow. Some temporal variations however, do occur due to fluctuations in the pump rate.

6. In the course of the present work, the mean velocity measured at a depth of 0.4 d is assumed to be representative of the flow irrespective of the boundary roughness. Strict Froude number similarity is not necessary because of the moderate ($Fr < 0.5$) Froude number.

7. The present study is restricted to non-cohesive particles that occur in a normal packing condition.

8. Minimal suspended sediment was present in this study. Since the effect of suspended sediment on turbulent flow structure is unknown, this may compromise the generality of the results.

9. Turbulent bursting may be important in the flume and is a hypothesized source of the fluctuating forces causing vibratory motion of particles. In natural river systems with a high relative roughness, the turbulence generated by breaking surface waves, hydraulic jumps and chutes may overwhelm the turbulence arising from the bursting process.

2.2 FLOW CONTROL AND FLUME OPERATION

Research was conducted in a small recirculating flume 0.47 m wide and 6.1 m long. Details of the pump and tilt mechanisms of the flume are shown in elevation (Figure 5). The slope may be adjusted by two jacks located at the downstream end of the flume so that uniform flow could be obtained.

Immediately above the pump is a 25.4 cm stainless steel honeycomb baffle

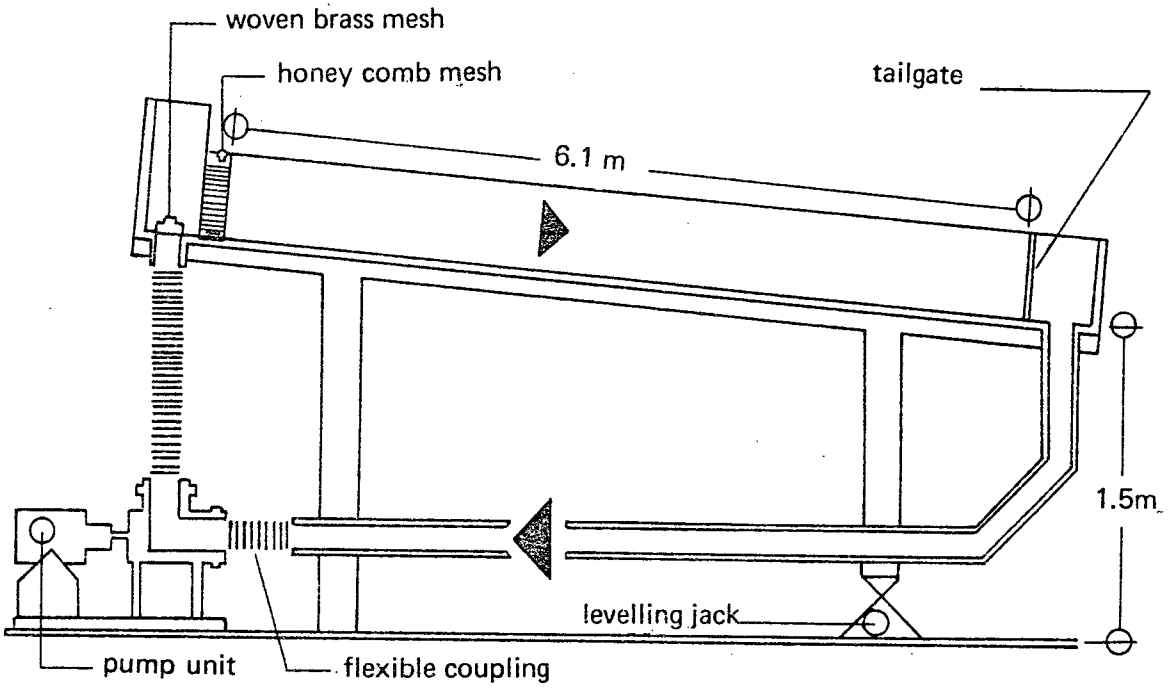

Fig. 5. Elevation view of flume at Simon Fraser University. (After Nowell, 1975).

with 2.54 cm square openings to rectify the flow. Wave action at the inlet is damped with a styrofoam float. At the downstream end, an adjustable tailgate provides fine adjustment to maintain uniform flow and isolate the vortex effect at the pipe outlet.

Uniform flow occurs when the energy gradient is subparallel to the slope of the bed so that there is no spatial variation in either flow velocity or depth. Uniform flow was obtained by adjusting the slope and tailgate. With some practice it was found that for varying bed roughness with a fixed slope, a constant, uniform mean velocity could be maintained from run to run with minor adjustments of the tailgate. Uniform flow conditions were checked by two independent methods:

a) Under operational conditions, the water depths were measured at two ports spaced 346 cm apart and adjustments made until the two depths were equal. The presence of low amplitude distortions of the free surface limits the accuracy to about one millimeter.

b) The energy gradient between two ports spaced 346 cm apart was measured using two inclined manometers. The computed differential was compared with the depth differential in still water. Low frequency fluctuations in the manometer also restricted accuracy to about one millimeter. A typical slope $s = 0.001$.

The flume walls are plexiglass with all fittings recessed to minimize side wall interference. A ground bubble machinist level straddling the flume sidewalls provided a check on the lateral level. A transverse slope would induce secondary circulation that is undesirable. Nowell (1975) made

an intensive investigation of the velocity distributions in this flume over the smooth, plane metal bed. He was unable to find any obvious pattern associated with the flume that would produce anomalous results. To ensure a fully developed flow boundary and to minimize end effects, all observations and measurements were made approximately 4 m from the inlet and 1.5 m from the tail gate.

Mean velocity was measured using a laboratory Ott current meter located at 0.4 of the flow depth on the flume center line. No adjustment was made for the change in flow conditions that resulted when the lego block concentrations were changed. To maintain consistency, the effective depth was measured from the lego baseboard when it was employed (see below, sections 2.5). To reduce the number of variables, flume slope, flow depth and water temperature were maintained as constant as possible from run to run. By holding all variables as constant as possible, the range of the Froude number was kept very small.

2.3 DEFINITION OF THE BED

2.3.1 Bed surfaces

Initial observations were made of isolated particles or packed gravel on a plane 'smooth' rigid flume boundary. Subsequent runs were made with a wake generator at fixed locations upstream of isolated particles. To eliminate or reduce slope factors, regular geometrical wake generators were used in the form of cylinders or squares. The effect of wake generator size compared with particle size was investigated using cylinders varying from

3 mm to 30 mm diameter. By varying the distance between the wake generator and the particle from 2 to 14 cm, the zone of influence of the wake shedding was observed.

Lego baseboard was fixed to the smooth flume bed to produce a regular hydrodynamically rough boundary. This allowed test runs with either a plane lego surface or with distributed roughness elements fixed in regular geometrical patterns. To remove problems associated with particle stability while resting on the lego surface, a test area was removed from the lego board so that the isolated test particle remained on the smooth bed of the flume.

To vary the effective roughness of the bed, lego blocks were distributed with different densities over the fixed lego baseboard (Figure 6). Here density is defined in terms of the ratio of plan areas of blocks to the total area. Density ranged from 1/8 to zero. Intermediate values of density were selected to correspond to values chosen by Nowell (1975, 1978), thus allowing direct comparison with his results.

2.3.2 Particle shape

In order to replicate results and make comparisons between runs using different bed configurations or roughness concentrations, 28 test particles were selected, painted and numbered. Particle sizes ranged from 11.2 mm to 40 mm. Later the number of particles was increased to include 5 - 9 mm pea gravel and coarse sand between 1 - 2 mm.

To distinguish effects attributable to shape, test particles were

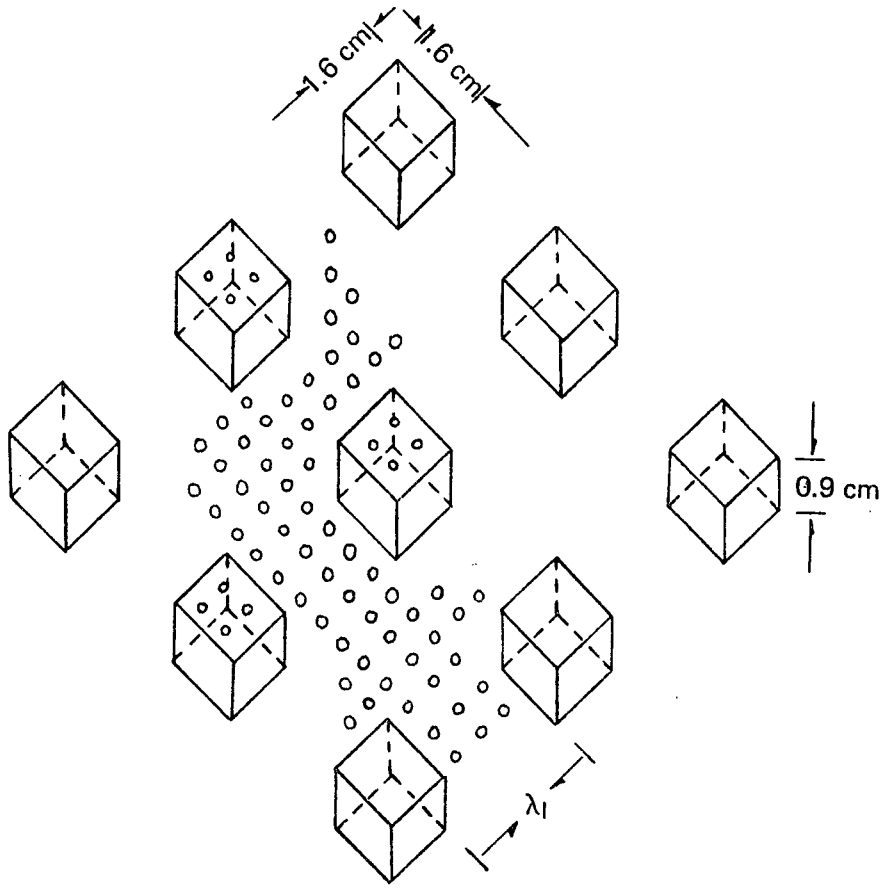

Fig. 6. Definition sketch of distributed lego block roughness elements. $3 \leq \lambda_e \leq 6$ cm.

differentiated using the classification procedure of Zingg (1935), based on the ratios of the particle axis length (Figure 7). Lengths of the three principal axes for each particle were measured and are tabulated in Table 1. This provided seven particles in each class ranging in size from 11.2 mm to 40 mm for disk, roller, blade or spherical shapes.

During observations, each test particle was oriented with the a -axis normal to the flow. Occasionally some particles would rotate to a different orientation. One run was made with the a -axis oriented at different angles to the flow to document the effects on the vibration frequency of changes in the projected area.

For some test runs, the effect of varying particle shape was eliminated by using marbles 15 mm in diameter in a close hexagonal packing arrangement on the flume bed. 'Cat's eye' marbles were found to be particularly easy to follow during oscillatory motion. Using this regular particle surface, the role of topographic lows or hollows was examined as well as particle interactions. The marbles, however, were rather difficult to use because of their pronounced instability.

Lastly, a natural, non-cohesive particulate boundary composed of sand and gravel was used. The bed configuration of the coarse material was either packed or crowded. After an hour or more of flume operation the sand had largely worked into the interstices of the coarse material creating a very stable bed.

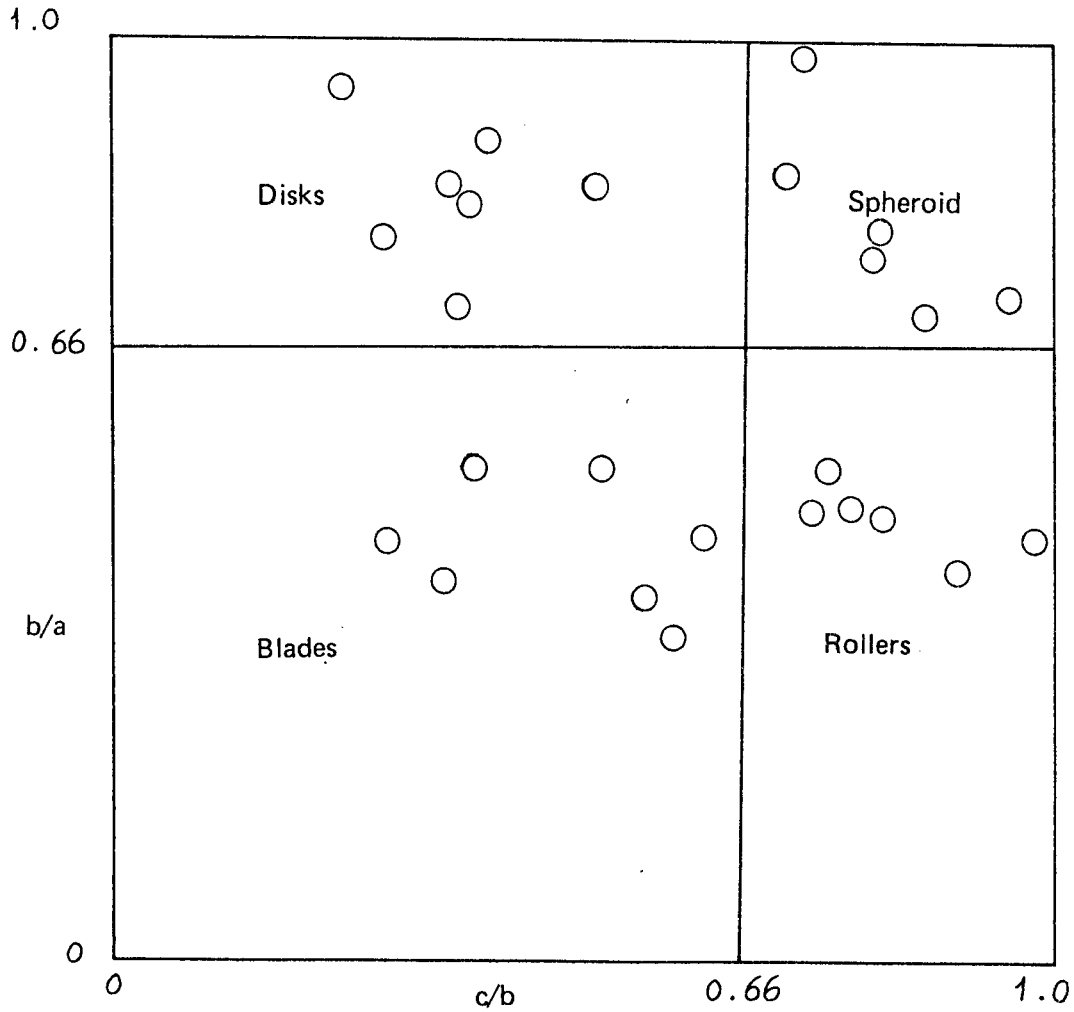

Fig. 7. Zingg diagram of test particles: a, b, c are dimensions of the principal clast axes for each particle.

Particle		1	2	3	4	5	6	7
Disks	a	26	31	25	36	31	39	48
	b	25	22	21	29	28	33	40
	c	6	8	11	8	11	12	15
Blades	a	36	42	35	39	48	46	49
	b	17	15	14	21	20	21	27
	c	5	9	8	8	7	13	14
Spheres	a	25	23	20	23	29	28	39
	b	18	16	17	23	22	22	28
	c	12	14	12	17	18	18	27
Rollers	a	28	28	31	32	29	41	46
	b	14	13	17	16	18	20	20
	c	11	13	13	12	12	16	18

Table 1. Axial dimensions (mm) of selected test particles, a,b,c are the principal particle axes.

2.4 FLOW VISUALIZATION

Flow visualization techniques in conjunction with motion photography were used in an attempt to obtain more information about the turbulent structure around individual roughness elements. Dye, aluminium powder and hydrogen bubbles were used in efforts to observe the flow structure.

2.4.1 Dye

Red food dye was injected into the flow using a 20 gauge hypodermic needle located in the bed of the flume. By varying the height of the dye reservoir with respect to the flow boundary, iso-kinetic injection could be achieved. The red dye was found to disperse rapidly in the high Reynolds number turbulent flow. In an attempt to reduce the dispersion rate, the dye was mixed with milk. Most milk available however has such a low fat content that no appreciable difference was observed.

Dye injected into the free stream dispersed so rapidly that no structure could be discerned. In order to visualize the flow structure around individual roughness elements, the injection needle was located beneath a fixed lego block that was intensely illuminated. The white lego surface provided good contrast for photography as the dye seeped from beneath and around the block. Dye seepage through gravel was not nearly so effective as it was difficult to control the location and size of the dye plume.

2.4.2 Aluminum powder and hydrogen generator

A very explicit and simple flow visualization technique involves

observation of highly reflective suspended tracer particles that are illuminated by an intense light source. The motion of fine aluminum flakes (Figure 8) used as tracer particles was photographed.

The amount of aluminum powder injected into the flow is quite arbitrary. The first visualization attempts used excessive amounts of powder making it difficult to see anything. The optimum amount of powder was found to be in the order of a teaspoon. If this quantity was injected in the outlet vortex, the aluminum would be dispersed throughout the flow in about half an hour.

Attempts were made to use a hydrogen bubble generator to place tracers in an organized pattern in the flow. This technique was largely unsuccessful due to problems associated with the optical density of the bubbles, fine particulate matter in the flume and the high Reynolds number flow over the rough boundary.

2.4.3 Visualization photography

A 16 mm Bolex camera was used to photograph the motion of the illuminated dye or aluminum powder. A close-up attachment fitted to an 86 mm lens gave a field of view of 28 by 36 mm at a minimum focal distance of 450 mm. Illumination from a 400 watt high pressure sodium light was collimated using two slits and a cylindrical condensing lens. Light losses were reduced by using reflective walls between the two slits (Figure 9). To minimize backscatter from the suspended tracer, room lights were extinguished during photography.

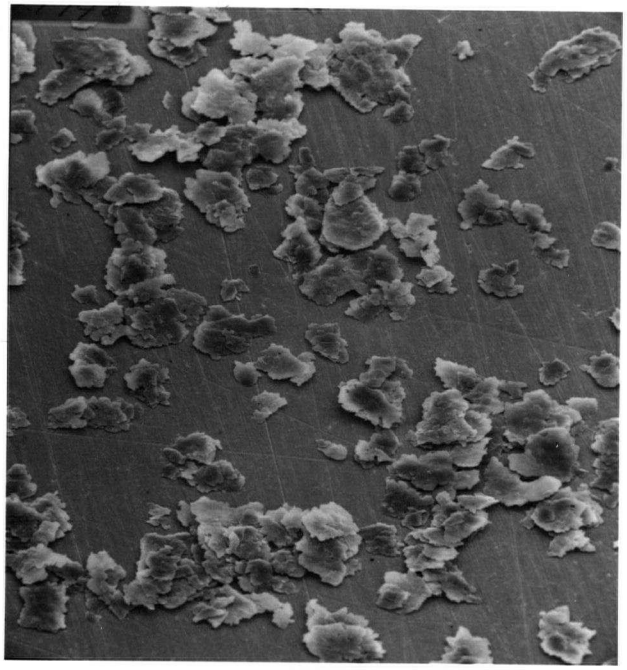

Fig. 8a. Electron microphotograph of aluminum flakes x 200.

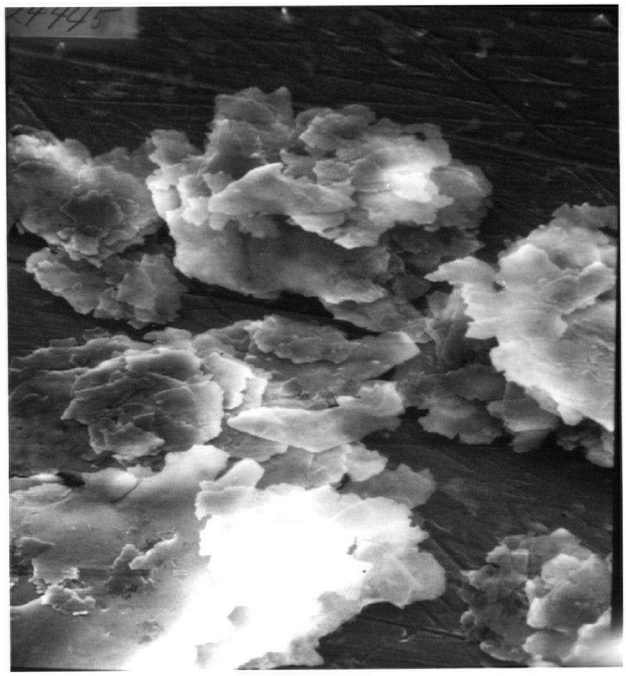

Fig. 8b. Electron microphotograph of aluminum flakes x 1000.

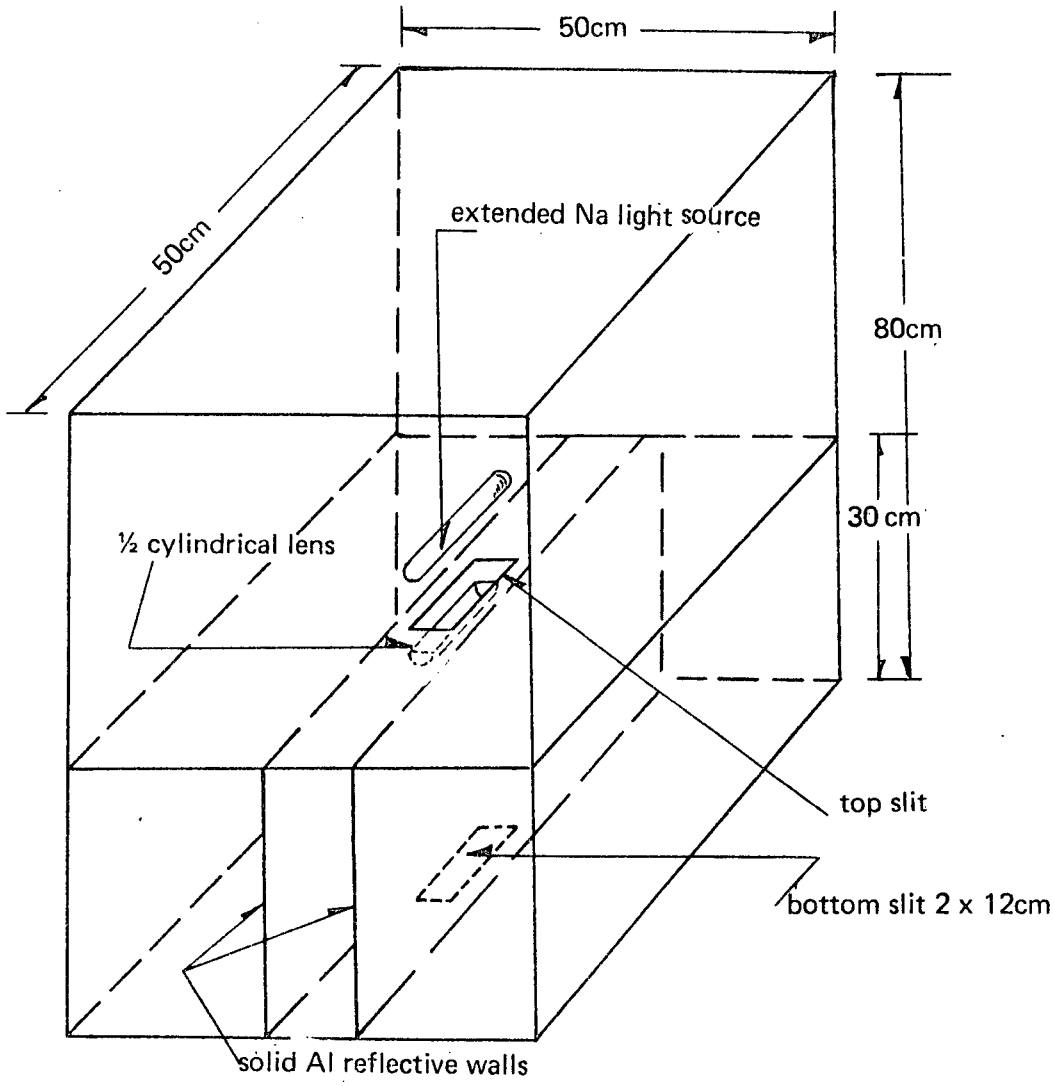

Fig. 9. Lamp housing and slit arrangement for flow illumination.

One hundred foot spools of Kodak 7278 Tri-X or 7277 4X black and white film were used for photography. Filming was done at speeds between 24 and 60 frames per second and viewed at 18 frames per second in order to slow down the motion and examine the pictures for possible coherent flow patterns.

2.5 DATA ANALYSES

The primary data in the current study consist of the vibration periods of gravel or sand of known sizes and shapes. A stable, representative value for the vibration period was obtained from 10 replications measuring the time required for 20 vibrations. That is, each individual period represents the mean of 200 vibrations. Occasionally a particle would move to a new location or orientation during a run. If seven or more replications had been made, measurements under the new configuration were not made. Ancillary data are flow depth and velocity, size and shape of particles and the bed roughness density. Prior to any statistical analysis, the data were checked for simple trends and support of inferences derived from the four research hypotheses.

Each vibration period, determined from 200 vibrations, allows the computation of a mean and standard deviation for each particle at specified roughness concentration. Within this set of data, significant variations in the vibration period within a roughness density as well as between different roughness densities were examined using a two-way cross-classification analysis of variance (Snedecor and Cochran, 1967). This provided information on the statistical significance of particle size and shape as well as the

roughness density.

By maintaining a fixed roughness concentration with the same group of particles, the role of flow depth and Froude number for a fixed threshold velocity can be examined. By differentiating on the basis of particle size and flow depth, a two-way cross classification analysis of variance was used to examine the statistical significance of the change in vibration period with flow depth.

For constant flow conditions at a specified roughness density, the influence of particle location was examined. To determine whether the mean vibration periods were identical, Duncan's New Multiple Range Test (Larkin, 1976) was used. For all statistical tests the level of significance was fixed at $\alpha = 0.05$.

Assuming that the flow depth d is an adequate approximation to the boundary layer thickness δ for depth limited flows and that an estimate of the free stream velocity U_∞ can be obtained from the mean velocity u, a non-dimensional period incorporating the vibration period T can be obtained. This non-dimensional period was plotted with the appropriate value of the momentum thickness Reynolds number and compared with the data of Rao, Narasimha and Badri Narayanan (1971) and Blinco and Simons (1975) for burst frequencies normalized with outer flow variables.

CHAPTER 3 EXPERIMENTAL RESULTS AND OBSERVATIONS

3.1 INITIAL OBSERVATIONS OF PARTICLE MOTION

Initially, observations were made of the motion of rocks 11.2 - 25 mm in diameter placed loosely on the bed of the flume. Mean flow velocity, depth and roughness characteristics were noted as well as the stability of various particles. As the flow velocity was gradually increased, randomly located particles were seen to vibrate intermittently. Both the number of particles moving and the frequency of vibration increased as the flow velocity increased. In order to obtain a stable vibration period, ten measurements were made using an electronic timer to measure the time required for 20 successive vibrations or oscillations.

Limitations imposed by flume operations prevented an increase in the flow velocity to a general threshold condition. The significance of this can be partially understood when the distribution of vibrating rocks is examined. For a typical run, six rocks may vibrate in the 2.6 meter section with uniform flow while the 0.8 meter end section subject to accelerating flow would have eight vibrating rocks. Increasing flow depth with constant slope and flow velocity resulted in fewer vibrating rocks. For the modified conditions, the mean basal shear stress increases, yet fewer vibrating rocks were observed. This may suggest either that mean values of the shear stress are not a useful index of vibratory motion or that unstable rocks susceptible to motion were quickly moved to more stable positions and exhibited no subsequent motion.

The vibratory motion of an unrestrained particle may variously be described as a rocking or flutter-like movement. The characteristic vibration of sand sized material has previously been described (Danel, Durand and Condolios, 1953; Sundborg, 1956) as a trembling or quivering motion. Descriptive terminology such as rocking or fluttering does not imply a specific operative process such as a lift or drag mechanism. Rather, this description reflects a perceived motion that is constrained by particle shape and orientation as well as support and pivot point location.

The persistance and character of the motion will be a function of the duration and magnitude of the impulsive forces modified by particle packing and geometry. A flat, blade shaped particle may be subjected to periodic forces that create a turning moment. The ratio of the axes or shape as well as pivot and support point locations may restrict the response so that motion is perceived as a flutter rather than a rocking motion.

Particle vibratory motion is not regular but is characteristically very intermittent. Motion often occurs as a flurry of movements followed by quiescent periods of irregular duration. In order to obtain a meaningful, stable value for the vibration period, 10 replications of the time required for 20 vibrations were measured. This permits computation of a mean period for one vibration and an associated standard deviation. Inter-movement times were frequently extremely brief and difficult to measure while at other times were of prolonged duration. Due to difficulties in obtaining consistent measures of the inter-movement time, it was not measured.

Some gravel sized particles exhibit a well defined vibration frequency with little variability in the amplitude of motion. Close observation of other particles however, discloses the existence of a low amplitude 'high' frequency vibration. In practice, vibrations whose period was less than 0.5 seconds ($f > 2$ Hz) were difficult to count visually and were considered 'high' frequency compared with periods of 1 - 5 seconds or more that constitute the low frequency motion. This higher frequency component appeared more prevalent while observing larger particles, although several smaller test particles were also observed to exhibit some 'high' frequency motion. In an attempt to be as consistent as possible, small amplitude motions that were barely perceptible were not counted.

This procedure introduces the subjective nature of the amplitude discrimination involved in counting vibration frequencies. The apparent difference in relative amplitudes of the high and low frequencies may arise from the superposition of two distinct mechanisms. Frequencies larger than 2 Hz might be a response to broad-band turbulence at the appropriate admittance frequency. Variations in the threshold of motion of individual clasts as well as particle inertia will introduce variability in the frequency and amplitude of motion.

3.2 TEST PARTICLES

3.2.1 Isolated particles

Observations were made of the vibratory motion of isolated gravel particles located on either a hydrodynamically smooth or rough rigid boundary. Keeping

a constant slope and a flow depth of approximately 8 cm, flow velocity over the smooth boundary was gradually increased. For conditions near the threshold, isolated particles were observed to exhibit low amplitude vibratory motions that were often difficult to count. Only small increases in velocity above that required to initiate vibration would result in the physical translation of the particles by sliding along the smooth bed. For some particles, the vibration was barely discernable and could not be counted. In general, motion occurred for velocities considerably below normal threshold values. This is likely a consequence of the low coefficient of friction for the immersed particles and the unusual exposure to mean drag for particles resting on the metal surface as well as the absence of restraint normally imposed by neighbouring particles.

Maintaining the same slope and flow depth, a velocity of 0.43 ms^{-1} was established over the lego baseboard. By removing a test section on the flume centerline, particles would sit on a smooth surface with easily replicable support conditions. The exposed surface was 12 cm long and 5 cm wide, located 4 meters downstream from the flow inlet. The vibration of the isolated test particles was observed to be more general and of larger amplitude by comparison with the smooth boundary results. Test particle vibration frequencies for a flow depth of 8 cm and mean velocity of 0.43 ms^{-1} over smooth and rough boundaries are presented in Table 2.

Generally, for a constant flow velocity, larger particles exhibited lower amplitude vibratory motions compared with smaller particles, while vibration frequency showed less variability. Several particles, notably

Particle	Smooth Metal Surface		Plain Lego Surface		Roughness Density 1/48		Roughness Density 1/16		Roughness Density 1/12		Roughness Density 1/8	
	$\bar{T}$	σ	$\bar{T}$	σ	$\bar{T}$	σ	$\bar{T}$	σ	$\bar{T}$	σ	$\bar{T}$	σ
D1					1.10	0.28	3.16	0.54	1.30	0.24		
D2			1.15	0.23	1.05	0.11	1.18	0.09	1.15	0.12	1.05	0.09
D3			1.13	0.14	1.52	0.20	1.24	0.12			1.28	0.20
D4									1.01	0.08		
D6			1.40	0.23	1.15	0.11	1.33	0.10				
D7					1.32	0.16	1.59	0.29	2.63	0.45	1.32	0.21
B1			1.04	0.13	0.99	0.08	0.90	0.10	1.16	0.10	1.08	0.04
B3			1.04	0.11	1.57	0.06	1.28	0.21	1.02	0.24		
B5	1.29	0.17			1.71	0.33	0.84	0.07	1.67	0.12	1.47	0.14
B6			0.98	0.10	2.24	0.58	1.12	0.09	1.98	0.29	1.30	0.09
B7			1.15	0.06	1.55	0.26	1.31	0.08				
S1			1.31	0.11	1.61	0.25	1.28	0.12				
S2			1.55	0.16	1.29	0.13	1.39	0.37	1.78	0.72		
S3	1.41	0.22	1.89	0.34	1.65	0.41	1.63	0.49	1.62	0.21	1.91	0.15
S4			1.42	0.19								
S5			1.56	0.26	1.61	0.32			1.98	0.42	1.90	0.23
S6			1.37	0.22								
S7			1.74	0.41			1.46	0.22	2.07	0.36	1.77	0.18
R1			1.38	0.19	1.15	0.11	1.38	0.25	1.53	0.08		
R2	1.37	0.27	1.56	0.24	1.45	0.15	1.21	0.07	1.69	0.27	1.35	0.17
R3			1.18	0.06	1.22	0.17	2.18	0.14	1.39	0.27		
R4	1.53	0.25	1.18	0.06	1.52	0.35	1.68	0.44	1.70	0.27	1.25	0.27
R6			1.71	0.09	1.27	0.36	2.85	0.46	1.44	0.10		
R7			1.74	0.14	2.25	0.57	1.57	0.27	2.66	0.67		

Table 2. Summary of mean vibration period (secs) over smooth and hydrodynamically rough (lego) surfaces.

D5, B4 and R5 were very stable and exhibited little or no vibration for any flow condition. For sufficiently large flow velocities these particles either flipped or slid along the flume bed.

3.2.2 Particle orientation

Particle orientation was found to be a significant factor influencing both the susceptibility to motion and the vibratory frequency. Previous investigators have found that particles larger than sand in alluvial deposits are generally arranged with the major (a) axis normal to the flow (Middleton and Southard, 1978). This provided the rationale for orienting particles with the a axis normal to the flow during the present study. As the axis of the particle was rotated from a normal to parallel orientation, the vibration period increased (Table 3). For parallel orientation, the particles were usually completely stable if the flow conditions remained constant.

3.3 PARTICLE INTERACTION

The existence of interaction effects has previously been suggested by other workers (Leopold, Emmett and Myrick, 1966; Helley, 1969; Nowell, 1975). For particles located on a smooth boundary, the amplitude of vibration appeared to be modified by the presence of other particles in the upstream neighbourhood. For a specific flow condition, a particle might not exhibit vibratory motion while the introduction of an upstream wake generator would frequently result in vibration.

Although irregular shaped gravel clasts upstream of a test particle

Particle B3	Time required for 20 vibrations (seconds).												$\bar{T}$	σ
a axis 90°	19.8	19.7	19.0	19.8	22.3	20.7	18.7						1.00	0.06
a axis 60°	30.1	34.7	52.9	53.4	32.9	58.8	44.2	39.2	46.1	44.1			2.18	0.48
a axis 30°	145.0	161.0	198.0	159.0	191.0	187.0	163.0	169.0					8.58	0.92
a axis 0°	No discernable motion.													
Particle R7														
a axis 90°	32.2	46.6	57.6	39.6	55.1	69.6	70.6	55.0					2.66	0.67
a axis 60°	50.9	79.8	64.6	80.1	66.4	70.9	64.3	91.2					3.55	0.62
a axis 30°	124.4	171.3											7.39	
a axis 0°	Stable													
Particle B5														
a axis 90°	34.4	29.3	36.7	33.9	31.2	34.7	33.1	30.9	34.6	35.7			1.67	0.12
a axis 45°	27,6	34,5	24,3	30.6	29.3	27.2	25.3	25.7	33.9	27.8	34.1	30.8	1.46	0.18
a axis 0°	Stable													

Table 3. Variation of particle vibration period with changing particle orientation. Flow depth 8 cm, mean velocity $\bar{v} = 0.44\ ms^{-1}$, roughness density 1/12.

could be used to study the interaction effects, regular geometric blocks and cylinders of different sizes were selected. This provided uniform, replicable conditions for comparison. Such a configuration may approximate the condition that may exist when a clast is located immediately downstream of a 'dominant' roughness element (White, 1940).

By placing either a disk, roller or blade shaped particle at varying distances downstream of a wake generator, interaction effects were investigated. Spherical particles were found to be so unstable on the smooth boundary that translation rather than vibration usually occurred. Wake generators whose diameter was much less than the test particle were found to be ineffective in modifying particle behavior. For those particles that did vibrate, the frequency and amplitude generally decreased with increasing distance downstream from the wake generator (Figure 10 a,b,c). In figure 10 a,b,c the non-dimensional distance is obtained by dividing the measured distance between the wake generator and particle by the diameter of the wake generator.

If a clast was located immediately adjacent to the wake generator (within one diameter distance), it usually exhibited no vibratory motion. In some instances, as the separation distance increased, the vibration period decreased before increasing sharply with larger separation distance.

All of the runs using a wake generator were made with flow velocities below the threshold of motion. The present results suggest that interaction effects may be important in modifying the threshold of motion. At increasing separation distances, the interaction effects become negligible. This is in

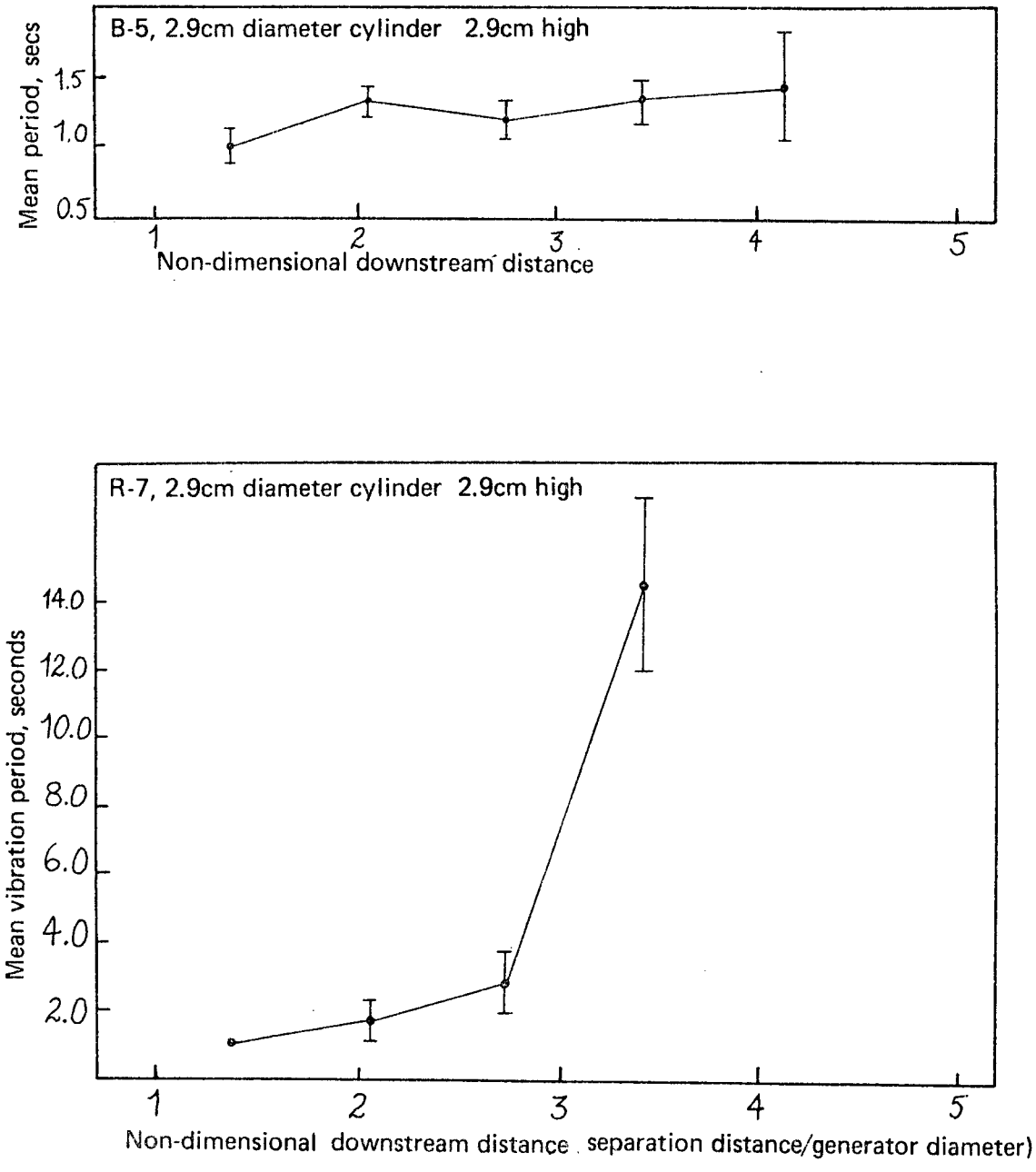

Fig. 10a. Variation of vibration period with increasing distance downstream from a wake generator.

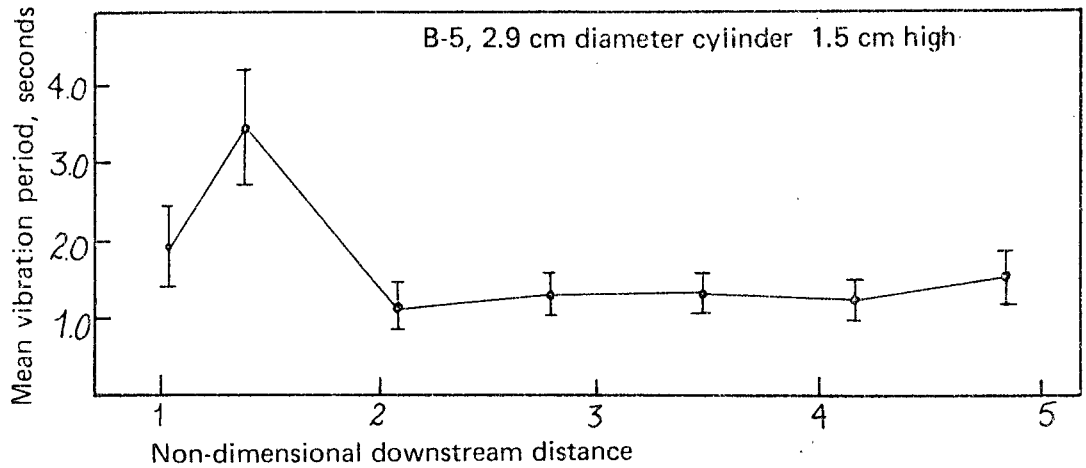

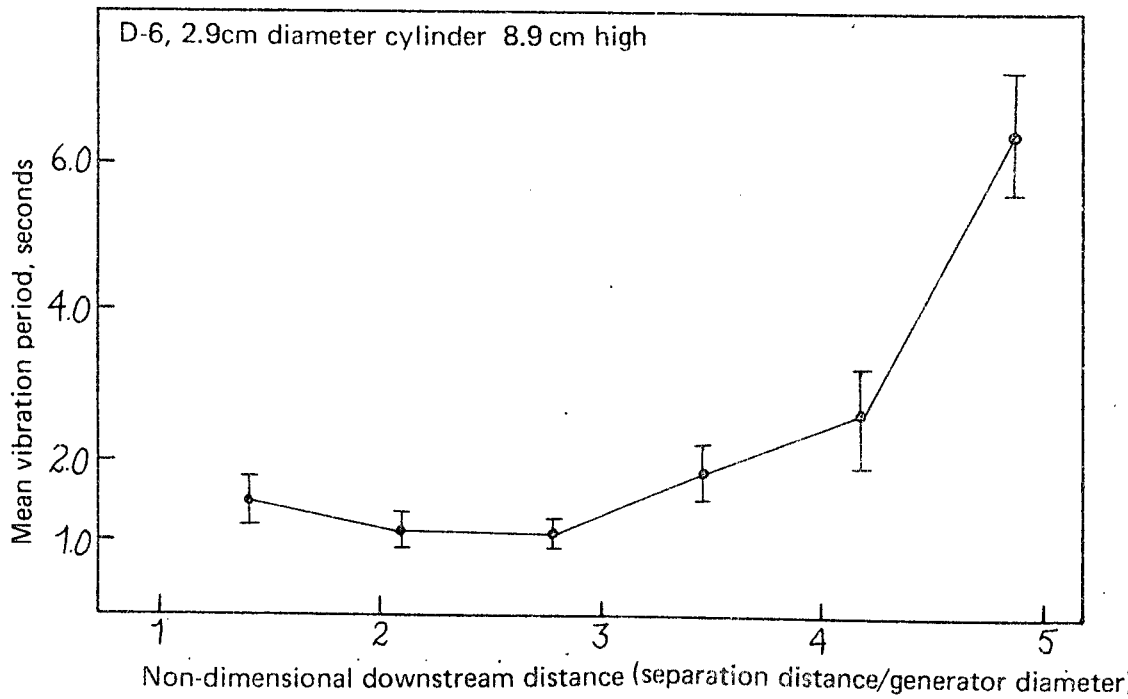

Fig. 10b. Variation of vibration period with increasing distance downstream from a wake generator.

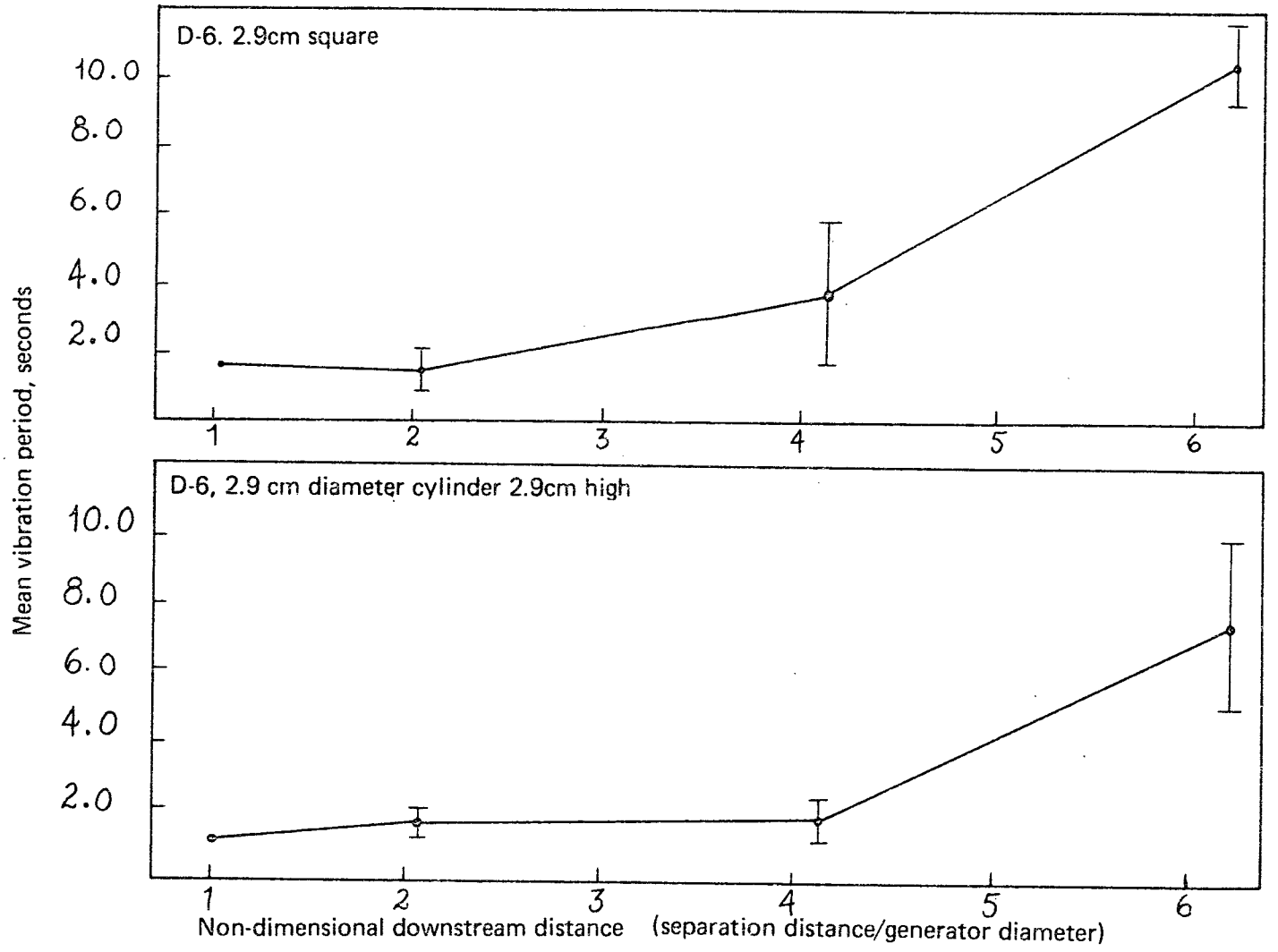

Fig. 10c. Variation of vibration period with increasing distance downstream from a wake generator.

accord with the findings of Leopold, Emmett and Myrick (1966), that interaction is negligible for spacings greater than about 8 diameters.

3.4 DISTRIBUTED ROUGHNESS ARRAYS

Nowell (1975) used lego blocks fastened to a lego baseboard to investigate the effects of distributed roughness concentration on the turbulence characteristics. Differences between isolated, wake interaction and skimming flows (Morris, 1955) arising from different roughness concentrations may appreciably alter particle response and vibration frequency. Differences may also arise resulting from interaction effects between particle size and shape and flow conditions arising from the roughness concentration.

3.4.1 Variation of vibration period within a roughness concentration

For each array of distributed roughness elements, the test particle was placed with the a axis normal to the flow on the test area, approximately in the location of the missing array element. For comparative purposes the slope, flow depth and mean velocity were kept as constant as possible from run to run. For each test particle, ten replications of the period required for 20 vibrations were measured. These are tabulated for each roughness concentration in Appendix I. The mean period of each particle at a specified roughness concentration is summarized in Table 2.

While no specific trend in the particle period at a selected roughness density is apparent, statistical tests of the range of mean values indicate that the periods are not drawn from the same population. Duncan's New

Multiple Range Test (Larkin, 1976) was used to test two hypotheses:

a) The measured periods determined within a roughness density were not identical.

b) Measured periods for each Zingg class (disk, roller, etc.) within a roughness density are drawn from the same population. Using a level of significance $\alpha = 0.05$, both hypotheses were rejected for each roughness density and all Zingg classes within each roughness concentration. This implicates particle size as a significant factor. In particular, the period for several larger particles - D7, S7 and R7 is slightly longer than average, which probably reflects the larger threshold forces necessary to initiate motion. Several of these particles exhibited higher frequency, low amplitude motion superimposed on the lower frequency motion. This motion was particularly difficult to discern and count consistently, so omission of the high frequency component may partially account for some of the frequency variation.

3.4.2 Variation of particle frequency between roughness concentrations

The mean period for the test particles in each roughness concentration are summarized in (Table 2). No consistent pattern is evident. Duncan's New Multiple Range Test (Larkin, 1976) was used to test whether the means for a specific particle at different roughness densities were identical. The hypothesis was rejected for all particles except D2 for a significance level of $\alpha = 0.05$.

Plotting the grand means and standard deviation for each roughness density - (Figure 11) shows a trend that peaks for a density of 1/12. While the overall trend is not significant, it does suggest that roughness

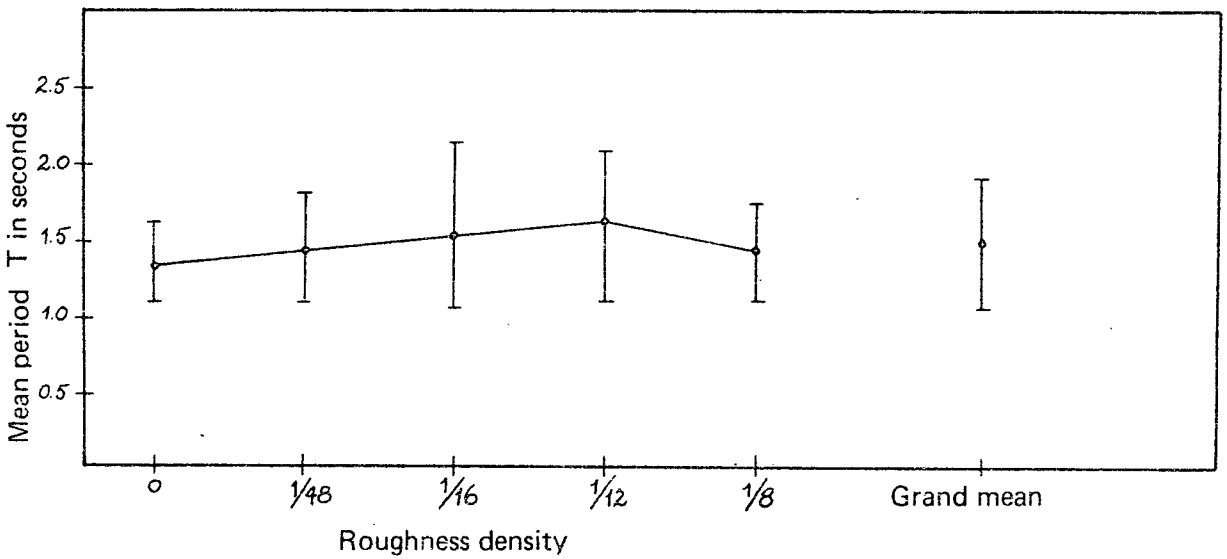

Fig. 11. Trend of mean vibration period for changing roughness density.

concentration modifies the particle vibration frequency.

The distribution of the variance was investigated using a two-way cross-classification analysis of variance (Snedecor and Cochran, 1967). The period variation for those particles where the data are complete, irrespective of the Zingg class (Table 4), for a restricted data set of common particle shapes (rollers) (Table 5), were examined using a two-way ANOVA test.

Particle size, roughness density and interaction effects were found to be significant for both data sets. A similar analysis to examine the distribution of variance between particle size and particle shape (Table 6 a, b) for a constant roughness density suggests that shape is an additional factor modifying the vibration period.

The present results indicated that particle size, shape, roughness density plus interaction effects individually contribute to variations in the vibration frequency. Besides the role of particle orientation, additional significant variation may have been introduced because mean velocity was measured at 0.4 of the flow depth as measured from the lego baseboard, irrespective of the roughness density. Disregarding particle shape, three different mean periods can be distinguished on the basis of particle size. For those particles less than 16.5 mm, 16.5 - 24 mm and greater than 24 mm, the mean period of vibration is 1.32, 1.52, and 1.78 seconds respectively.

3.4.3 Role of particle position

While examining the effects of a wake generator upstream of a particle,

Source	df	Sum Squares	Mean Square	F Calc.	F Tab. $\alpha = 0.05$
Total	445	55081.86			
Variation Among	47	35454.22			
Roughness Density	3	1751.05	583.68	11.84	2.62
Different Particles	11	21427.51	1947.96	39.50	1.81
Inter-action	33	12275.66	371.99	7.54	1.49
Residual	398	19627.64	49.32		

Table 4. Results of two-way cross classification ANOVA to investigate distribution of variance. Particles used were D2, B1, B3, B6, S2, S3, R1, R2, R3, R4, R6 and R7 for roughness densities 0, 1/48, 1/16, 1/12.

Source	df	Sum Squares	Mean Square	F Calc.	F Tab. $\alpha = 0.05$
Total	222	29300.32			
Variation Among	23	22570.35			
Roughness Density	3	323.17	107.72	3.19	2.65
Particle Size	5	12214.43	2442.89	72.23	2.26
Inter-action	15	10032.75	668.85	19.78	1.74
Residual	199	6729.97	33.82		

Table 5. Summary of results for two-way cross classification ANOVA to investigate distribution of variance. All particles were rollers of different sizes (R1 - R7) for roughness density of 0, 1/48, 1/16 and 1/12.

Source	df	Sum Squares	Mean Square	F Calc.	F Tab. $\alpha = 0.05$
Total	147	12256.01			
Among	15	3593.45			
Particle Shape	3	958.28	319.43	4.87	2.68
Particle Size	3	914.83	304.94	4.65	2.68
Inter-action	9	1720.34	191.15	2.91	1.95
Residual	132	8662.56	65.63		

Table 6a. Summary of two-way ANOVA to investigate the distribution of variance within Zingg Classes. Classes are separated into disks, blades, spheres and rollers. Roughness density of 1/48.

Source	df	Sum Squares	Mean Square	F Calc.	F Tab. $\alpha = 0.05$
Total	192	28531.17			
Among	19	23542.05			
Particle Shape	3	4460.36	1486.79	51.55	2.66
Particle Size	4	3840.12	960.03	33.29	2.42
Inter-action	12	15241.57	1270.13	44.04	1.81
Residual	173	4989.12	28.84		

Table 6b. Summary of two-way ANOVA to investigate the distribution of variance within Zingg classes. Roughness density of 1/16.

it was observed that separation distance was a significant parameter. Chen and Roberson (1974) have shown that the distribution of Reynolds stress rapidly decreases for increasing distance downstream of a roughness element.

During the runs using distributed roughness arrays of lego blocks, the unconstrained particle was located at a site corresponding to the missing element in the array. In order to determine whether the location was important, the vibration frequencies for a variety of test particles were measured at a distance ranging from 4 to 12 cm downstream of an element in the array.

Of the seven test particles investigated (Table 7), only D6 and S7 exhibited much of a variation in vibration period from one location to another. The difference may arise from an aberrant run or reflect the influence of particle size. Making a comparison at a density of 1/12 is unfortunate since this is the optimum roughness configuration (Nowell, 1975) which probably has a uniform turbulence level downstream of the roughness elements. The possibility remains that the vibration period depends on location downstream of a roughness element (Nowell, 1975) at other roughness densities.

3.5 CHANGING FLOW PARAMETERS

For depth limited turbulent boundary layer flows, the presence of a free surface restricts the vertical scale of motion and redistributes energy from the vertical component to the horizontal downstream and cross stream

Particle	Distance cm	$\overline{T}$ secs	Standard Deviation
B3	2	1.02	0.24
	6	1.07	0.13
	8	1.20	0.33
	12	1.12	0.30
D3	2	1.25	0.19
	6	1.15	0.09
	10	1.12	0.12
S4	2	1.12	0.18
	6	0.98	0.11
	10	1.08	0.22
R3	2	1.32	0.11
	6	1.39	0.27
	10	0.84	0.05
B7	6	1.17	0.18
	10	1.32	0.11
D6	6	2.17	0.57
	10	1.12	0.13
S7	2 - 4	1.15	0.15
	6	2.07	0.36
	10	1.11	0.12

Table 7. Variation of particle vibration period with changing distance downstream of roughness elements. Density 1/12, d = 8 cm., v = 0.45 ms^{-1}.

velocity components via the pressure-velocity correlation. For a constant mean velocity, a change of length scale in the turbulent flow should also result in adjustments to the temporal scales of motion within the flow.

Maintaining a constant flume slope with a roughness concentration of 1/12, the role of flow depth in constraining length and time scales was examined. Using an almost constant mean flow velocity (0.40 - 0.42 ms^{-1}) depths of 5, 8, and 20 cm were used while observing the motion of individual test particles. Data for these runs are presented in (Table 8).

Although only a small number of test particles was used during the runs at 5 and 20 cm flow depth, it is evident that the particle vibration period is strongly correlated with flow depth. For flow depths of 5, 8 and 20 cm, the mean periods of vibration were 0.94, 1.61 and 2.63 seconds respectively (Figure 12).

Both lower and upper bounds on the available flow depth resulting from flume dimensions and the difficulty of resolving differences in vibration frequencies permitted only three different flow depths. A two-way cross-classification ANOVA of the vibration periods measured for flow depth of 8 and 20 cm suggest that flow depth as well as particle shape and interaction affects are important (Table 9). A similar statistical analysis was not made for the periods measured when the flow depth was 5 cm because of the small sample size with two values listed as less than one second.

Flow Depth	Mean Velocity	Mean Period	Standard Deviation
5 cm	0.40 ms^{-1}	0.94 secs	0.11
8 cm	0.42 ms^{-1}	1.61 secs	0.54
20 cm	0.42 ms^{-1}	2.63 secs	0.60

Table 8. Variation of mean vibration period for constant roughness density of 1/12 and variable flow depth.

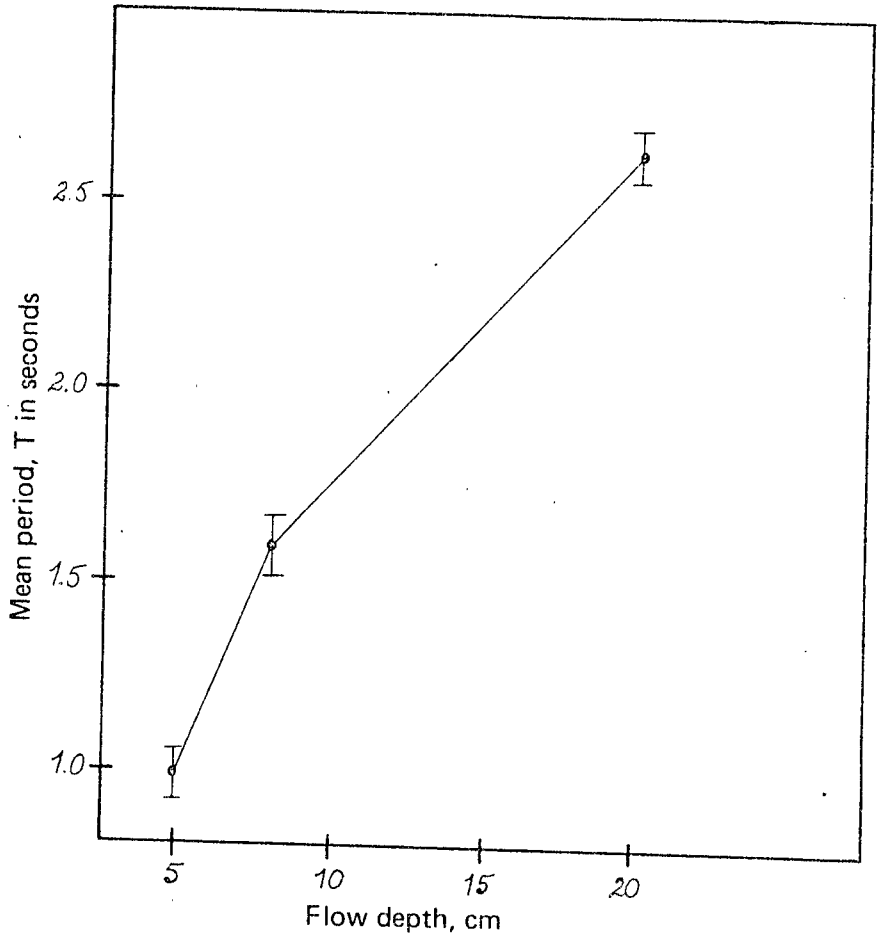

Fig. 12. Variation of mean vibration period with changing flow depth, flow velocity approximately 0.42 ms^{-1}.

Source	df	S.S.	M.S.	F calc	F tab $\alpha = 0.05$
Total	134	33201.38			
Among	11	25095.08			
Flow depth	1	17440.66	17440.66	264.65	3.92
Particle	5	6001.29	1200.26	18.21	2.29
Interaction	5	1653.13	330.63	5.02	2.29
Residual	123	8106.30	65.90		

Table 9. Two-way ANOVA for particle vibration period and flow depths of 8 and 20 cm.

3.6 PARTICLE SIZE AND DISTRIBUTION

Observations of particle vibration frequency in distributed roughness arrays were restricted to particles ranging in size from 11.2 to 45 mm. In order to investigate more closely the role of particle size, the behavior of 1.2 mm coarse sand and 5.6 - 11.2 mm pea gravel was examined. Additional observations used marbles to eliminate shape factors while mixtures of sand and gravel in varying proportions modeled more closely natural conditions.

3.6.1 Motion of sand

Maintaining a constant flow depth of 8 cm, the mean velocity was reduced to 0.27 ms^{-1} over the coarse sands. A large number of sand grains were observed to vibrate but it was extremely difficult to obtain a stable average period. The relatively large number of moving sand grains within the field of view made it very difficult to concentrate on one grain. This was accentuated by the small size of individual grains and the high frequency of particle motion. Seldom would a sand grain remain in one location long enough to record five successive replications, let alone ten replications of 20 vibrations. Calculations indicate that threshold flow conditions existed for particles about 1 mm in diameter. Only one reliable determination of particle vibration with a period of 1.08 seconds (Table 10) was obtained. Other particles had similar vibration periods of about one second.

3.6.2 Motion of pea gravel

Individual gravel particles ranging in size from 5.6 to 11.2 mm diameter

Particle	Time for 20 vibrations											$\bar{T}$ secs	σ
1.0-2.0 mm Sand	18.8	24.6	23.0	17.8	15.2	27.3	17.9	22.3	25.5	21.8	23.8	1.08	0.19
Pea Gravel	41.5	42.2	31.0	46.5	38.9	27.0	26.8	27.8	33.7	30.3		1.73	0.36
	32.6	25.1	30.7	22.8	33.0	24.4	34.8	21.9	19.0	22.4		1.33	0.28
Roller	23.0	20.8	27.8	32.5	24.8	35.8	24.9	30.3	21.9	24.3		1.33	0.24
Disk	19.3	24.7	21.8	24.0	16.8	24.2	19.9	17.0	23.1	25.7		1.08	0.16
Sphere	18.6	17.0	17.1	18.9	20.2	24.2	17.8	19.0	17.4	22.5		0.96	0.12
Disk	18.8	27.3	25.6	19.4	23.8	21.2	31.5	32.0	-	-		1.25	0.26
Blade	17.0	14.6	16.8	17.0	18.3	21.4		Very unstable				0.88	0.11

Table 10. Particle vibration period for sand (1.0 - 2.0 mm), $v = 0.274\ ms^{-1}$, and 5.6 - 11.2 mm pea gravel, roughness density 1/12, d = 8 cm, $v = 0.44\ ms^{-1}$.

were observed in a distributed roughness array with a density of 1/12. For a flow depth of 8 cm and mean velocity of 0.44 ms^{-1}, vibration periods ranged from 0.88 to 1.73 seconds with a mean of 1.2 seconds. Variations in particle size, shape and orientation probably account for most of the range in the vibration periods (Table 10).

3.6.3 Motion of marbles

To minimize effects resulting from particle shape, a number of runs were made utilizing 15 mm diameter marbles on the bed of the flume in close hexagonal packing. Many of the marbles in this single layer exhibited random and irregular quivering motion.

In order to determine the vibration frequencies, isolated 'cat's eye' marbles were placed on top of the closely packed marbles. The patterns within the otherwise clear marbles helped in the ability to discern and follow individual motions. As might be expected, these marbles were extremely unstable, frequently being entrained during an observation period.

3.6.4 Gravel in gravel

Non-cohesive particles within a gravel matrix exhibited vibration in a random, unpredictable manner. Over protracted periods, some particles would cease to vibrate, moving to more stable positions. Some particles would vibrate intermittently with prolonged quiescent periods while other particles would vibrate regularly for several hours. The uncertain response of any selected particle made observations difficult and frustrating. For the predominant size range 11.2 - 25 mm in diameter used in the present

study, general threshold conditions could not be attained due to flume limitations. Attempts to make specific clasts at pre-determined locations vibrate were seldom successful. Even for those occasions when rocks were made to vibrate, no consistent condition was apparent.

While the occasional particle was observed to vibrate with a large period, most moved within a narrow range of frequencies. During one set of observations, the period of a number of particles was measured at a low flow velocity. When the flow velocity was increased from 0.30 to 0.40 ms^{-1}, three particles remained in motion, the others having ceased to move or rolled to more stable positions. Maintaining a relatively constant flow depth and slope, the frequency of vibration was observed to increase (decreased period T) with increasing flow velocity (Table 11).

The most diverse vibrational modes, rocking, flutter, rotational and jumping motions were exhibited within the gravel matrix. Under some circumstances it was possible to find four or five clasts moving within a 10 cm square area. The vibrational period of these rocks was very similar and yet as far as could be determined by visual observations, they moved independently of each other.

3.6.5 Gravel-sand mixtures

Sand less than 1 mm in diameter was introduced while maintaining constant flow conditions over the gravel bed. Within a short period, the sand packed between the interstices and worked down into the gravel framework, increasing particle stability and reducing the number of vibrating particles. As the

	Time required for 20 vibrations - secs.										$\bar{T}$	σ
				d = 7.6 cm			v = 0.30 ms^{-1}					
16 - 25 mm P1	43.9	37.3	55.0	50.5	68.6	58.9	52.2	50.0	34.2	59.2	2.55	0.52
16 - 25 mm P2	66.2	74.1	36.3	54.5	87.7	72.8	93.8	94.8	88.0	102.5	3.85	1.03
11.2 - 16 mm P3	42.0	35.0	39.3	33.6	37.2	34.1	40.5	38.0	-	-	1.87	0.15
				d = 7.6 cm			v = 0.40 ms^{-1}					
P1	24.1	25.2	22.2	29.1	20.9	24.0	18.8	18.7	23.3	22.2	1.14	0.15
P2	25.7	29.0	19.6	26.2	26.8	23.1	17.6	21.0	18.2	19.4	1.13	0.20
P3	17.1	24.8	24.4	22.5	23.4	22.5	moved to more stable position				1.12	0.14

Table 11. Vibration periods with changing flow velocities, d = 7.6 cm, gravel in gravel.

amount of sand increased, vibration of the gravel clasts ceased. Sporadically, sand grains between the gravel interstices were observed to move in groups but the frequency was not measured.

3.7 REPLICATION OF VIBRATION PERIODS

In order to ensure a meaningful vibration period, ten successive measurements of the time required for 20 vibrations were made. Under some conditions the mean period obtained in this manner could be easily replicated (eg. see Table Appendix I) although occasionally quite different values were obtained (Table 2). For example, when measuring the vibration period 6 cm downstream from a wake generator using the same conditions on three successive days, values obtained for particle D5 were 1.16, 1.18 and 1.14 respectively. The variance of individual measurements was generally very small indicating a well defined excitation frequency.

For distributed roughness arrays, the periods for particle vibration had a large variance, possibly a reflection of the role of intermittency as well as particle orientation. Extended observations when 20 successive measurements rather than 10 were made suggest that some variation arises from a low frequency component due to flume conditions. This periodicity is most evident in Table 21 for particles R4 and S7 when the flow depth was 20 cm. The temporal record is graphed in Figure 13.

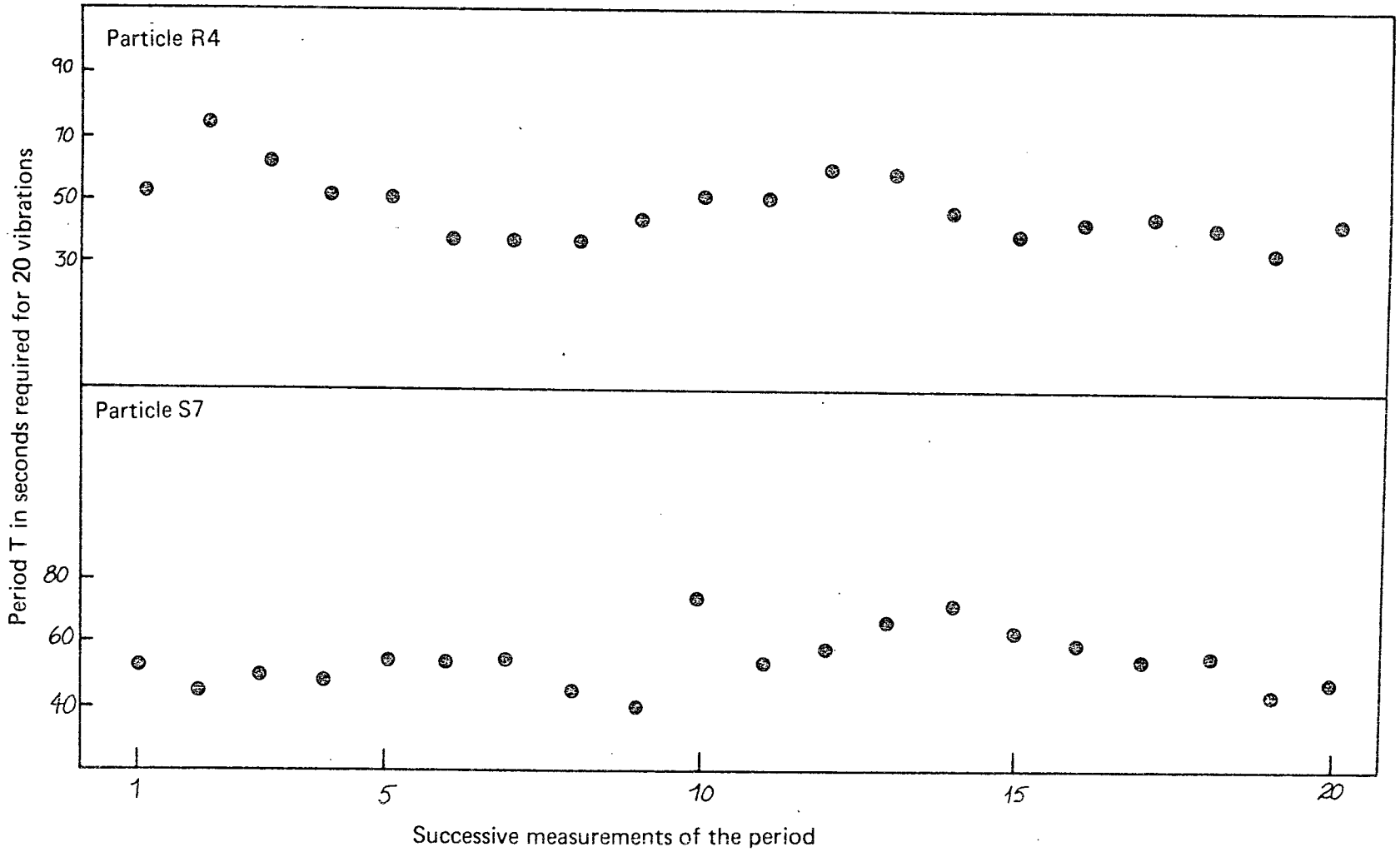

Fig. 13. Temporal variation of successive measurements of the time required for 20 vibrations; flow depth 20 cm, roughness density 1/12, velocity 0.42 ms^{-1}.

3.8 A SPECIFIC EXAMPLE OF PARTICLE VIBRATION

The preceding observations and measurements may be clarified by examining a specific instance of vibratory motion. For the threshold of motion of individual particles, atypical responses may be expected as a result of unusual particle configurations. This suggests that in interpreting the behavior of specific particles it is important to determine whether the behavior is atypical, along with the statistical significance of the response.

For conditions near the threshold of motion, the mean fluid force on a particle may result in the generation of an overturning moment. If the moment generated by the fluid force is insufficient to overturn the particle, it may simply be rotated and held against a downstream fulcrum or pivot point.

A number of examples were observed in which the particle appeared to 'fall back' periodically as if a support (mean fluid force) had been removed. In several instances, reduction of the mean velocity resulted in the particle returning to a more stable position, typically that which occurred in the absence of any flow. Behavior such as this might occur near the threshold of motion if the velocity of the fluid is significantly reduced momentarily. A similar response would occur if the particle were subjected to an adverse pressure gradient.

CHAPTER 4 PARTICLE VIBRATION MECHANISMS AND DISCUSSION

4.1 INTRODUCTION

Although a qualitative investigation such as the present study is unable to demonstrate conclusively a cause and effect mechanism to explain particle vibration, it may suggest possibilities for further study.

A tentative explanation proposes that particle vibration occurs in response to quasi-periodic forces imposed on the boundary by the turbulent bursting phenomenon. Non-dimensional scaling of the vibration periods determined in the present study conforms to the scaling relationships for the turbulent burst period. Additional support for this explanation may be found by re-examining data obtained by other investigators using sand sized material.

If particle vibration is important in the entrainment process, any explanation should be consistent with an entrainment mechanism as well as known structural features of turbulent flows. A modification of Sutherland's (1967) entrainment mechanism could incorporate the turbulent bursting phenomenon and be consistent with the structural features observed within the turbulent flows.

4.2 POSSIBLE MECHANISMS INITIATING VIBRATION

4.2.1 Mechanical instability

The mechanical instability hypothesis proposed that particle vibration occurred in response to random turbulent fluctuations impinging on an unstable

particle. Three specific conditions were differentiated in section 1.5.1:

a) Vibration frequencies are controlled by the particle admittance function. This is expected to vary considerably with particle size and shape.

b) An aerodynamic instability may occur where the particle is able to 'fly' into the mean flow. Once perturbed however, the change in attitude destroys the lift.

c) 'Loosely constrained' particles may move when subjected to fluid force. Collision with an adjacent particle and reduction in the net fluid force allows the particle to return toward its original position.

Observations of vibratory motion irrespective of particle shape or the presence of adjacent particles indicate that neither aerodynamic instability nor constraint by nearby particles is a primary factor causing vibration. Variations in vibration frequency resulting from changes in particle orientation as well as the absence of motion for some clasts indicate that particle instability is important.

If vibration occurs in response to random turbulent fluctuations impinging on unstable particles, a considerable variation in vibration period is to be expected. This is supported by the observations of the vibration period. Statistical analyses indicate that both particle size and shape are significant factors controlling the vibration period. In section 1.5.1 however, it was suggested that for particles whose size spans almost two orders of magnitude a similar range in particle vibration period may be expected for constant flow conditions near the particle threshold of motion. For the range of particles used with almost constant flow conditions, the

threshold of motion will not always be strictly realized, yet the range of vibration periods is surprisingly small - generally 1 - 3 seconds.

The relatively small range in vibration periods compared with the range in particle sizes may be due to particles having a flat admittance function (Figure 4b). In this case the particle vibration frequency should correspond rather closely to the peak in the turbulent energy spectrum (as suggested by Lyles, 1970) and not be particularly sensitive to changes in velocity and flow depth (Nowell, 1975).

The results tabulated in Table 11 for particles subjected to different flow velocities indicate that the vibration period is significantly modified by variations in the mean flow velocity. Furthermore Table 8 and Figure 12 demonstrate that for almost constant mean velocity, the flow depth is also a significant parameter controlling the vibration period. The present results show a very strong positive correlation between the period of vibration and the flow depth.

While no conclusive evidence is presented to refute the hypothesis that vibration is a response to random turbulent fluctuations impinging on mechanically unstable particles, the results do suggest this is too simplistic an explanation. Mechanical instability is likely to be a necessary but not sufficient condition to explain the observed phenomenon.

It may be argued that even an unconditionally stable particle such as a square or rectangular block with a flat surface will exhibit vibratory motion

if it is subjected to periodic impulsive forces whose magnitude is close to the overturning moment. Thus particle stability reflects the magnitude of the forces necessary to achieve threshold conditions. As flow conditions approach the threshold of motion, individual particles become less stable and are able to respond more readily to fluctuations in pressure and velocity. Possible responses however will be restricted by interparticle geometry and particle inertia.

4.2.2 Particle vibration from self-excitation

In section 1.5.2 it was hypothesized that vibration may be a response to self excitation. This mechanism requires that vortices, shed alternately from separation points on the particle afterbody, create oscillatory forces that initiate vibratory motion. If the formation region, controlled by the effective hydraulic diameter of the body, is reduced, the shear layers are brought closer together facilitating their interaction and resulting in a decrease of the shedding period.

Specific observations that would support this hypothesis are enumerated in section 1.5.2. Observations and measurements of vibration periods for particles located on either smooth or rough boundaries, irrespective of the presence of other bluff bodies support the hypothesis. For increasing turbulent intensity, the vibration period might be expected to increase for specific particles. This is partially supported by the trend of increasing period with increasing roughness density (Figure 11).

Since the vortex shedding period is dependent on the hydraulic diameter

of the body, the mean vibration period for constant flow conditions should increase with increasing particle size. While variations in the vibration period attributable to particle size are statistically significant (Table 5) there is by no means a consistent relationship between size and period.

For sufficiently small particles that subsist within the viscous sublayer, vortex shedding does not occur so these particles should exhibit no vibratory motion. For sand, the particle Reynolds number Re^* is in the transition range ($3.5 \leq Re^* \leq 70$) so that viscous effects rather than wake shedding should be dominant. Observations, however, of small sand grains in the order of 1 mm diameter indicated that vibration of a period comparable to that of larger clasts does occur.

When the relative roughness $d/D > 3$, the wake shedding frequency might be expected to be independent of the flow depth. If the relative roughness is less than three, distortion of the free surface may significantly modify the wake shedding frequency. In the course of the present study, the relative roughness was always greater than three while the particle vibration period was strongly correlated with flow depth.

While evidence of particle vibration in sands and the dependence on flow depth does not conclusively refute self-excitation as a mechanism, it does suggest that this is not the primary operative process initiating particle vibration. Furthermore, if vortex shedding from a bluff body is at all irregular, it is likely that destructive rather than constructive interference occurs that would increase the overall periodicity of the effective fluctuations.

4.2.3 Wake interaction and vorticity amplification

The hypotheses of wake interaction and vorticity amplification (Section 1.5.3) proposes that periodic fluctuations in the pressure-velocity field arise either from wakes shed from upstream roughness elements or energy concentration at a preferred frequency. Both mechanisms require the presence of an upstream roughness element to create the necessary conditions.

If either wake interaction or vorticity amplification is important, then no motion should occur on either hydrodynamically smooth or rough boundaries in the absence of neighbouring upstream particles. For flow states approaching the threshold condition, a number of particles were observed to exhibit vibratory motion in the absence of other particles in the neighbourhood. This suggests that neither mechanism is specifically responsible for initiating vibratory motion.

Subsequent observations demonstrated that one or the other of these mechanisms may, under the correct conditions, initiate particle vibration. For subcritical conditions, vibration did not occur for isolated particles. Placing wake generators immediately upstream, whose hydraulic diameter was as large as or larger than that of the particle, frequently resulted in vibratory motion. Thus it would appear that upstream roughness elements have the effect of reducing the mean conditions necessary to create vibratory motion. This may arise either because of the increased turbulent intensity immediately downstream and hence larger fluctuations, or because energy is preferentially concentrated at specific frequencies due to vorticity amplification.

Small material (like coarse sand) is not expected to show evidence of vibration since amplified frequencies or wake interaction effects will rapidly be dominated by viscous effects. This is contrary to the present observations.

In the case of distributed roughness arrays it is suggested that neither wake shedding nor vorticity amplification is the dominant mechanism initiating particle vibration but may be implicated in modifying the frequency of vibration or the 'high' frequency component that was observed superimposed upon the high amplitude, low frequency motion.

If the vortex shedding from a three-dimensional bluff body is irregular this has implications for the downstream action upon other particles through the mechanism of wake interaction. Thus we might expect an irregular quasi-periodic vibration rather than either a regular or random motion.

4.2.4 Turbulent bursting

The remaining hypothesis proposes that particle vibration is a response to fluctuating forces imposed upon the boundary by turbulent bursting. Either the adverse pressure gradient associated with the high speed sweeps or the high frequency large amplitude fluctuations in the wall shear stress may be the primary mechanism initiating vibration. Specific observations that would support this hypothesis were detailed in section 1.5.4.

If turbulent bursting is the operative process, then particle vibration should occur for particles near the threshold of motion, irrespective of the

boundary roughness or presence of neighbouring particles. This is supported by observations of vibratory motion on hydrodynamically smooth and rough boundaries in the absence of other particles. The results for the particle vibration period, independent of the roughness concentration, are somewhat equivocal. A two-way cross classification analysis of variance indicates that differences of vibration period between the roughness concentration, are larger than expected (Table 4). This is further demonstrated by the trend in the mean vibration period which peaks for a roughness density of 1/12 (Figure 11). Note, however, that the variation is well within one standard deviation of the grand mean period. The weak dependence of vibration period on roughness density may be associated with difficulties of obtaining consistent representative velocities or secondary effects introduced by wake interaction.

If the turbulent structure and associated bursts are affected by the overall flow conditions, then factors such as flow depth and velocity will become significant. The present observations, although limited in number, show a strong positive correlation (Figure 12) between the period of vibration and the flow depth. This would be expected if the flow depth and presence of a free surface constrain the spatial and temporal scales of motion.

While the present results indicate a curvilinear relationship between vibration period and flow depth, the possibility of a linear relation cannot be rejected. Difficulties in accurately measuring the 'high' frequency motion occurring for a flow depth of 5 cm, small sample sizes and slight differences

in mean flow velocities will all contribute to the uncertainty in the mean values.

The vibration period is sensitive to the mean flow velocity (Table 11). Some dependence on the mean velocity is expected since threshold conditions are required to produce unstable particles. Mean velocity or free stream velocity is also important as a scaling parameter for the bursting frequency and hence may affect the particle vibration frequency.

Variations in the free stream velocity may also account for some of the differences in the vibration period measured between roughness densities. During the experimental procedure, the mean flow velocity was measured at 0.4 of the flow depth as measured from the basal surface, irrespective of the roughness density. This implicitly assumes a logarithmic velocity profile which may be inappropriate for high relative roughness (Nowell and Church, 1979).

If the frequency of turbulent bursting is independent of wall characteristics, then for appropriate threshold conditions, individual particles should vibrate in response to the turbulent burst period rather than being controlled by particle size or shape. A two-way cross-classification analysis of variance indicates that both particle size and shape are important parameters (Table 5, 6a, 6b) that appear to modify the vibration period. Variations due to particle size were not unexpected since, for constant flow conditions, considerable variation will occur in the threshold criterion. This will be reflected in the particle instability and response characteristics

of individual particles. Additional variations in the determination of the particle vibration period was introduced by particle orientation (Table 3), low frequency variations in flow characteristics (Figure 13) and imprecise measurements of the vibration period that arise from the arbitrary, subjective nature of the amplitude discrimination.

The variation in the vibration period of particles ranging in size from coarse sand to gravel is relatively small compared with the range in particle sizes. This is consistent with the hypothesis of turbulent bursting where flow depth and velocity will be the principle determinants of the bursting period, rather than particle size, assuming conditions are approximately near the threshold of motion.

The present observations indicate that the particle vibration period T is strongly dependent on the flow depth d or boundary layer depth δ. The results of Table 11 indicate an inverse relationship between the period and flow velocity U. While some sensitivity to velocity changes may be an artifact of the measurement technique, the pattern in Figure 11 for a density of 1/8 does not support this idea.

From the two-way cross classification analysis of variance (Tables 4, 5 and 6) there are apparent effects arising from the roughness density k, particle size, shape and orientation as well as interaction effects. The maximum projection sphericity $Sp = (c^2/ab)^{1/3}$ has been shown by Sneed and Folk (1958) to be a good measure of hydraulic behavior. Thus the variable Sp can be used to combine effects of particle shape and orientation.

Thus $T = f\left(d, \frac{l}{u}, Sp, k, D\right)$.

The first two effects implicate turbulent bursting. The remainder implicate secondary effects such as mechanical stability and wake interactions. The effect due to particle size D is a result of inertia and is a threshold phenomenon. This factor may also incorporate constraint factors of adjacent particles.

While the turbulent bursting phenomenon may superficially explain particle vibration, it will be necessary to specify an event and its associated structure along with its relation to an entrainment mechanism if any, before the explanation is satisfactory.

4.3 NON-DIMENSIONAL BURST PERIODS

4.3.1 Scaling relationships

A time series analysis of the products of the streamwise and normal velocity fluctuations i.e. the instantaneous Reynolds stress, shows that the major contributions to the long term average of the Reynolds stress - $\overline{\rho u'v'}$ occur intermittently over a short period and is associated with the phenomenon of turbulent bursting (Kim et. al., 1971). In between burst events, the production of turbulent energy is very small. The peak production of turbulent energy is found to occur in the regions immediately adjacent to the wall (Kline et. al., 1967) so it would be expected that burst periodicity and the associated fluctuations in the Reynolds stress should scale on inner wall variables.

Using a hot wire anemometer in a turbulent boundary layer in air, Rao, Narasimha and Badri Narayanan (1971) measured the mean period between turbulent bursts. Their data, along with similar measurements in water obtained at Stanford, showed that the mean period was strongly dependent upon the Reynolds number. A weak dependence upon the Reynolds number remained if the period was non-dimensionalized using the shear velocity U_* and the boundary layer depth δ. A more satisfactory scaling relationship was obtained by using the free stream velocity U_∞ and the displacement thickness δ^*. For fully developed, depth limited flow, the boundary layer depth δ will be approximately equal to the flow depth d while the displacement thickness δ^* will be considerably less than δ or d (Massey, 1975).

Over a range of Reynolds numbers spanning two orders of magnitude with the period Tv determined from visual observations, the non-dimensional period $T^* = U_\infty Tv/\nu$ is approximately equal to 5 while if the displacement thickness is used, $T^* = U_\infty Tv/\delta^* \approx 32$ (Rao, Narasimha and Badri Narayanan, 1971). Additional support for the validity of this scaling relationship in depth limited flows using water is provided by the work of Blinco and Simons (1975). Using the non-dimensional period $T^* = U_\infty Tv/\delta$, a slight dependence on Reynolds number remains with T^* decreasing to around 4. This is apparent in both the results of Rao, Narasimha and Badri Narayanan (1971) and those of Blinco and Simons (1975). Some scatter in the non-dimensionalized period may be attributed to difficulties of measuring the mean period between bursts and the amplitude discrimination level selected to define a burst.

Using data obtained from the hot wire anemometer, Rao, Narasimha and Badri Narayanan (1971) found that the measured period Tm for the burst frequency was approximately one half that obtained for the period Tv determined from visual observation. This would provide a non-dimensional period $T^* = U_\infty Tm/\delta \approx 2.4$. A consistent relationship between Tv and Tm is dependent upon the amplitude discrimination used to identify a burst. The latter value for the non-dimensional period closely corresponds to that obtained by Antonia, Danh and Prabhu (1976) in which the burst frequency for laboratory data was found to be approximately one half the zero crossing frequency of the velocity signal.

In order to obtain suitable non-dimensional periods from the present work for comparison with published data on burst periodicity, several assumptions were required. An estimate of the free stream velocity U_∞ was obtained by multiplying the mean velocity by 1.2. This is a value suggested by Leopold, Wolman and Miller (1964) although the results of Vanoni (1964) indicate that the factor is closer to 1.14. Since no velocity profiles were measured, neither the displacement thickness δ^* nor the momentum Reynolds number Re_θ can be computed. A suitable estimate of the momentum thickness θ may be obtained from the relationship $\theta \sim 0.1\delta$ (Jackson, 1976) which in turn allows computation of the momentum Reynolds number.

Using the mean period Tv from each set of observations, four estimates of the non-dimensional period T^* ranging from 4.85 to 9.6 were obtained (Table 12). Although these values are slightly high, they compare favorably

Particles/ Condition	Flow Depth m	Mean Velocity	Mean Period $\bar{T}$	Free stream Velocity U_∞	Re_θ	$T^* = T \frac{U}{\delta}$
Gravel test particles in distributed roughness arrays 1/12	0.08 m	0.43 ms^{-1}	1.49 s	0.52 ms^{-1}	3440	9.60
Gravel test particles in a distributed roughness array, density 1/12.	0.05 m	0.40 ms^{-1}	0.94 s	0.48 ms^{-1}	2000	9.02
Gravel test particles in distributed roughness array 1/12	0.20 m	0.44 ms^{-1}	2.57 s	0.53 ms^{-1}	8800	6.80
1 - 2 mm coarse sand	0.08 m	0.27 ms^{-1}	1.08 s	0.33 ms^{-1}	2190	4.85

Table 12. Summary table of flow parameters and non-dimensional period T^*.

with previous data presented by Rao, Narasimha and Badri Narayanan (1971) (Figure 14).

4.3.2 Burst frequencies in fine material

Vanoni (1964) conducted a series of experiments to determine the critical shear stress for fine sands having a geometric mean sieve size of 0.102 mm. Approaching the threshold condition for the initiation of motion, the fine sediment was observed to move intermittently. Many grains moved simultaneously during each event over areas varying from 7 to 18 mm in diameter.

By observing a small area, Vanoni counted the number of events within a time interval and estimated the average number of grains in motion during each event. The event frequency and number of grains in motion were found to be strongly correlated and formed the basis for judging the occurrence of critical conditions. When the event or burst frequency fell between 0.33 and 1 Hz, Vanoni considered that threshold conditions had been reached. If the frequency of events was below 0.1 Hz, the rate of movement was negligible while for frequencies greater than 1 Hz, general movement of sediment occurred.

Table 13 summarizes data from Vanoni (1964, of Table 5, p. 23). Using his values of the flow depth d, free stream velocity U_∞ and burst period Tv, a non-dimensional period T^* ranged between 1.78 and 14.0 with a mean of 5.49.

The non-dimensional period T^*, calculated from the results of Vanoni, can be differentiated on the basis of sediment motion. In the absence of

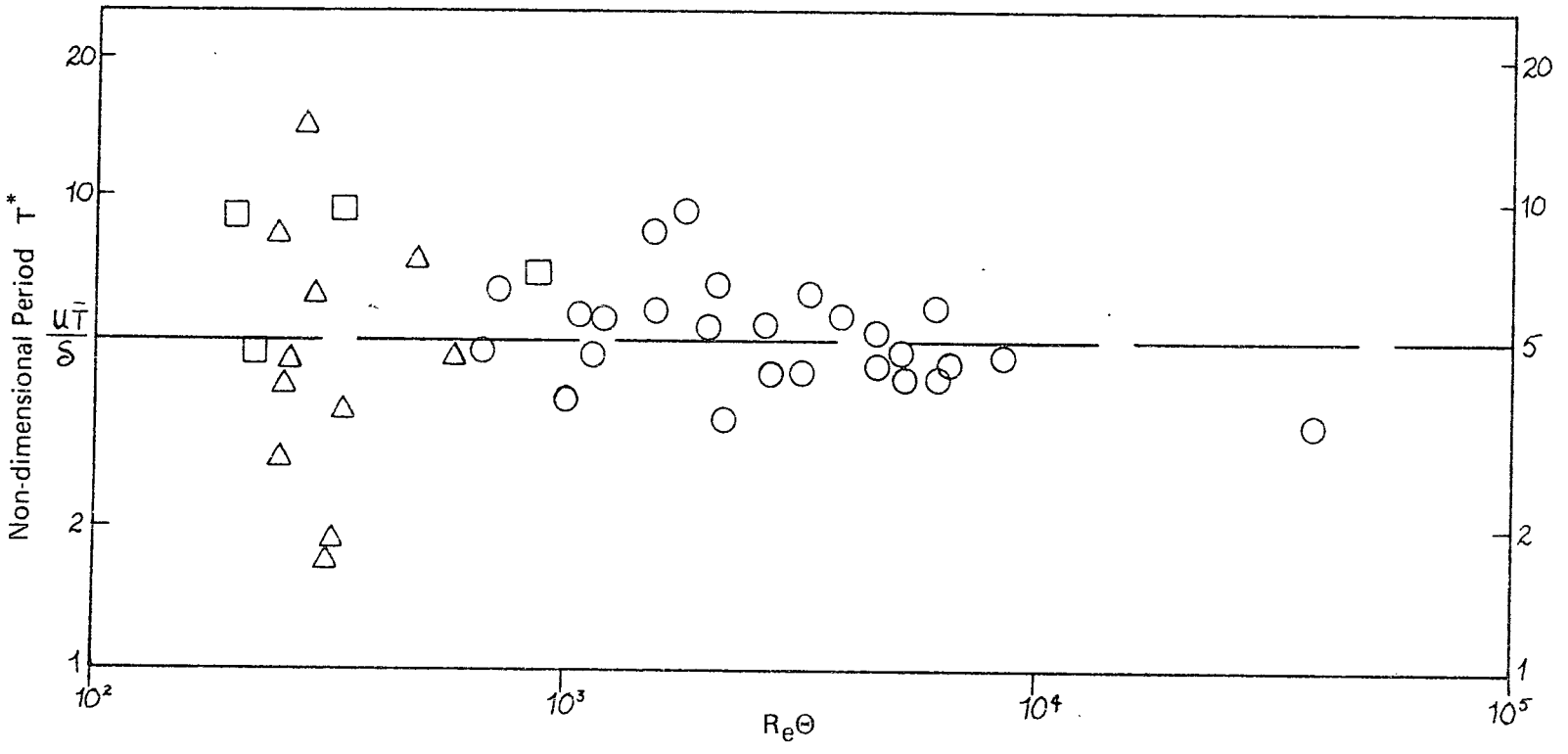

Fig. 14. Vibration period or burst rate normalized with outer variables. Data of Rao, Narasimha and Badri Narayanan (1971) ○ ; present values for vibration of sand and gravel □ ; results of Vanoni, 1965 △ .

Run Number	Flow Depth	Free Stream Velocity U_∞	Burst Frequency	T Secs.	$T^* = \frac{U_\infty T}{d}$	Sediment Motion	Re_θ
VANONI							
R-3	0.119 m	0.247 ms^{-1}	1/3	3.5	6.21	small	2939
R-4	0.119	0.281	2/3	1.5	3.54	critical	3343
R-7	0.119	0.238	1/7	7.0	14.0	small	2832
R-11	0.093	0.262	1/3	3.0	8.47	small	2436
R-12	0.093	0.262	1	1.0	2.82	critical	2436
R-13	0.093	0.285	0.667	1.5	4.59	critical	2650
R-15	0.092	0.293	0.667	1.5	4.78	critical	2695
	0.092	0.328	2	0.5	1.78	general	3017
	0.092	0.344	2	0.5	1.87	general	3164
31-B	0.215	0.228	1/7	7.0	7.41	small	4902
31-C	0.215	0.263	1/4	4.0	4.89	small	5654
					$T^* = 5.49$		
SUTHERLAND							
visual	0.106 m	0.313 ms^{-1}	0.5	2.0	5.91	critical	3317
film	0.100	0.271		0.5	1.36	critical	2710
LYLES							
tapioca	1.93 m	19.65 ms^{-1}	1.8 ± 0.3	0.56	5.63	critical	

Table 13. Summary of flow conditions and non-dimensional period T^* for the data of Vanoni (1964), Sutherland (1967) and Lyles (1970).

visual bursting processes, no sediment was observed to move while rare bursts resulted in negligible sediment motion. For 'small' amounts of sediment motion the non-dimensional period averaged $T^* = 8.2$. For conditions judged 'critical', $T^* = 3.9$ while for general motion $T^* = 1.8$. This suggests that the non-dimensional period T^* may be a potential discriminator for determining threshold conditions. The results are also consistent with the burst periods obtained by Rao, Narasimha and Badri Narayanan (1971). For conditions approximating general motion, the burst frequency might be expected to conform closely to that measured by hot wire anemometry, providing a non-dimensional period $T^* = 2.4$.

During the course of an investigation into the mechanisms by which sediment grains are first moved, Sutherland (1967) using rounded quartz sand having a geometric mean size of 0.564 mm, made visual observations and photographs of the bursts of sediment motion. For a mean flow velocity of 26.1 cm^{-1} and flow depth of 10.6 cm, Sutherland judged that threshold conditions existed when the grain motions occurred about every two seconds. Using a factor of 1.2 to convert the mean velocity to the free stream velocity U_∞ (Leopold, Wolman and Miller, 1964), the non-dimensional period $T^* = 5.9$.

Using a 16 mm camera. Sutherland (1967) recorded the motion of dye ejected into the sublayer over the sediment bed. The dye filaments were observed to be periodically ejected from the vicinity of the bed, grains moving only in the larger bursts. The ejected dye was carried downstream along paths inclined between 10° and 20° from the horizontal. This is in

accord with the work of Brown and Thomas (1977) who found that the structure associated with the turbulent burst was inclined at an angle of approximately 18°.

From one photo sequence presented by Sutherland where the mean velocity is 22.6 cm s^{-1}, flow depth is 10 cm and burst period T is 0.5 sec., the non-dimensional period $T^{*} = 1.36$. While Sutherland judged this to correspond to critical conditions, this value may not be representative since it is obtained from a single measurement observed and recorded on 16 mm film. Sutherland judged that critical conditions for grain motion generally occurred when bursts occurred about every two seconds for any chosen spot. For the preceding flow conditions this would correspond to a non-dimensional period $T^{*} = 5.4$, rather than 1.36.

In discussing flow visualization with fine colloidal sized particles, Corino and Brodkey (1969) noted that a collective movement of particles often occurred simultaneously with a fluid ejection that followed the lift-up of a wall streak. Grass (1974) used fine sand particles to visualize events in the bursting process, suggesting a direct link between fluid ejection and particle motion.

Lyles (1970) observed the motion of fine sand grains and tapioca particles in a wind tunnel. As the mean wind speed approached the threshold value, some of the particles began to vibrate or rock back and forth. Vibrations were seldom steady but occurred in flurries. If the mean wind speed was increased considerably above the threshold, vibration could not

be observed due to the rapidity of entrainment.

By counting 25 successive vibrations, Lyles was able to estimate the mean frequency of vibrations of the tapioca particles (6.1 mm diameter) to be 1.8 $\pm$ 0.3 Hz. With an available flow depth of 193 cm at a mean speed of 16.3 ms^{-1}, the non-dimensional period $T^* = 5.6$. This is of the same order of magnitude as the non-dimensional period for vibrating particles at the threshold conditions in water.

The results of Lyles must be used with caution since it is not clear that the flow depth of the wind tunnel should be used. Although vibration frequencies for various sizes of sand are reported, no information is provided on the mean wind speed so further checks could not be made.

4.3.3 Burst frequency in gravel

Tables 2 and 11 list vibration periods for different sized gravel test particles or changing flow velocities. For a constant flow velocity, the smaller clasts should be nearer the threshold of motion compared with the larger particles. Similarly, increased flow velocities will result in conditions approaching the threshold of motion.

Test particles were differentiated on the basis of clast size into three groups: particles 1 - 3 (11.2 - 16.5 mm); particles 4 - 6 (16.5 - 24 mm) and particles 7 - 8 (> 24 mm). From Table 2 three mean vibration periods corresponding to the respective particle sizes can be obtained. These can be used to calculate specific values of the non-dimensional period

T^* (Table 14) as the threshold condition is approached. Similarly, changes in the vibration period for increasing flow velocity provide additional estimates of T^*.

Table 14 provides evidence that the non-dimensional period T^* decreases as threshold conditions are approached. It is very plausible that for threshold criterion, the non-dimensional period would closely approximate the value $T^* = 5$ found by Rao, Narasimha and Badri Narayanan (1971) to scale the turbulent bursts when the period was visually determined. For the reduced amplitude discrimination that would prevail at the onset of general motion, burst frequencies and particle motion, as indicated by Vanoni's data, might well be expected to approximate the non-dimensional period $T^* = 2.4$, determined from hot wire anemometry.

4.4 ENTRAINMENT MECHANISMS

In an early study of turbulent flows over gravel, Thompson (1963) postulated the existence of distinct rotating eddies that were responsible for particle entrainment. In Thompson's model, vortices whose axes were normal to the boundary would impart a lifting force to particles as the rotating fluid element was convected along the bed. This is very similar to the action of 'kolks' proposed by Matthes (1947) where strong vortex motion at the stream bed lifts materials by suction. The kolks have a surface manifestation in the form of boils.

Sutherland (1967) appears to be the first investigator who attempted to

Particle Size	Flow Depth	Mean Velocity	Mean Period $\bar{T}$	Free Stream Velocity U_∞	Re_θ	$T^* = \frac{TU}{\delta}$
11.2 - 16.5 mm	0.080 m	0.43 ms^{-1}	1.32 s	0.52 ms^{-1}	3440	8.58
16.5 - 24 mm	0.080 m	0.43 ms^{-1}	1.52 s	0.52 ms^{-1}	3440	9.88
24 mm	0.080 m	0.43 ms^{-1}	1.78 s	0.52 ms^{-1}	3440	11.57
16.5 - 24 mm	0.076 m	0.30 ms^{-1}	2.76 s	0.36 ms^{-1}	2280	13.07
16.5 - 24 mm	0.076 m	0.40 ms^{-1}	1.13 s	0.48 ms^{-1}	3040	7.14

Table 14. Variation in the non-dimensional period T^* with changing particle size or velocity.

explain the mechanism of sediment entrainment from observations of the turbulent flow. According to Sutherland's model, particle lift-up and entrainment result from an advected eddy, whose lowermost portion is rotating in the same direction as the mean flow, impinging on a particle. The increased velocity associated with the eddy results in a large increase in the instantaneous drag force, which, as a result of the rotation within the eddy, is inclined at a small angle to the bed. When the vertical component of the drag force exceeds the immersed particle weight and restraining forces arising from contact with neighbouring particles, the particles will be lifted from the bed and entrained.

On the basis of observations of the motion of heavy, isolated particles in an open channel, Sumer and Oğuz (1978) propose some modifications to Sutherland's entrainment mechanism. Rather than an eddy whose flow along its lowermost portion rotates in the same direction as the mean flow, Sumer and Oğuz propose that a so-called recirculation cell rotates in the opposite direction. This would be consistent with models of the turbulent structure (Offen and Kline, 1975; Praturi and Brodkey, 1978) where high speed fluid having a negative vertical velocity overtakes slower speed fluid near the boundary forming transverse vortices whose flow along the lowermost portion is counter to the mean flow direction. The transverse vortex imposes a temporary adverse pressure gradient that results in lift-up and ejection of low momentum fluid. The fluid inrush, transverse vortex formation, lift-up and ejection of low momentum fluid leading to the chaotic break up referred to as a burst, form a sequence of events with a characteristic periodicity or burst frequency. Hence a particle near the threshold of motion will be

subjected to periodic velocity fluctuations corresponding to some specific event within this semi-deterministic sequence.

The mobilization of particles is a threshold phenomenon arising from particle inertia and energy transfer efficiency. Hence even if the non-dimensional burst period T^* is a constant, at flows well below threshold, only extreme burst events can possibly give rise to particle vibration so Tp^* (particle) will be greater than T^*. As threshold conditions are approached, Tp^* should converge to the value T^*.

The present results support this behavior in the particle non-dimensional period Tp^*. As the threshold of motion is approached, Tp^* decreases until it approximates the value $T^* = 5$, which was determined on the basis of visual observations. For more general sediment motion, $Tp^* < 5$, indicating that the detection of bursts is an amplitude-controlled effect and the sediment responds to lower amplitude burst events. Under these conditions Tp^* converges to a value $Tm^* = 2.4$ as determined from the analysis of velocity signals (Rao, Narasimha and Badri Narayanan, 1971; Antonia, Danh, and Prabhu, 1976).

The variation in the particle non-dimensional period and the convergence of Tp^* toward Tm^* at and above threshold conditions provides considerable support for the importance of burst events in particle mobilization. This does not, however, implicate any specific event within the burst sequence. While Sutherland's entrainment mechanism implies that a particle will be lifted from the bed when the vertical component of the drag force exceeds the

restraining force, Sumer and Oğuz's model views the lifting of a particle as a response to an adverse pressure gradient imposed by the transverse vortex.

In the turbulent structural model for a smooth boundary, the adverse pressure gradient associated with the transverse vortex initiates fluid uplift and ejection from the viscous sublayer. Although insufficient information exists for rough boundary conditions, available evidence suggests that bursting is the dominant process. According to Grass:

> "...it is envisaged that the smooth boundary viscous sublayer fluid and fluid trapped between the roughness elements simply forms a 'passive' reservoir of low momentum fluid which is drawn on during ejection phases. Entrainment was extremely violent in the rough boundary case, with ejected fluid rising almost vertically from between the interstices of the roughness elements."
> Grass (1971, p. 252).

Transverse vortices, originating as part of the burst sequence, modify the pressure distribution on the wall. Evidence exists, however, for large scale structures that may control the burst frequency and modify wall conditions. Correlation measurements over the entire flow depth (Grass, 1971; Brown and Thomas, 1977) indicate that a large scale structure exists that encompasses most of the flow depth. This large, organized structure appears to be inclined at an angle of 18° from the horizontal (Brown and Thomas, 1977). These workers propose that the passage of the large structure results in a high frequency, large amplitude wall shear fluctuation that precedes the local maximum in the 'slowly varying' wall shear component.

Thus particle vibration may be a response to the high frequency, large amplitude wall shear fluctuations associated with the passage of the large structure, rather than with transverse vortices generated in the burst sequence. During the course of the present work, flow visualization using aluminum powder and recorded on 16 mm film provide some evidence for the existence of a large structure over a hydrodynamically rough boundary. It is apparent that aluminum particles become concentrated in a linear pattern which would correspond to the stagnation zone on the back of the large structure. It proved difficult however to measure either the angle of inclination or periodicity of this structure.

CHAPTER 5 CONCLUSIONS AND RECOMMENDATIONS FOR FURTHER STUDIES

5.1 CONCLUSIONS

Starting with the four hypotheses for particle vibration:

1) mechanical instability of the particle in the flow;
2) oscillatory forces arising due to vortex shedding from a particle;
3) advected eddies interacting with particles downstream;
4) response of particles to turbulent bursting,

a series of observations was made that would reject some of the hypotheses. The phenomenon of particle vibration is complex, but it is concluded that burst effects appear to dominate. Mechanical instability may be a necessary but insufficient condition for vibratory motion to occur.

For conditions of general sediment motion and deformation of the free surface by wave action, wake formation rather than turbulent bursting, may be more significant in sediment dynamics.

Particle vibration period appears to be a function of flow depth, velocity, particle size, shape and orientation as well as local roughness density. The proposed functional relationship is:

$$T = f\left(d , \frac{1}{u} , Sp , k , D\right)$$

The principal parameters at the threshold of motion are flow depth and velocity.

The vibration frequency was measured for particles ranging in size from coarse sand to gravel. Using the outer flow variables δ and U_∞, the non-dimensional period for particle vibration is the correct order of magnitude compared with the relationship $T^* = TU/\delta$ formulated for turbulent bursting. Data previously obtained by Vanoni (1964), Sutherland (1967) and Lyles (1970) also conform to this relationship.

The magnitude of the non-dimensional period T^* may be a possible measure of the threshold of motion. As the threshold of motion was approached, a consistent decrease in the magnitude of T^* was observed. It is suggested that at the threshold of motion the non-dimensional period T^* for particle vibration will be approximately five. This is the mean value determined for turbulent bursts using visual identification. As threshold conditions are exceeded, the non-dimensional period decreases to a value approximating $T^* \sim 2.4$. This is a value determined by analysis of the velocity signals. The uncertainty in this approach involves the amplitude discrimination level required to detect or record a burst event.

5.2 FUTURE INVESTIGATIONS

The present study has provided some qualitative evidence to indicate that the phenomenon of turbulent bursting and associated structures may be very important in the entrainment process. Considerable work will be necessary to verify these tentative conclusions. A number of questions need to be addressed.

1) During the present study, particles were occasionally observed to vibrate with a high frequency, low amplitude motion that was superimposed upon the lower frequency, high amplitude vibratory motion. It would be useful to determine whether this is related to the threshold condition or whether the two vibratory frequencies represent two distinct populations resulting from different excitation mechanisms.

2) While the limited data available conforms to a non-dimensional scaling relationship, considerably more information is required to determine if the vibration period is inversely proportional to the flow velocity and directly proportional to the flow depth.

3) As the threshold of motion is approached for a specific particle, the non-dimensional period T^* decreases to approximately five while for more general motion, T^* may decrease further. The exact behavior of T^* near the threshold of motion will provide some evidence regarding the influence of wake and general turbulence intensity effects producing additional entrainment events.

4) Useful information may be provided by determining the limiting particle sizes that exhibit vibratory motion.

5) The present work is unable to assess the relative importance of either the burst event or passage of a large structure that may initiate particle vibration. Limited photographic evidence suggests that discrete large scale structures that encompass the entire flow depth are present over

hydrodynamically rough surfaces. Does particle vibration occur in response to high frequency, large amplitude fluctuations in the wall shear stress caused by the passage of a large structure, or by an adverse pressure gradient imposed by a transverse vortex that forms in the burst sequence?

6) In the present study all runs were made for a constant, fixed energy slope. Some observations should be made to ascertain whether slope is a significant parameter in determining the vibration period. It should not be important if the vibration is a response to a specific turbulent structure.

7) Previous work has determined that in a positive pressure gradient, bursting becomes more violent and frequent while in negative pressure gradients the rate of bursting is reduced. In a sufficiently accelerating flow, the bursting ceases entirely. If sediment entrainment and mobilization is influenced or initiated by burst amplitude and periodicity, the role of pressure gradients may have important implications for the formation of pool/riffle sequences.

For flows over a riffle or through a chute, the accelerating flow should have a reduced burst frequency. In a pool, the decelerating fluid creates a positive pressure gradient which should result in more frequent and violent bursting. If particle vibration and entrainment is related to some aspect of turbulent bursting, then the changing pressure gradients in the pool/riffle sequence will regulate the bursting process and hence the entrainment and movement of material.

BIBLIOGRAPHY

ANTONIA, R.A., DANH, H.G. AND PRABHU, A. 1976. Bursts in turbulent shear flows. Physics of Fluids, 19; No. 11, 1680 - 1686.

BAGNOLD, R.A. 1941. The physics of blown sand and desert dunes. Methuen, London, 265 pp.

BISAL, F. AND NIELSEN, K.F. 1962. Movement of soil particles in saltation. Can. J. Soil Sci., 22; 81 - 86.

BLINCO, P.H. AND SIMONS, D.B. 1975. Turbulent structure near smooth boundary. ASCE. J. Eng. Mech. Div., 101; No. EM3, 241 - 255.

BROWN, G.L. AND THOMAS, A.S.W. 1977. Large structure in a turbulent boundary layer. Physics of Fluids, 20; No. 10, Pt. II S243 - S252.

BRADSHAW, P. 1971. An introduction to turbulence and its measurement. Pergamon Press, New York. 218 pp.

CHEN, C.K. AND ROBERSON, J.A. 1974. Turbulence in wakes of roughness elements. ASCE J. Hy. Div., 100; No. HY1, 53 - 67.

CHEPIL, W.S. 1959. Equilibrium of soil grains at the threshold of movement by wind. Soil Sci. Soc. Am. Proc., 23; No. 6, 422 - 428.

CHURCH, M. AND GILBERT, R. 1975. Proglacial fluvial and lacustrine environments. In A.V. Jopling and B.C. McDonald, editors, Glaciofluvial and glaciolacustrine sedimentation. Soc. of Econ. Paleontologists and Mineralogists, Special Publication. 23; 22 - 100.

CORINO, S.R. AND BRODKEY, R.S. 1969. A visual investigation of the wall region in turbulent flow. J. Fluid Mech., 37; 1 - 30.

DANEL, P., DURAND, R. AND CONDOLIOS, E. 1953. Introduction a l'etude de la saltation. Houille Blanche, 8; No. 6, 815 - 829. Engl. Transl. Supp. No. 1, 1955.

DAVENPORT, A.G. 1964. The buffeting of large superficial structures by atmospheric turbulence. Annals of New York Acad. Sci., 116; 135 - 160.

EINSTEIN, H.A. AND EL SAMNI, S.A. 1949. Hydrodynamic forces on a rough wall. Rev. Mod. Phys., 21; 520 - 524.

FENTON, J.D. AND ABBOTT, J.E. 1977. Initial movement of grains on a stream bed: the effect of relative protrusion. Proc. Roy. Soc. London Ser. A., 332; 443 - 471.

FRANCIS, J.D.R. 1973. Experiments on the motion of solitary grains along the bed of a water stream. Proc. Roy. Soc. London Ser. A. 332; 443 - 471.

GERRARD, J.H. 1966. The mechanics of the formation region of vortices behind bluff bodies. J. Fluid Mech., 25; Part 2, 401 - 413.

GESSLER, J. 1971. Beginning and ceasing of sediment motion. Chapter 7 in Shen, H.W. (ed), River Mechanics, Water Resources Pubs., Fort Collins, Colorado. 21 pp.

GILBERT, G.K. 1914. The transportation of debris by running water. U.S. Geol. Survey Professional, Paper 86. 263 pp.

GRASS, A.J.. 1971. Structural features of turbulent flow over smooth and rough boundaries. J. Fluid Mech., 50; 233 - 255.

GRASS, A.J. 1974. Transport of fine sand on a flat bed: turbulence and suspension mechanics. Euromech., 48; 33 - 34.

HELLEY, E.J. 1969. Field measurement of the initiation of large bed particle motion in Blue Creek near Kalamath, California. U.S. Geol. Survey Prof. Paper 562-G, 19 p.

HINZE, J.O. 1975. Turbulence. McGraw Hill, New York. 2nd Ed. 790 pp.

JACKSON, R.G. 1976. Sedimentological and fluid-dynamic implications of the turbulent bursting phenomenon in geophysical flows. J. Fluid Mech., 77; Part 2, 531 - 560.

JOHANSSON, C.J. 1963. Orientation of pebbles in running water. A laboratory study. Geog. Annaler, 45A; 85 - 112.

KENNEDY, J.F. 1969 . The formation of sediment ripples, dunes and antidunes. Ann. Revs. of Fluid Mech., 1; 147 - 168.

KIM, H.T. ET. AL. 1971. The production of turbulence near a smooth wall in a turbulent boundary layer. J. Fluid Mech., 50; 133 - 160.

KLINE, S.J. ET AL. 1967. The structure of turbulent boundary layers. J. Fluid Mech., 30; 741 - 773.

KNIGHT, D.W. AND MACDONALD, J.A. 1979. Open channel flow with varying bed roughness. ASCE J. Hy. Div., 105; HY 9, 1167 - 1183.

KOSTER, E.H. 1974. Flume studies on isolate gravel fabric on a sand bed. Geol. Surv. Can. Paper, 74-1; Pt. 8, 247 - 249.

LARKIN, P.A. 1976. Biometrics: a handbook of elementary statistical tests. U. of British Columbia, Vancouver, 163 pp.

LEOPOLD, L.B., WOLMAN, M.G. AND MILLER, J.P. 1964. Fluvial processes in geomorphology. W.H. Freeman, San Francisco, 522 pp.

LEOPOLD, L.B., EMMETT, W.W. AND MYRICK, R.M. 1966. Channel and hillslope processes in a semi-arid area, New Mexico, U.S. Geol. Surv., Prof. Paper 352-G, 61 pp.

LYLES, L. 1970. Turbulence as influenced by surface roughness in a wind tunnel boundary layer and subsequent effects on particle motion. Unpld. Ph. D. Diss., Kansas State University, Manhattan, 69 pp.

LYLES, L. AND WOODRUFF, M.P. 1971. Boundary layer flow structure: effects on detachment of non-cohesive particles. in Shen, H.W. (ed) 'Sedimentation'. Symposium to honor H.A. Einstein, Shen, Fort Collins. Chapter 2, 16 pp.

MASSEY, B.S. 1975. Mechanics of Fluids, 3rd Ed. Van Nostrand Reinhold, New York, 528 pp.

MIDDLETON, G.V. AND SOUTHARD, J.B. 1978. Mechanics of sediment movement. S.E.P.M. Short Course No. 3, Binghamton, New York.

MILLER, R.L. AND BYRNE, R.J. 1966. The angle of repose for a single grain on a fixed rough bed. Sedimentology, 6; 303 - 314.

MORRIS, H.M. 1955. A new concept of flow in rough conduits. Trans. ASCE, 120; 373 - 398.

NORDIN, C.F. ET AL. 1972. Hurst phenomenon in turbulence. Wat. Res. Res., 8; 1480 - 1486.

NOWELL, A.R.M. 1975. Turbulence in open channels: an experimental study of turbulence structure over boundaries of differing hydrodynamic roughness. Unpld. Ph. D. Diss., U. of British Columbia, 349 pp.

NOWELL, A.R.M. 1978. Dissipation and fine-scale structure in turbulent open channel flow. Wat. Res. Res., 14; 519 - 526.

NOWELL, A.R.M. AND CHURCH, M. 1979. Turbulent flow in a depth-limited boundary layer. J. Geophys. Res., 84; No. C8, 4816 - 4824.

NYCHAS, S.G., HERSHEY, H.C. AND BRODKEY, R.S. 1973. A visual study of turbulent shear flow. J. Fluid Mech., 61; Pt. 3, 513 - 540.

OFFEN, G.R. AND KLINE, S.J. 1974. Combined dye-streak and hydrogen-bubble visual observations of a turbulent boundary layer. J. Fluid Mech., 62; Pt. 2, 223 - 239.

OFFEN, G.R. AND KLINE, S.J. 1975. A proposed model of the bursting process in turbulent boundary layers. J. Fluid Mech., 70; Pt. 2, 209 - 228.

PRATURI, A.K. AND BRODKEY, R.S. 1978. A stereoscopic visual study of coherent structures in turbulent shear flow. J. Fluid Mech., 89; Pt. 2, 251 - 272.

RAO, K.N., NARASIMHA, R. AND BADRI NARAYANAN, M.A. 1971. The 'bursting' phenomenon in a turbulent boundary layer. J. Fluid Mech., 48; Pt. 2, 339 - 357.

REYNOLDS, A.J. 1974. Turbulent flow in engineering. John Wiley, New York. 462 pp.

SADEH, W.A. AND CERMAK, J.E. 1972. Turbulence effects on wall pressure fluctuations. ASCE J. Eng. Mech. Div., 98; 365 - 1379.

SHIELDS, A. 1936. Anwendung der Ähnlichkeitsmechanik und der Turbulenzforschung auf die Geschiebebewegung: Preussische Versuchsanstalt Für Wasserbau und Schiffbau. Berlin, Mitteilungen #26 70 pp. (Also as U.S. Dept. Agric. Soil Cons. Service, Co-op Lab., California Institute of Tech.)

SNEDECOR, G.W. AND COCHRAN, W.G. 1967. Statistical Methods. Iowa State University Press, Ames 6th Ed., 593 pp.

SNEED, E.D. AND FOLK, R.L. 1958. Pebbles in the Lower Colorado River, Texas: a study in particle morphogenesis. J. Geology, 66; 114 - 149.

SUMER, B.M. AND OĞUZ, B. 1978. Particle motions near the bottom in turbulent flow in an open channel. J. Fluid Mech., 86; Pt. 1, 109 - 127.

SUNDBORG, A. 1956. The river Klaralven: a study of fluvial processes. Geografiska Annaler, 38; 127 - 316.

SURRY, D. AND STATHOPOULOS, T. 1977/78. An experimental approach to the economical measurement of spatially averaged wind loads. J. Indust. Aerodynamics, 2; 385 - 397.

SUTHERLAND, A.J. 1967. Proposed mechanism for sediment entrainment by turbulent flows. J. Geophys. Res., 72; 6183 - 6194.

TENNEKES, H. AND LUMLEY, J.L. 1972. A first course in turbulence. The MIT Press, London. 300 pp.

THOMPSON, S.M. 1963. A study of the transportation of gravel by turbulent water flows. Unpld. M.Sc. Diss., U. of Canterbury, Christchurch. 161 pp.

URBONAS, B.R. 1968. Forces on a bed particle in a dumped rock stilling basin. Unpld. M.Sc. thesis, Colorado State, Fort Collins, 69 pp.

VANONI, V.A. 1964. Measurements of critical shear stress for entraining fine sediments in a boundary layer. W.M. Keck Lab. Hydraulics and Water Resources. Calif. Instit. Tech. 47 pp.

WHITE, C.M. 1940. The equilibrium of grains on the bed of a stream. Proc. Roy. Soc. London Ser. A, 174; 322 - 338.

YALIN, M.S. 1977. Mechanics of sediment transport. Pergamon Press, New York. 2nd Ed. 298 pp.

YALIN, M.S. AND KARAHAN, E. 1979. Inception of sediment transport. ASCE J. Hy. Div., 105; No. HY 11, 1433 - 1443.

ZINGG, T. 1935. Beitrag zür Schotteranalyse: Schweizerische Mineralogische und Petrologische Mitteilungen, 15; 39 - 140.

Particle	Time required for 20 vibrations (seconds).										$\bar{T}$ secs	σ
D 6	very low amplitude, difficult to count											
B 5	26.1	21.0	26.8	30.8	23.0	21.7	24.8	27.1	25.9	31.0	1.29	0.17
S 1	completely unstable and rolls away											
S 2	completely unstable and rolls away											
S 3	25.6	35.9	22.9	28.5	26.8	30.0	rolls away				1.41	0.22
S 7	very low amplitude, difficult to count											
R 2	24.1	24.2	36.4	30.5	36.5	20.8	23.8	24.4	24.6	29.1	1.37	0.27
R 5	39.2	26.7	29.4	26.5	31.3	26.7	32.1	39.2	28.4	26.9	1.53	0.25

Table 15. Time required for 20 vibrations on a smooth, metal boundary. Flow depth 8 cm, $\bar{v} = 0.42\ ms^{-1}$.

Particle	Time required for 20 vibrations (seconds).										$\bar{T}$	σ
D 2	22.8	35.3	21.5	22.1	22.2	18.7	21.6	20.0	23.4	21.5	1.15	0.23
D 3	20.8	21.1	23.5	18.4	24.8	21.3	25.8	22.8	20.4	27.4	1.13	0.14
D 6	29.8	25.0	30.5	23.8	24.5	25.7	22.3	35.4	35.3	27.0	1.40	0.23
B 1	21.8	16.8	17.8	23.4	23.0	22.4	20.0	-	-	-	1.04	0.13
B 3	24.8	22.3	19.5	20.0	23.7	18.2	20.6	17.7	20.2	20.4	1.04	0.11
B 5	very low amplitude, barely perceptible motion										-	-
B 6	17.6	19.8	19.0	22.5	17.3	18.7	22.4	18.2	21.1	-	0.98	0.10
B 7	22.7	23.9	24.1	21.9	20.7	21.9	23.8	23.4	24.7	-	1.15	0.06
S 1	22.7	26.5	22.9	29.7	26.7	28.8	26.1	27.5	25.6	25.9	1.31	0.11
S 2	33.1	29.4	27.6	26.9	34.7	35.4	27.7	33.4	29.7	37.7	1.55	0.16
S 3	44.8	37.8	29.3	27.9	46.1	39.2	42.3	34.5	-	-	1.89	0.34
S 4	28.7	33.0	32.6	27.9	30.7	24.3	28.1	22.4	-	-	1.42	0.19
S 5	39.9	37.3	26.0	26.8	30.1	36.8	27.6	28.1	28.7	-	1.56	0.26
S 6	23.7	21.6	25.7	36.5	27.2	28.5	26.4	28.9	-	-	1.37	0.22
S 7	38.0	51.1	40.7	37.5	35.5	24.8	29.7	29.7	26.1	-	1.74	0.41
R 1	27.8	24.8	26.6	24.3	26.6	26.6	26.3	28.5	-	-	1.38	0.19
R 2	38.1	30.1	33.4	24.2	22.2	36.5	28.2	27.1	26.8	35.4	1.56	0.24
R 3	24.0	23.6	22.9	25.2	24.1	21.4	23.5	-	-	-	1.18	0.06
R 4	24.9	23.2	21.9	25.5	23.6	21.7	24.6	23.7	24.1	-	1.18	0.06
R 6	31.8	41.5	28.2	34.3	34.9	42.5	31.2	30.8	33.2	-	1.71	0.09
R 7	39.3	35.1	38.6	30.7	34.0	31.9	33.7	36.1	33.3	-	1.74	0.14

Table 16. Time (seconds) required for 20 vibrations on a plain lego baseboard. Flow depth 8 cm, $\bar{v} = 0.41\ ms^{-1}$.

Particle	Time for 20 vibrations (seconds).													$\bar{T}$	σ
D 1	19.2	16.5	21.1	17.5	18.8	21.4	32.5	28.6						1.10	0.28
D 2	18.6	21.3	26.0	19.1	19.8	19.1	22.9	20.8	21.9	20.2				1.05	0.11
D 3	29.0	31.2	25.0	30.7	32.6	26.9	37.9	27.1	33.5					1.52	0.20
D 6	20.6	21.4	26.1	24.5	20.1	22.1	26.8	22.7	24.5	21.8				1.15	0.11
D 7	19.8	24.4	27.3	28.6	25.0	27.7	31.6	28.4	24.4	27.2				1.32	0.16
B 1	20.1	22.4	18.2	20.6	20.0	18.9	18.3	19.6	17.6	21.5				0.99	0.08
B 3	30.9	30.1	31.7	31.4	32.4	31.5	29.7	33.2						1.57	0.06
B 5	28.2	24.9	27.1	37.2	42.5	42.9	35.8	37.8	31.2					1.71	0.33
B 6	34.4	27.8	47.3	43.4	61.7	44.6	55.2	weak	motion					2.24	0.58
B 7	30.3	23.3	28.0	29.0	34.2	28.5	40.1	35.0						1.55	0.26
R 1	21.4	21.6	19.8	23.3	24.2	27.6	20.8	22.3	24.6	23.6				1.15	0.11
R 2	29.3	27.4	33.4	25.3	32.1	33.6	26.7	28.2	27.3	26.4				1.45	0.15
R 3	27.2	26.4	23.7	22.7	23.5	22.5	27.0	22.3	23.7	19.6	32.6			1.22	0.17
R 4	35.1	41.9	27.4	25.9	24.9	22.3	22.0	31.7	33.2	39.3				1.52	0.35
R 6	21.8	24.6	29.8	35.3	44.0	22.0	18.1	22.5	20.5	21.4	20.8	23.9	25.4	1.27	0.36
R 7	44.0	30.7	36.2	56.4	55.0	60.1	47.4	47.9	27.8					2.25	0.57
S 1	34.2	31.6	39.3	36.4	36.9	29.3	24.9	31.1	26.3					1.61	0.25
S 2	23.3	23.1	25.2	27.9	23.9	24.3	30.8	28.9	23.7	27.3				1.29	0.13
S 3	29.9	45.8	26.6	28.8	28.2	25.0	44.6	35.6						1.65	0.41
S 5	46.0	28.0	28.6	23.4	35.1	31.5	36.1	29.8	31.2					1.61	0.32

Table 17. Time (seconds) required for 20 vibrations with a roughness concentration of 1/48, flow depth = 8.1 cm, $\bar{v}$ = 0.43 ms^{-1}.

Particle	Time for 20 vibrations (seconds)										$\bar{T}$	σ
D 1	51.4	52.5	71.5	73.0	72.6	60.3	70.6	76.1	57.9	46.0	3.16	0.54
D 2	24.6	23.4	22.0	23.0	25.3	22.1	27.3	21.1	24.1	23.3	1.18	0.09
D 3	25.8	27.2	28.6	23.9	20.4	23.4	25.1	22.9	26.1	25.5	1.24	0.12
D 6	22.9	26.5	25.2	29.6	26.9	29.1	27.1	26.5	24.1	27.6	1.33	0.10
D 7	33.8	25.6	30.0	29.2	29.8	30.9	39.1	34.5	33.4	-	1.59	0.19
B 1	16.5	19.0	20.2	20.4	16.2	19.9	15.0	16.7	16.3	18.9	0.90	0.10
B 3	19.7	27.5	25.0	33.5	23.1	24.3	29.9	22.7	23.8	-	1.28	0.21
B 5	16.8	14.8	16.5	17.3	14.9	18.6	18.1	17.9	17.4	15.6	0.84	0.07
B 6	20.0	22.3	23.7	22.7	22.8	23.5	24.4	19.4	-	-	1.12	0.09
B 7	25.8	26.4	27.4	24.6	24.2	30.0	25.4	26.1	25.3	27.2	1.31	0.08
S 1	23.9	27.7	22.6	25.7	22.5	25.4	29.5	27.9	26.7	25.0	1.28	0.12
S 2	21.8	29.1	46.1	29.8	28.1	25.8	19.9	30.1	24.9	23.0	1.39	0.37
S 3	27.0	29.2	43.4	39.9	38.7	47.1	24.7	36.5	18.7	20.4	1.63	0.49
S 4	26.9	38.4	38.5	33.3	23.5	28.4	27.9	23.5	25.5	31.5	1.49	0.28
S 7	32.7	32.1	25.3	28.0	20.4	33.9	28.1	26.5	31.2	33.5	1.46	0.22
R 1	23.4	28.6	26.8	35.4	31.2	33.6	22.7	19.1	27.4	27.9	1.38	0.25
R 2	23.0	26.9	22.9	23.4	25.5	24.6	23.9	23.2	24.5	-	1.21	0.07
R 3	25.3	22.7	20.3	21.9	23.4	20.6	25.0	29.9	22.8	24.0	1.18	0.14
R 4	27.6	35.1	25.9	41.8	44.0	42.6	39.7	23.6	21.8	-	1.68	0.44
R 6	41.0	45.8	59.2	55.2	64.6	60.0	65.1	68.5	54.0	-	2.85	0.46
R 7 (a)*	51.9	61.6	55.3	69.4	60.1	55.5	51.6	59.2	60.0	-	2.95	0.25
(b)	23.6	27.7	37.7	39.6	25.6	31.2	29.4	28.2	35.2	36.5	1.57	0.27

* a axis rotated 180° from (b)

Table 18. Time (seconds) required for 20 vibrations with a roughness density of 1/16, flow depth d = 8 cm, $\bar{v}$ = 0.44 ms^{-1}.

Particle	Time for 20 vibrations (seconds).												$\overline{T}$	σ
D 1	34.0	21.1	29.5	21.9	30.2	22.8	22.9	30.1	26.2	20.3			1.30	0.24
D 2	25.8	22.6	20.4	25.8	20.1	23.4	23.9	26.2	21.5	20.5			1.15	0.12
D 4	22.8	20.6	18.5	20.2	21.5	19.6	17.0	20.5	21.2	19.6			1.01	0.08
D 7	38.9	54.2	45.1	54.5	61.8	60.8	low amplitude motion						2.63	0.45
B 1	23.9	20.7	25.6	23.0	25.8	21.0	21.9						1.16	0.10
B 3	21.2	22.3	19.0	33.4	18.1	18.6	16.3	20.2	18.4	17.4			1.02	0.24
B 5	34.4	29.3	36.7	33.9	31.2	34.7	33.1	30.9	34.6	35.7			1.67	0.12
B 6	31.8	47.2	41.9	38.6	39.0	45.3	44.9	32.7	34.2				1.98	0.29
S 2	45.1	50.7	29.7	48.9	35.6	54.2	49.1	21.1	19.0	18.4	20.0		1.78	0.72
S 3	26.9	20.2	19.1	29.6	20.2	19.5	25.5	22.9	21.4	22.4	20.8		1.13	0.17
S 3	30.4	28.8	28.5	33.4	40.7	39.1	29.8	31.2	31.5	30.4			1.62	0.21
S 5	32.0	33.5	34.3	46.3	56.4	45.8	45.9	34.6	35.2	37.3			1.98	0.42
S 7	38.3	36.9	44.8	34.5	41.5	47.8	45.5	55.9	27.3	42.0	43.5	38.3	2.07	0.36
S 7*	22.0	20.8	23.3	21.2	19.3	24.1	29.7	20.9	25.8	22.4			1.15	0.15
R 1	30.8	29.2	30.8	29.5	32.8	28.7	33.4	29.8					1.53	0.08
R 2	30.0	35.8	28.9	38.1	41.5	24.7	38.5	36.2	28.7	35.2			1.69	0.27
R 3	30.0	38.7	28.3	24.3	23.5	25.0	24.4						1.39	0.27
R 4	37.0	41.6	35.5	24.7	27.6	39.6	31.6	35.6	32.7				1.70	0.27
R 6	28.3	32.3	26.4	28.2	27.8	28.1	31.0	31.8	27.4	27.5			1.44	0.10
R 7	32.2	46.6	57.6	39.6	55.1	69.6	70.6	55.0					2.66	0.67

* $\overline{v} = 0.45\ ms^{-1}$

Table 19. Time (seconds) required for 20 vibrations for a roughness density of 1/12, flow depth = 8 cm, $\overline{v} = 0.42\ ms^{-1}$.

Particle	Time for 20 vibrations (seconds).										$\bar{T}$	σ
D 2	19.5	22.4	18.6	19.8	23.1	22.9	20.1				1.05	0.09
D 3	29.6	21.9	23.7	27.7	29.7	28.1	30.5	23.5	21.3	20.1	1.28	0.20
D 7	32.7	19.6	23.9	23.2	23.8	30.8	30.2	29.8	24.2	25.0	1.32	0.21
B 1	22.0	22.0	22.1	20.4	21.5	22.2	20.7				1.08	0.04
B 5	24.8	25.6	32.6	33.0	30.7	29.4	31.6	30.1	28.7	27.3	1.47	0.14
B 6	23.0	26.2	29.0	26.2	25.9	26.1	27.8	24.2			1.30	0.09
S 3*	39.6	36.6	43.0	32.9	38.1	41.2	39.2	37.1	36.7		1.91*	0.15
S 5*	37.8	30.7	45.3	40.5	36.7	33.4	41.9	37.2			1.90*	0.23
S 7	43.4	30.9	35.1	36.2	31.9	37.2	32.9	34.4	36.2		1.77	0.18
R 2	28.5	21.9	24.9	32.3	27.4	26.9	29.8	22.7	27.7		1.35	0.17
R 4	24.3	22.0	32.9	34.8	20.9	29.8	22.6	19.9	23.7	19.8	1.25	0.27

* run @ $\bar{v} = 0.37\ ms^{-1}$.

Table 20. Time (seconds) for 20 vibrations using a roughness concentration of 1/8, flow depth d = 8 cm, $\bar{v} = 0.44\ ms^{-1}$.

Particle	Roughness density 1/12, d = 5 cm, $\bar{v}$ = 0.40 ms^{-1}										$\bar{T}$	σ
D 6	18.3	18.8	21.8	24.6	22.1	21.0	24.5	18.7	17.1	18.3	1.03	0.13
B 3	16.2	16.4	17.3	16.1	18.6	20.5	18.2	15.9	18.5	18.3	0.88	0.07
S 2	18.4	20.5	19.0	17.7	17.6	18.5	17.0	17.9	17.4	20.9	0.92	0.07
S 7	Low amplitude, high frequency motion, very difficult to count.										< 1.00	
R 4	Low amplitude, high frequency motion, very difficult to count.										< 1.00	

Particle	Roughness density 1/12, d = 20 cm, $\bar{v}$ = 0.42 ms^{-1}											T	σ
D 6	70.5	40.6	37.9	52.5	52.8	40.4	46.6	54.1	65.8	53.2	43.1	2.53	0.52
B 3	48.5	41.8	39.6	38.4	52.6	44.1	-	-	-	-	-	2.21	0.27
B 5	82.9	63.9	59.5	51.1	66.7	70.0	62.2	73.7	62.4	65.6	-	3.29	0.42
S 2	55.0	42.2	49.4	64.2	58.1	57.4	53.6	62.4	58.1	83.0	61.7	2.93	0.51
S 3	35.2	38.7	32.9	30.7	30.4	44.6	40.2	31.7	-	-	-	1.78	0.26
S 7	55.4	46.9	52.0	50.2	56.3	55.9	57.7	45.3	41.3	76.5			
	57.6	59.9	69.7	74.6	66.3	61.1	57.3	58.4	47.6	50.3		2.85	0.47
R 4	54.8	74.5	62.3	52.3	51.2	38.3	38.2	37.5	43.9	51.3			
	49.2	59.7	58.2	46.8	40.8	43.3	44.7	41.5	34.8	43.2		2.42	0.50

Table 21. Time required for 20 vibrations when flow depth is changed from 8 cm. to either 5 or 20 cm.

Particle B5 Distance														$\overline{T}$	σ
	Wake generator, 2.9 cm diameter cylinder, 1.5 cm high.														
2 cm	41.9	47.2	32.6	35.8	24.7	42.3	29.2	33.9	36.8	39.9	41.4	64.9		1.96	0.51
4 cm	57.3	71.8	50.3	62.1	56.2	83.4	90.1	86.1						3.48	0.77
6 cm	25.1	23.8	21.4	23.0	27.6	23.7	22.4	28.4	21.2	23.0	20.5	20.4		1.16	0.13
6 cm	22.4	28.3	24.7	26.9	17.7	21.6	27.0	28.7	21.5	21.7	21.6	21.1		1.18	0.17
6 cm	23.6	20.5	18.0	27.4	21.4	20.2	27.7	24.6	32.7	22.7				1.14	0.20
8 cm	27.9	26.4	25.7	27.4	20.5	25.4	23.3	30.9	22.9	30.6				1.31	0.17
10 cm	22.0	29.0	24.2	26.1	29.3	26.4	29.5	22.6	21.3	26.4				1.28	0.15
12 cm	21.8	24.6	26.6	26.0	26.0	21.3	28.5	21.4	32.5	27.7	24.0	21.9	20.6	1.24	0.17
14 cm	23.2	30.0	23.6	23.9	25.2	28.6	27.4	35.5	34.7	34.3	31.4	40.7		1.49	0.28
	Wake generator, 2.9 cm diameter cylinder, 2.9 cm high.														
4 cm	15.4	16.9	18.7	13.1	17.5	20.6	24.5	25.3	24.5	21.7	21.0			1.00	0.20
4 cm	20.0	22.5	20.6	19.3	15.6	17.8	20.4	24.2	15.3	23.8	18.4	16.9		0.98	0.14
6 cm	17.8	24.1	26.8	21.6	24.8	31.8	31.4	25.7	27.9	27.8	33.1	28.5		1.34	0.22
6 cm	23.6	24.3	28.4	22.7	25.9	26.3	32.2	31.6	29.3	28.8	29.9	28.8		1.38	0.15
8 cm	32.9	24.3	23.8	22.1	24.6	19.5	23.2	23.2	18.9	18.5	23.4	25.3		1.20	0.21
10 cm	25.4	20.6	24.3	22.0	22.7	32.0	28.3	37.6	28.9	32.5	22.4	26.0		1.34	0.25
12 cm	25.3	23.9	25.0	20.9	21.1	49.4	38.2	34.4	25.5	21.8				1.43	0.46

Table 22. Vibration period of clasts downstream of a wake generator, flow depth d = 7.8 cm, $\overline{v}$ = 0.39 ms^{-1}.

Particle	Time for 20 vibrations (seconds).												$\overline{T}$	σ
B3 @ 2 cm	21.2	18.7	23.2	26.8	20.2	18.9	22.2	18.5	21.5	23.6			1.02	0.24
@ 6 cm	21.2	22.3	19.0	33.4	18.1	18.6	16.3	20.2	18.4	17.4			1.07	0.13
@ 8 cm	17.0	19.8	29.9	16.1	18.4	25.3	19.8	35.0	26.1	31.8			1.20	0.33
@ 12 cm	37.1	18.1	24.9	19.9	17.7	16.4	20.3	24.6	21.3	23.0			1.12	0.30
D3 @ 2 cm	23.2	21.8	23.7	22.3	24.0	26.2	32.4	28.2	19.5	28.6			1.25	0.19
@ 6 cm	22.7	25.8	22.2	23.5	21.3	21.1	22.6	21.3	26.2				1.15	0.09
@ 10 cm	20.5	22.4	22.4	19.5	21.7	24.2	19.9	27.9	21.7	23.0			1.12	0.12
S4 @ 2 cm	21.1	22.5	22.7	17.6	19.2	18.9	20.7	23.7	28.4	28.3			1.12	0.18
@ 6 cm	23.1	20.4	17.4	21.0	21.4	17.3	17.9	22.2	18.6	17.6			0.98	0.11
@ 10 cm	18.9	26.0	29.9	22.1	25.8	18.3	16.9	17.4	19.6	20.4			1.08	0.22
R3 @ 2 cm	30.7	25.6	26.1	24.3	25.8	23.7	24.4	27.5	28.4	28.0			1.32	0.11
@ 6 cm	30.0	38.7	28.3	24.3	23.5	25.0	24.4						1.39	0.27
@ 10 cm	17.5	16.6	16.9	15.2	15.9	18.6	17.5	16.7					0.84	0.05
B7 @ 6 cm	22.2	23.3	19.6	28.7	21.7	19.0	28.8	21.2	26.4	22.1			1.17	0.18
@ 10 cm	26.6	22.1	27.7	25.7	26.7	30.0	24.5	27.3	27.1				1.32	0.11
D6 @ 2 - 4 cm	no motion													
@ 6 cm	36.1	40.0	28.7	31.1	57.3	61.6	47.8	55.4	39.7	36.7			2.17	0.57
@ 10 cm	21.9	20.1	20.3	23.7	22.4	19.2	20.4	23.4	25.8	26.9			1.12	0.13
S7 @ 2 - 4 cm	22.0	20.8	23.3	21.2	19.3	24.1	29.7	20.9	25.8	22.4			1.15	0.15
@ 6 cm	38.3	36.9	44.8	34.5	41.5	47.8	45.5	55.9	27.3	42.0	43.5	38.3	2.07	0.36
@ 10 cm	19.4	22.4	25.8	24.8	23.1	19.4	24.9	21.4	19.7				1.11	0.12

Table 23. Variation of vibration periods at varying distances with roughness density of 1/12, flow depth d = 8 cm, $\overline{v}$ = 0.45 ms^{-1}.